Fakultät für Medizin
der Technischen Universität München

Targeting of the tumor-associated urokinase-type plasminogen activation system: recombinant single chain antibody scFv-IIIF10 directed to human urokinase receptor

Angela Kirschenhofer

Vollständiger Abdruck der von der Fakultät für Medizin der Technischen Universität München zur Erlangung des akademischen Grades eines

Doktors der Medizin

genehmigten Dissertation.

Vorsitzender : Univ.-Prof. Dr. D. Neumeier
Prüfer der Dissertation:
1. Priv.-Doz. Dr. V. Magdolen
2. Univ.-Prof. Dr. M. Schmitt

Die Dissertation wurde am 9.01.2007 bei der Technischen Universität München eingereicht und durch die Fakultät für Medizin am 18.07.2007 angenommen.

Acknowledgements

The experimental part of this work was performed during January 2001 and April 2003 in the Clinical Research Group of the Women's Hospital of the Technical University in Munich under supervision of PD Dr. Viktor Magdolen.

I want to cordially thank PD Dr. Viktor Magdolen for providing the subject of this thesis, for the patient and steady support in every arisen question, for the inspiring ideas when discussing experimental problems and for being my mentor at all times.

I want to thank Prof. Dr. Manfred Schmitt, the head of the Clinical Research Group, as well as PD Dr. Ute Reuning for their kind support in answering questions especially on the experiments in cell biology.

Many special thanks to Volker Böttger, who kindly provided the phages and gave me the technical support in phage display experiments; many special thanks to Prof. Dr. Achim Krüger and Dr. Charlotte Koppitz for their kind support in animal experiments.

Sincere thanks are given to Sabine Creutzburg for her competent guidance through cloning experiments, Christel Schnelldorfer for her friendly and competent assistance with FACS experiments and Anke Benge for the encouragement in cell culture.

I want to thank all collegues and persons who are not mentioned here, but have been involved in my work.

Elke Guthaus, Stefanie Neubauer and Juliane Farthmann are to thank for their always positive attitude, the nice atmosphere at work and their friendship.

I want to thank Oliver, who was always there for me, for his patient help and support.

My dear parents and sister Constanze is to thank for their mental support. Without their encouraging words I couldn´t have completed my dissertation.

Index

Abbreviations

1. Introduction 1

1.1 The role of the uPA/uPAR-system for tumor invasion and metastasis 1

1.1.1 Urokinase-type plasminogen activator receptor (uPAR, CD 87) 2

1.1.2 Urokinase-type plasminogen activator (uPA) and its inhibitors (PAI-1 and PAI-2) 6

1.1.3 Clinical relevance of uPA/uPAR 7

1.2 Antibodies interfering with uPA/uPAR-interaction 8

1.3 Generation of monoclonal antibodies directed to human uPAR 9

1.4 Generation of single-chain antibody scFv-IIIF10 9

1.4.1 Single-chain antibodies 9

1.4.2 Characterization of the binding epitope of mAb-IIIF10 11

1.4.3 Generation of a recombinant scFv-version of mAb-IIIF10 and expression in *E. coli* 12

1.5 Clinical application of therapeutic molecules 14

2. Objective 16

3. Materials and Methods 17

3.1 Materials 17

3.1.1 Cell lines 17

3.1.2 *E. coli* bacterial strain 17

3.1.3 Mammalian expression vector pSecTag2/HygroB 17

3.1.4 Chemicals 19

3.1.5 Instruments 19

3.2 Methods 20

3.2.1 Molecular biology 20

3.2.1.1 *E. coli* culture 20

3.2.1.2 Long term storage of *E. coli* 20

3.2.1.3 Plasmid preparation from *E. coli* (Mini-prep) 21

3.2.1.4 Plasmid preparation from *E. coli* for DNA sequencing 22
3.2.1.5 Restriction analysis of DNA-fragments 22
3.2.1.6 Ligation of DNA fragments with T4-ligase 22
3.2.1.7 Transformation of plasmid DNA in *E. coli* 23
3.2.1.8 Polymerase chain reaction (PCR) 23
3.2.1.9 RT-PCR 25
3.2.1.10 Proteinase K digestion 26
3.2.1.11 DNA gel electrophoresis 27
3.2.1.12 Isolation of DNA from agarose gels (“freeze and squeeze“) 27
3.2.2 Protein chemical methods 28
3.2.2.1 Solid phase binding assay with rec-uPAR$_{1-277}$ 28
3.2.2.2 SDS-polyacrylamide gel electrophoresis (SDS-PAGE) 28
3.2.2.3 Western blot 30
3.2.2.4 Stripping of Western blot membranes 31
3.2.2.5 Purification and concentration of scFvIIIF10 and TF$_{1-214}$ 31
3.2.2.6 FACS analysis 31
3.2.3 Cell biology 34
3.2.3.1 Cell culture 34
3.2.3.2 Stable transfection of V79, CHO and OV-MZ-6#8 cells 34
3.2.3.3 Phage-display 35
3.2.3.3.1 Phage amplification and purification 35
3.2.3.3.2 Phage-titration 36
3.2.3.3.3 Solid phase binding assay phage ELISA 37
3.2.3.3.4 Phage-binding assay 38
3.2.3.4 Cell proliferation assay 39
3.2.3.5 Cell adhesion assay 39
3.2.3.5.1 Cell-matrix adhesion assay 39
3.2.3.5.2 Cell-cell adhesion assay 40
3.2.4 Tumor model 41
3.2.5 Statistical analysis 42

4. Results 43

4.1 Mammalian expression plasmids encoding scFv-IIIF10 43

4.2 Generation of stable transfectants in eukaryotic cells 47
4.3 Purification and characterization of soluble scFv-IIIF10 and soluble TF_{1-214} from eukaryotic cell culture supernatants 48
4.4 Detection of membrane anchored variants of scFv-IIIF10 *via* M-13 phages 51
4.5 Interaction of membrane bound scFv-IIIF10 with human uPAR 52
4.6 Characterisation of the proliferation of OV-MZ-6#8 cells transfected with soluble scFv-IIIF10 54
4.7 Determination of the adhesive capacities of the transfected OV-MZ-6#8 cells to different ECM-Proteins 55
4.8 Effects of scFv-IIIF10 secretion on *in vivo* tumor growth of human ovarian cancer cells 55

5. Discussion 57
5.1 scFv-IIIF10 as a therapeutic molecule 57
5.2 Limitations in the design and application of single chain fragments 58
5.3 Currently applied antibodies in clinical trials 60
5.4 Future prospects of antibody therapy 62

6. Summary 64

7. References 66

8. Curriculum vitae and publications 82

Abbreviations

aa	amino acid
Amp	ampicillin
APS	ammoniumperoxodisulfate
ATF	aminoterminal fragment
bp	base pair
BPB	bromphenol-blue
BSA	bovine serum albumine
CEA	carcinoembryonic antigen
cDNA	complementary desoxyribonucleic acid
CHO	chinese hamster ovary
CMV	Cytomegalovirus
DMEM	Dulbecco´s modified Eagle´s medium
DMSO	dimethylsulfoxide
DNA	desoxyribonucleic acid
dNTP	desoxyribonucleictriphosphate
E. coli	Escherichia coli
e.g.	*exempli gratia* (for example)
ECM	extracellular matrix
EDTA	ethylendiamin-tetra-acetic acid
EGFR	epidermal growth factor receptor
ELISA	enzyme linked immunosorbent assay
GFD	growth factor-like domain
GPI	glykosylphosphatidylinositol
FACS	fluorescence activated cell sorting
FCS	fetal calf serum
FDA	Food and Drug Administration
FIGO	Fédération Internationale de Gynécologie et d´Obstetrique
h	hour
HEPES	2-{(4-(hydroxyethyl)-1-piperazin}ethansulfonic acid
HMW	high molecular weight
HSV	Herpes simplex virus

kDa	kilo dalton
K_D	dissociation´s constant
LB-medium	Luria-Bertani-medium
LMW	low molecular weight
mAb	monoclonal antibody
min	minute
MOPS	3-(N-morpholino)-propanesulfonic acid
MMP	matrixmetalloproteinase
Ni-NTA	nickel-nitrilotriacetic acid
OD_x	optical density at x nm
OS	over all survival
p.a.	*per analysis*
PAGE	polyacrylamide gel electrophoresis
PAI	plasminogen activator inhibitor
PBS	phosphate buffered solution
P:C:I	phenol:chloroform:isomylalcohol, 25:25:1
PCR	polymerase chain reaction
PEG	polyethyleneglycol
PMA	phorbol-12-myristat-13-acetate
POX	peroxidase labeled
PVDF	polyvinylidenfluoride
RFS	relapse free survival
rpm	rounds per minute
RT	room temperature
scFv	single chain fragment
SDS	sodium dodecyl sulfate
SDS-PAGE	SDS-polyacrylamide gel electrophoresis
suPAR	soluble urokinase-type plasminogen activator receptor
TBS	tris buffered solution
TCD	transmembrane domain
TEMED	N,N,N`,N`-tetramethylethylendiamine
TMB	3,3´,5,5´-tetramethylbenzidine
TKI	tyrosin kinase inhibitor

tPA	tissue type plasminogen activator
Tris	N-[tris-(hydroxymethyl-)]aminomethane
U	unit
uPA	urokinase-type plasminogen activator
uPAR	urokinase-type plasminogen activator receptor
o/n	over night
wt	wild type

amino acids

A	Ala	alanine	M	Met	methionine
C	Cys	cysteine	N	Asn	asparagine
D	Asp	aspartic acid	P	pro	proline
E	Glu	glutamic acid	Q	Gln	glutamine
F	Phe	phenylalanine	R	Arg	arginine
G	Gly	glycine	S	Ser	serine
H	His	histidine	T	Thr	threonine
I	Ile	isoleucine	V	Val	valine
K	Lys	lysine	W	Trp	tryptophan
L	Leu	leucine	Y	Tyr	tyrosine

1. Introduction

1.1 The role of the uPA/uPAR-system for tumor invasion and metastasis

One of the principle properties of malignant cells, which distinguish them from normal or benign cells, is their capability to cross tissue boundaries and to metastasize. Once detached from the primary tumor, they are able to invade into the surrounding extracellular matrix (ECM) and into blood or lymphatic vessels, followed by adhesion to and invasion through the endothelium to finally re-implant at distant loci accompanied by neovascularization. The degradation of the surrounding ECM is facilitated, when certain extracellular proteolytic enzymes are present: matrix-metalloproteinases (MMPs), cysteine proteases (including cathepsin B and L) and serine proteases such as plasmin and the urokinase-type plasminogen activator (uPA) (overview in Andreasen et al., 1997; Danø et al., 1999; Reuning et al., 1998; Schmitt et al,. 2000; Allgayer 2006).

The proteolytic urokinase-type plasminogen activator system encompasses the serine protease urokinase-plasminogen activator (uPA), its receptor uPAR (CD 87) and its inhibitors PAI-1 and PAI-2 (**Figure 1**). In concert with other members of the serine protease family (plasmin, tissue kallikreins, membrane type serine-proteases), matrix-metalloproteinases (MMPs) and cysteine proteases, it mediates the pericellular proteolytic events leading to focal degradation of the basement membrane and extracellular matrix in cancer growth, tumor cell invasion and metastasis (Andreasen et al., 2000; Del Rosso et al., 2002; Ragno, 2006).

Binding of uPA to its tumor cell surface receptor uPAR converts the single polypeptide chain plasminogen into its two-chain form plasmin and thereby not only focuses its plasminogen activation function to the tumor cell, but also induces a cascade of other biological events including cell proliferation, adhesion, migration, chemotaxis and angiogenesis (Rabbani and Mazar, 2001; Blasi and Carmeliet, 2002; Reuning et al., 2003). This conversion can also be catalyzed by tPA (tissue type plasminogen activator), an enzyme triggering the intravascular fibrinolysis, and certain bacterial proteins (Andreasen et al., 1997). The proteolytic activity of uPA is controlled by its inhibitors PAI-1 and PAI-2 (Blasi, 1997).

Due to the lack of a transmembrane domain, uPAR needs to functionally cooperate with other transmembrane receptors in order to conduct intracellular signalling. A cross talk with the adhesion and signalling receptors of the integrin superfamily has been reported (Chapman and Wei, 2001). Integrins are transmembrane cell surface receptors which upon binding to ECM

proteins exert regulatory functions in many processes such as cell adhesion, migration and proliferation (Blasi and Carmeliet, 2002; Reuning et al., 2003). Recently it was reported, that uPAR functionally interacts also with a G-protein coupled receptor involved in chemotaxis, the high affinity receptor (FPR) for the fMet-Leu-Phe peptide (fMLP). fMLP is a peptide of bacterial origin that is a strong leukocyte chemoattractant. fMLP-dependent cell migration requires uPAR expression (Montuori et al., 2002; Le et al., 2002).
Upon binding, the enzymatically active uPA is focused to the cell surface resulting in a higher state of uPA activity and a several fold enhanced rate of conversion of cell-surface associated plasminogen to plasmin (Ellis et al., 1999). Plasminogen is a serineprotease present in plasma and extracellular fluids with a high activity spectrum towards various extracellular matrix components such as fibrin, fibronectin, laminin and collagen IV, thereby leading to ECM degradation (**Figure 1**). In fact, in a variety of malignancies such as breast, ovarian, esophageal, gastric, colorectal or hepatocellular cancer, a strong clinical value of the plasminogen activation system in predicting relapse free and overall survival in cancer patients has been demonstrated (Harbeck et al., 2002; Look et al., 2002).

1.1.1 Urokinase-type plasminogen activator-receptor (uPAR, CD87)

uPAR, the cellular receptor for uPA, is a cysteine-rich glycoprotein attached to the lipid bilayer of the plasma membrane *via* a glycosyl-phosphatidyl-inositol (GPI) anchor (Ploug et al., 1991). It comprises three homologous, structurally related protein domains of approximately 90 amino acids with four to five disulphide bonds (DI, DII and DIII as numbered from the N-terminus, Behrendt et al., 1991; Llinas et al., 2005; see **Figure 2**). Domain I is located on the N-terminal part of the receptor and is important for uPA binding (Behrendt et al., 1991). However, uPA binding studies showed that the affinity of domain I-uPAR to uPA is several hundred fold lower than the affinity of the complete uPA receptor (Rettenberger et al., 1994; Ploug et al., 1998, 2002) suggesting that uPA/uPAR- binding rather requires the complete three-domain molecule for high-affinity interaction.

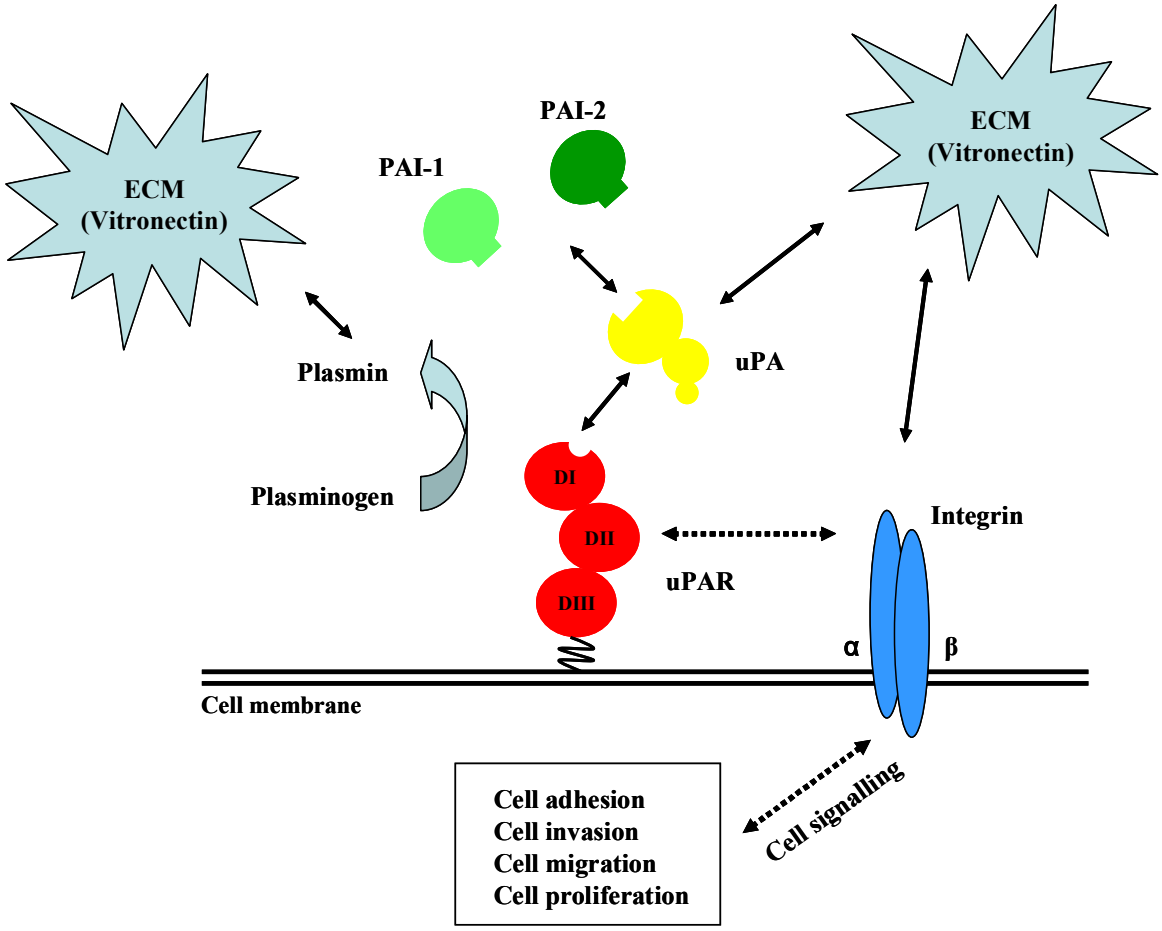

Figure 1. ***Schematic overview of the role of the uPA/uPAR-system in tumor invasion and metastasis.*** Binding of uPA to its tumor cell surface receptor uPAR converts the single polypeptide chain plasminogen into its two-chain form plasmin, thereby leading to degradation of the ECM, but also inducing a cascade of other biological events including cell adhesion, invasion, migration and proliferation. The proteolytic activity of uPA is controlled by its inhibitors PAI-1 and PAI-2. Using integrins as co-receptors, the uPA/uPAR-system is able to conduct intracellular signalling.

By various methods, it has been demonstrated that domain I of uPAR harbors important determinants for uPA-binding: (i) a uPAR mutant with four aa substitutions (His47, Glu49, Lys50 and Arg53 exchanged by alanine) did not longer interact with uPA, while other triple or quadruple mutations in other regions of uPAR did not significantly affect binding to uPA (Pollänen, 1993); (ii) exchange of the only glycosylation site, Asn52, of domain I of human uPAR to Gln52 by *in vitro* mutagenesis (and thus leading to a nonglycosylated domain I) resulted in a uPAR variant with considerably reduced affinity for uPA compared to wild-type uPAR (Moller et al., 1993); (iii) chemical modification of uPAR with tetranitromethane, which resulted in efficient and specific nitration of solvent-accessible tyrosine residues, identified Tyr57 of uPAR to be intimately engaged in the interaction with uPA (Ploug et al., 1995); (iv) by photoaffinity labelling of the uPA receptor specific sites involved in ligand binding were shown to include Arg53 and Leu66 (Ploug ,1998); (v) a systematic Ala scan identified the residues Arg53, Leu55, Tyr57, and Leu66 to be essential for uPA/uPAR complexation (Gårdsvoll et al., 1999); (vi) recently, the crystal structure of a uPAR-soluble form bound to an antagonist peptide was solved, thus confirming that the three domains of the uPAR form an almost globular receptor with a breach between DI and DIII generating a cavity (19 angstroms deep), where the ligand peptide is located; domain I plays a predominant role in this ligand interaction by providing half of the binding interface (Llinas et al., 2005); additionally, the crystal structure of ATF/suPAR was reported (Barinka et al., 2006). (vii) in a recent study performed by Gårdsvoll et al. (2006), the functional epitope on the uPAR for uPA-binding was characterized. The alanine-scanning-mutagenesis clearly showed that the high affinity binding of pro-uPA critically depends on both uPAR domain I (9 positions) and domain2 (21 positions). Although the alanine-scanning-mutagenesis did not reveal any important role for domain III in uPA binding, this domain nevertheless plays a stabilizing role on the assembly of a functional, ligand-binding cavity in the three-domain uPAR.

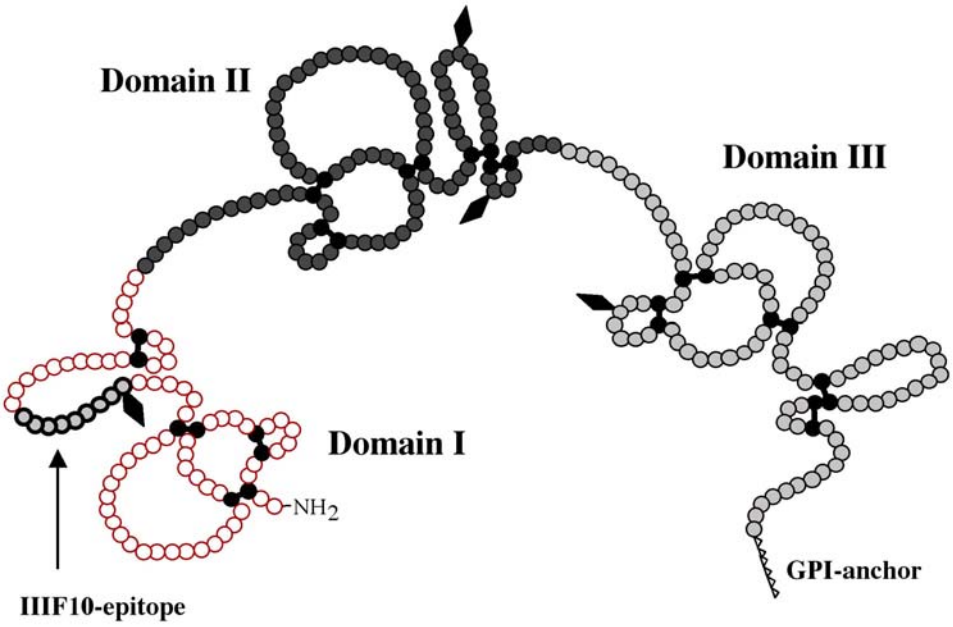

Figure 2. ***The domain structure of the uPA receptor.*** uPAR consists of three structurally homologous domains and is linked to the cell surface *via* a C-terminal glycan lipid GPI-anchor (modified according to Ploug et al. 1994). Glycosylation sites (^{52}NRT, ^{162}NDT, ^{172}NTT, ^{200}NST; Ploug et al., 1998) are indicated by a rhombus, disulfide bonds are depicted in black. The epitope of mAb IIIF10 (aa 52-60 of uPAR) in the N-terminal domain I, which harbors main determinants for uPA binding, is indicated in grey. mAb IIIF10 binds with high affinity to both glycosylated and non-glycosylated uPAR (Luther et al., 1997).

Besides its proteolytic function, the uPA/uPAR-system has also mitogenic and chemotactic properties. The three domains of the uPAR are joined by linker sequences, the linker region connecting domains I and II exhibits an extreme proteolytic sensitvity and can be cleaved by several proteolytic enzymes. Such cleaved forms (c-uPAR) lacking domain I have been detected on the surface of different cell lines in normal and cancer tissues. An epitope has been identified residing within the peptide region connecting DI and DII, which upon exposure to proteolytic cleavage mimicks uPA/uPAR-mediated chemotactic activity (Andolfo et al., 2002; Fazioli et al., 1997). Both, full length and cleaved uPAR can be shed, thus generating soluble uPAR forms (suPAR and c-suPAR respectively). Soluble uPAR forms are found in biological fluids *in vitro* and *in vivo*. Such variants may arise by differential splicing or phospholipase C cleavage of the GPI-anchor (Høyer-Hansen et al., 1992; Montuori et al., 2002, 2005).

Moreover, uPA/uPAR-system shows cell adhesive capacity by the ability of uPAR and PAI-1 to bind to the ECM protein vitronectin. Domain II and III have been reported to bind to vitronectin, an ECM-protein with high affinity (Waltz and Chapman, 1994).
Due to the lack of a transmembrane domain, uPAR cooperates with other transmembrane receptors in order to conduct intracellular signalling. Hereby, the adhesion and signalling receptors of the integrin superfamily seem to play an important role (Chapman et al., 2001). uPAR has been reported to be able to associate with ß1-integrins as immunoprecipitates with anti-uPAR antibodies (Wei et al., 1996). Recently it was reported, that uPAR functionally interacts also with a G-protein coupled receptor involved in chemotaxis, the high affinity receptor (FPR) for the fMet-Leu-Phe peptide (fMLP). fMLP is a peptide of bacterial origin that is a strong leukocyte chemoattractant. fMLP-dependent cell migration requires uPAR expression (Montuori et al., 2002; Le et al., 2002).

1.1.2 Urokinase type plasminogen activator (uPA) and its inhibitors (PAI-1 and PAI-2)

There are two types of plasminogen activators, the urokinase-type (uPA) and the tissue-type (tPA). Both are capable of activating the inactive zymogen plasminogen to the active proteinase plasmin, which can degrade extracellular matrix proteins. tPA is synthesized in endothelial cells and plays a primary role in intravascular fibrinolysis.
uPA is a 55 kDa serine protease which is produced by various normal and cancer cells as an inactive single-chain protein. Pro-uPA, the zymogen of uPA has a several hundred fold lower activity than the activated two-chain uPA (Andreasen et al., 1997).
uPA consists of two disulfide bridge-linked polypeptide chains, the C-terminal serine protease domain (B-chain) with its catalytic site, and the A-chain. The A-chain, so called aminoterminal fragment (ATF), consists of two domains, a “growth factor-like domain“ (aa 1-46) harboring the binding site for uPAR (Appella et al., 1987) and a kringle domain (aa 47-135), which has structural similarities to other protein domains like tPA, plasmin and thrombin and is able to bind to uPAR.
The action of uPA on plasminogen is controlled by the inhibitors PAI-1 and PAI-2, PAI-1 being the most efficient inhibitor. Alternatively, when PAI-1 binds to uPAR-bound uPA, a complex is formed with α_2-macroglobulin/LDL-receptor-related protein (LRP), a multifunctional transmembrane receptor, and is then rapidly endocytosed (Cubellis et al.,

1990). Upon internalization the complex is then degraded and uPAR recycled to the cell surface (Nykjaer et al., 1997).

1.1.3 Clinical relevance of uPA/uPAR

As early as 1988, elevated uPA levels in primary breast tumor tissue were shown to be associated with a highly invasive phenotype and poor prognosis (Duffy et al., 1988). Jänicke et al. (1991; 2001) were the first to describe the prognostic significance of PAI-1 in breast cancer patients. High PAI-1 level as determined by ELISA was shown to be an independent and significant predictor of poor prognosis.

Harbeck et al. (2002) demonstrated in a multivariate prospective analysis of 3424 primary breast cancer patients that uPA and PAI-1 have not only a clinically relevant prognostic but also predictive impact in primary breast cancer. This paper provides additional evidence supporting the use of uPA/PAI-1 in the clinic by demonstrating how effects of adjuvant systemic therapy differ in patients with high uPA/PAI-1 levels. Node-negative patients with low uPA/PAI-1 may even be candidates for being spared the burden of adjuvant chemotherapy. Similar findings were observed in a pooled analysis of prognostic impact of uPA and PAI-1 in 8377 breast cancer patients (Look et al., 2002). Apart from lymph node status, high levels of uPA and PAI-1 were the strongest predictors of both poor relapse free survival and poor overall survival in the analysis of all patients. For lymph node-negative breast cancer, uPA and PAI-1 measurements in primary tumors may be especially useful for designing individualized treatment strategies.

Leissner et al. (2006) observed that high PAI-1 mRNA expression represents a strong and independent unfavourable prognostic factor for the development of metastases and for breast cancer specific survival in lymph node- and hormone receptor-positive breast cancer patients, whereas uPA mRNA levels did not demonstrate significant independent prognostic value, suggesting that PAI-1 is a stronger prognostic factor than uPA.

Elevated tumor antigen levels of uPA, PAI-1 and uPAR are associated with poor disease outcome, high tumor grade and are conductive to tumor cell spread and metastasis (Schmitt et al., 1997; Reuning et al., 1998; Duffy, 2002; Harbeck et al., 2002). This strong correlation between elevated uPA, uPAR or PAI-1 values on one hand and cancer spread on the other made the uPA system serve as a novel target for the development of new tumor biology-based therapeutics, which either inhibit the enzymatic activity of uPA, reduce the expression of the

components of the uPA system or block binding of uPA to uPAR (Schmitt et al., 2000; Sperl et al., 2001; Muehlenweg et al., 2001; Reuning et al., 2003).
As tumor metastasis is one of the crucial mechanisms in patients suffering from certain tumors, new therapeutic strategies are in development to inhibit tumor cells from invading the ECM and metastasize.

1.2 Antibodies interfering with uPA/uPAR-interaction

A strategy to interfere with the uPA/uPAR-interaction is the use of specific blocking antibodies directed to either uPA or uPAR. In fact, it has *e.g.* been demonstrated in *in vitro* studies that antibodies which inhibit binding of uPA to uPAR, (i) distinctly reduced tumor cell surface-associated plasminogen activation (Magdolen et al., 2001), (ii) inhibited uPA-mediated stimulation of proliferation of ovarian cancer cells (Fischer et al., 1998), (iii) disrupted the uPA-mediated activation of the ERK signalling pathway and promoted apoptosis in breast cancer cells (Ma et al., 2001) and (iv) significantly inhibited the formation of new micro-vascular structures in fibrin matrices by human microvascular endothelial cells (Kroon et al., 1999). In a proof of principle-experiment, the anti-metastatic efficacy of an antibody directed to the uPA binding domain of rat uPAR was evaluated in a syngeneic model of rat breast cancer (Rabbani and Gladu, 2002). For this, rat breast cancer cells, which overexpressed uPAR upon stable transfection, were inoculated into the mammary fat pad of syngeneic female Fischer rats. Subsequently, the antibodies were topically and daily applied for one week. The animals displayed a marked decrease in tumor growth and a significant inhibition of metastasis to retroperitoneal and mesenteric lymph nodes as well as an obvious delay of metastasis to lung, liver and spleen, respectively, when compared to control tumor-bearing animals receiving the same dose of pre-immune rabbit IgG.
Bauer et al. (2005) evaluated the effect of anti-uPAR monoclonal antibodies with and without chemotherapy on primary tumor growth, retroperitoneal invasion and hepatic metastasis *in vivo*. Human pancreatic carcinoma cells were injected into the pancreatic tail of nude mice. It was demonstrated that mice systemically treated with a combination of gemcitabine and anti-uPAR mAb led to about 92% tumor reduction compared to the control or either agent alone the tumor capsule remaining intact.

1.3 Generation of monoclonal antibodies directed to human uPAR

The Clinical Research Group of the Women's Hospital of the Technical University in Munich together with the Institute of Pathology of the TU in Dresden have generated a series of monoclonal antibodies (mAbs) directed against uPAR by using non-glycosylated, recombinant human uPAR (spanning aa 1-284) expressed in *E. coli* as the immunogen (Luther et al., 1997). By flow cytofluorometrical analysis, some of these mAbs (3/12) were shown to bind to native human uPAR present on the cell surface of monocytoid U937 cells. Interestingly, one of these mAbs, IIIF10, efficiently reduced binding of uPA to uPAR, indicating that the epitope detected by mAb IIIF10 is located within or close to the uPA-binding site of uPAR. Subsequent epitope mapping with overlapping synthetic peptides (Luther et al., 1997) revealed that the epitope covers the linear sequence of amino acids (aa) 52-60 of the N-terminal domain I of uPAR **(Figure 2 and 4)**.
The inhibitory properties of mAb IIIF10, together with the other findings described above, strongly suggest that the mAb IIIF10-epitope, aa 52-60 of human uPAR, is located at the uPA-binding site of uPAR.

1.4 Generation of single-chain antibody scFv-IIIF10

1.4.1 Single-chain antibodies

Although mAbs display high specificity and *in vivo* stability, clinical application as therapeutic molecules, especially against solid tumors, has been rather unsuccessful which is in part due to the inability of the mAbs to penetrate into the tumor (Reff and Heard, 2001). Single chain antibodies (scFv), *i.e.* fusion proteins consisting of the antibody's variable heavy (VH) and light (VL) chain connected *via* a flexible linker, represent novel powerful agents for the achievement of targeted therapy, since they are much smaller in size and, thus, more likely to penetrate into the tumor mass **(Figure 3)**.

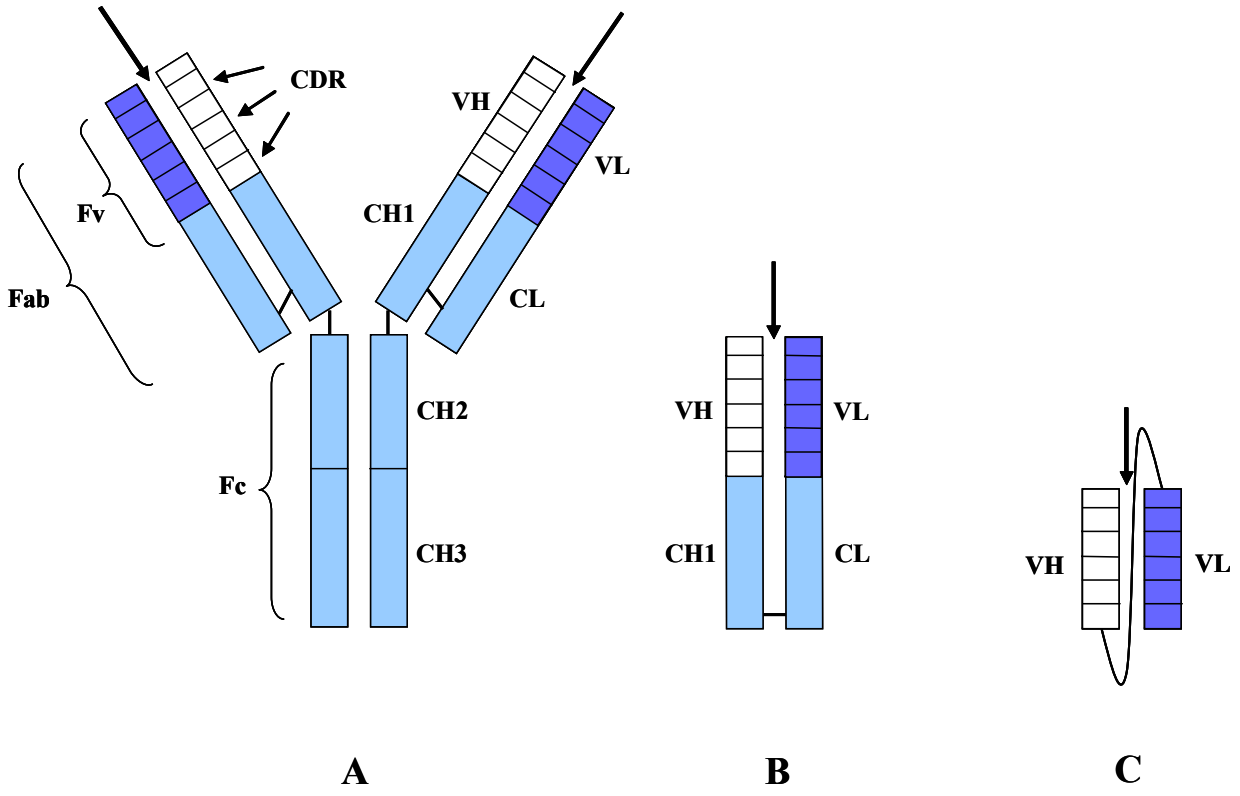

Figure 3: ***Structure of a human antibody and antibody fragments.***
(**A**) A human IgG antibody consists of two heavy and two light chains, each of the polypeptide chains bearing variable regions (VH = variable region of heavy chain, VL = variable region of light chain) being responsible for antigen binding and constant regions (CH = constant region of heavy chain, CL = constant region of light chain) being responsible for the biologic function. The combination of these chains and the amino acid sequences in addition to the six complementary determining regions (CDR) determine the antigen binding activity for a single antibody.
(B) An antibody may be degraded by proteolytic enzymes into two distinct components, the Fab fragment (= fragment antigen binding) with the antigen binding site and the Fc fragment (= fragment crystallisable) which is responsible for cell attachment. A Fab fragment consists of the heavy and light chains with the antigen binding site. The two chains are held together by interaction of the CL and CH1 domains.
(C) The smallest antibody component that has been generated is the single chain fragment (scFv). It consists of the variable regions only (VH and VL = fragment variable = Fv) connected *via* a polypeptide linker. Antigen binding pockets are indicated by an arrow (→).

Sanz et al. (2002) demonstrated as a proof of principle a direct *in vivo* therapeutic effect of an anti-laminin scFv derived from a human phage-display library. This scFv inhibits angiogenesis in the chick embryo chorioallantoic membrane assay and prevents the establishment and growth of subcutaneous tumors in mice either when administered as bolus protein therapy or when produced locally by gene-modified mammalian tumor cells.

Furthermore, modification of the scFv, *e.g.* fusion with additional effector functions such as a prodrug converting enzyme, an antiangiogenic or thrombogenic factor (Helfrich et al., 2000) or a toxin (Fan et al., 2002), can easily be achieved by recombinant technologies. scFv-targeting of molecular processes associated with malignancies may even be utilized to enhance the effects of conventional therapeutics such as chemotherapy and radiation or to modulate immune response (Leath et al., 2004). 5T4 positive leukemia cells were successfully targeted with a fusion protein consisting of an anti-5T4-scFv and human IgG1 Fc domain. This strategy bound 5T4 positive tumor cells and provoked an antibody-dependent cell cytotoxic immune response against the malignant cells (Myers et al., 2002).
Finally, efficient gene therapeutic approaches can be envisioned, because *in vivo* expression of a therapeutic scFv molecule is much more efficient as compared to the synthesis and correct assembly of a heteromeric mAb (Vitaliti et al., 2000). In recent years, an increasing number of reports has in fact demonstrated that scFvs directed to various tumor-associated target molecules (*e.g.* VEGF, laminin, erbB2 or mesothelin) are powerful tools to interfere with tumor growth or block vascularization either when administered as bolus protein therapy or when produced locally by gene-modified tumor cells (Vitaliti et al., 2000; Sanz et al., 2002; Arafat et al., 2002; Fan et al., 2002). Also, members of tumor-associated proteolytic systems such as cathepsin L or membrane-type serine protease 1 (MT-SP1) have been selected as targets for the development of scFv-based therapeutic molecules (Guillaume-Rousselet et al., 2002; Sun et al., 2003).

1.4.2 Characterization of the binding epitope of mAb IIIF10 by employing phage based random peptide libraries

In initial experiments, which are part of another study (Kirschenhofer et al., 2003), the binding epitope of mAb IIIF10 was characterized by employing phage-based random peptide libraries with repertoires of hundreds of millions of unique peptide sequences (Smith and Scott, 1993) to select mAb IIIF10 binding peptides. In a process known as biopanning, mAb IIIF10 was incubated in solution with an aliquot of the peptide-displaying phage libraries, antibody-bound phages were eluted, amplified and again selected for mAb IIIF10 binding. Finally, the peptide-encoding DNA of individual mAb IIIF10-binding phages was sequenced and the corresponding amino acid sequences were deduced. As depicted in **Figure 4**, amino acids present in both phage and uPAR sequences in identical positions confirm the mAb

IIIF10 epitope location on human uPAR: Furthermore, they define residues which are likely essential for mAb IIIF10 binding to its natural target (*e.g.* the SYR-motif).

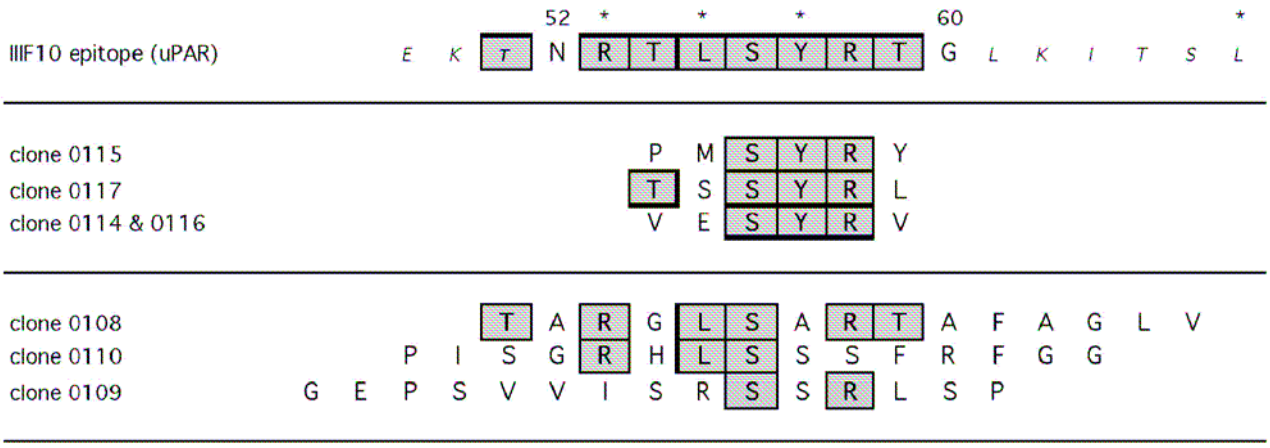

Figure 4. ***Isolation of phage-encoded epitopes using mAb IIIF10: verification of previous peptide mapping studies using uPAR-derived peptides.*** Phage-based random peptide libraries were employed to select mAb IIIF10 binding peptides (for technical details see Böttger, 2001). mAb IIIF10 was incubated in solution with an aliquot of phage libraries ($4.5x10^{10}$ to $2x10^{11}$ phage) displaying 6 or 15mer random peptides. Antibody-phage complexes were captured on magnetic beads (Protein A Dynabeads). Antibody-bound phage were eluted, amplified and again selected for mAb IIIF10 binding (2nd biopanning). Single clones were isolated from the selected phage pools and ELISA-tested for specific binding to IIIF10. Six unique peptide sequences were obtained and aligned to each other and to the epitope sequence of mAb IIIF10 defined on uPAR by an overlapping peptide approach (aa 52-60; Luther et al. 1997). Amino acids present in both phage and uPAR sequences in identical positions are highlighted. Arg53, Leu55, Tyr57, and Leu66 which were previously identified to be essential for uPA/uPAR complexation by an Ala-scan approach (Gårdsvoll et al., 1999) are indicated by asterisks.

1.4.3 Generation of a recombinant scFv-version of mAb IIIF10 and expression in *E. coli*

mRNA of mAb IIIF10-producing hybridoma cells was prepared and the fragments encoding the variable regions of heavy (VH) and light (VL) chain were amplified by RT-PCR using gene-specific primers with added restriction sites. Subsequently, VH- and VL-gene segments were cloned into a phagemid vector (pCantab6, McCafferty et al., 1994) allowing the expression of the variable regions as single chain antibody (scFv). scFv-IIIF10 protein was detected *via* a C-terminal *c-myc* tag sequence using antibody 9E10 (for technical details of

scFv production, secretion and detection see: Kay et al., 1996). To evaluate the binding specificity of scFv-IIIF10, peptides were employed which had been used to map the epitope of mAb IIIF10 on human uPAR (Luther et al., 1997). It was shown that only a peptide whose sequence comprises the complete IIIF10 epitope on uPAR (51-65) is able to prevent both scFv-IIIF10 and mAb IIIF10 from binding to recombinant uPAR. Another peptide with an incomplete epitope sequence (encompassing aa 48-59 of uPAR) is more than 100 times less efficient. Neither of the peptides block binding of control scFv (Z5) to its target protein (unrelated to uPAR, data not shown here).

As tested by flow cytofluorometry, scFv-IIIF10 binds also to native human uPAR, presented on the surface of PMA-stimulated U937 cells. Pre-incubation of scFv-IIIF10 with soluble rec-$uPAR_{1-277}$ prevented binding of scFv-IIIF10 to the cell surface. Control scFvs (D7 and Z5, both directed to uPAR-unrelated epitopes) do not bind to U937 cells (**Figure 5**).

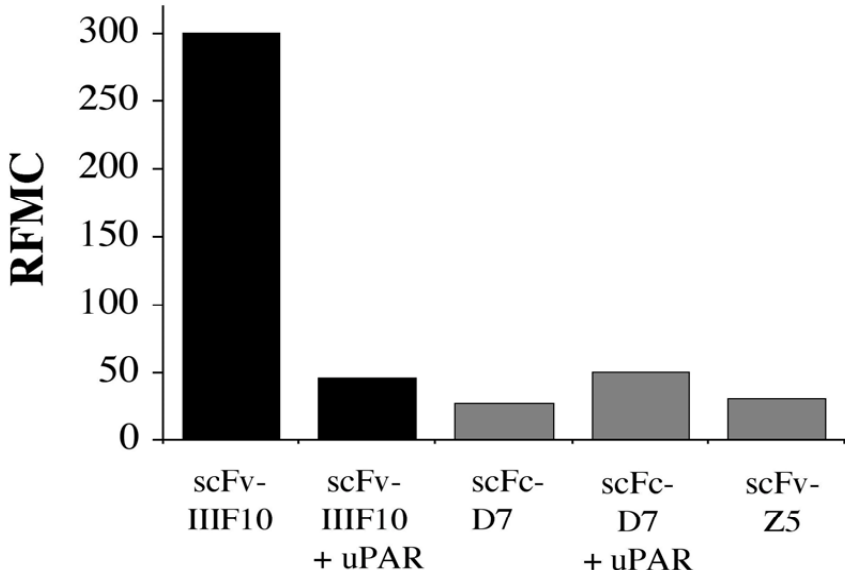

Figure 5. ***uPAR-binding characteristics of scFv-IIIF10 expressed in* E. coli.** scFv-IIIF10 binds also to native human uPAR, presented on the surface of PMA-stimulated U937 cells. Pre-incubation of scFv-IIIF10 with soluble rec-$uPAR_{1-277}$ prevented binding of scFv-IIIF10 to the cell surface. Control scFvs (D7 and Z5, both directed to uPAR-unrelated epitopes) do not bind to U937 cells. Bound scFv was detected by a sequential incubation with the monoclonal anti-*c-myc* antibody 9E10 and Alexa-labelled anti-mouse antibodies. Cell-associated fluorescence was determined by flow cytofluorometry. Fluorescence intensities are expressed as relative fluorescence mean channel (RFMC). For details see Kirschenhofer et al. (2003).

1.5 Clinical application of therapeutic molecules

In the last few years, biotechnology and drug development has made great progress. Antibodies or antibody fragments (*i.e.* Fab-fragments or scFvs) in tumor therapy have entered clinical trials and some are already commonly used in clinical settings.

Trastuzumab (Herceptin®) is a humanized mAb recognizing an epitope on the extracellular domain of HER-2/*neu* (c-erbB-2), a cell-surface protein from the EGFR (epidermal growth factor receptor) family overexpressed in ca. 25% of primary breast cancer patients. Herceptin® is used as a common standard therapy either alone or in combination with chemotherapy in the treatment of women with metastatic breast cancer and HER-2/*neu* overexpression (Adams et al., 2005).

For radioimmune-guided surgery a radio-labeled anti-CEA scFv has been developed. CEA (carcino-embryonic antigen) is a well characterized tumor-associated glycoprotein expressed on endodermally derived gastrointestinal-tract neoplasms and other adenocarcinomas. Injected intravenously before surgery, the radio-labeled anti-CEA scFv locates the tumor tissue in the operative field (Mayer et al., 2000). Some scFvs are currently being examined in clinical trials. In an ongoing phase I trial, 15 patients suffering from recurrent intra-abdominal ovarian or extra-ovarian adenocarcinoma that had failed standard therapy were treated with an intraperitoneally administered adenovirus encoding a scFv against erbB-2. Based on the hypothesis that the intracellular expressed anti-erB-2 scFv prevents erbB-2 mediated signal transduction and induces apoptosis, 38% of the patients had stable disease. Acceptable toxicity was noted with no vector related toxicity experienced (Alvarez et al., 2000). Oh et al. (2004) evaluated the tumor targeting properties of L19, a dimeric $scFv_2$-molecule. ^{123}I-conjugated dimeric L19 selectively localized lung, colorectal or brain carcinomas in a phase I trial.

As antibody therapy often bears the problem of severe side effects, *i.e.* the development of a human anti-mouse immunoglobulin antibody response (HAMA) or human anti-chimeric antibody response (HACA), other niches of new therapeutic drugs and protein engineering are currently explored.

Novel biopharmaceuticals for the treatment of cancer such as small therapeutic molecules have been developed and are now tested in several clinical trials. For example, gefitinib (Iressa®, ZD 1839) is a low molecular weight, synthetic aniline-quinazoline. It is a competitive inhibitor of the intracellular tyrosine kinase of the EGFR receptor. In phase I

trials, oral application of gefitinib is well tolerated and active in patients with non-small-cell lung cancer (NSCLC) and other solid tumors (Herbst et al., 2002). Erlotinib (Tarceva®, OSI-774), is also a quinazoline-based agent which inhibits the intracellular tyrosine kinase of the EGFR receptor. It shows promising results in phase I trials in patients with NSCLC (Hidalgo et al., 2001). For both therapeutic molecules several phase III trial are ongoing comparing their application in combination with chemotherapy (Martin et al., 2006).

Lapatinib (Tycerb®) is an orally-active tyrosine kinase inhibitor (TKI) that targets both c-erbB-receptors (c-erbB-1 and -2). Its dual mode of action distinguishes it from existing TKIs such as gefitinib and trastuzumab, which are single EGFR and HER2/*neu* receptor inhibitors respectively. It is hoped, that dual TKIs may help to address the problem of drug resistance that can arise following treatment with single receptor inhibitors. There is an actual ongoing clinical phase III trial (so called TEACH) evaluating and comparing the efficacy and safety of lapatinib versus placebo in women with early-stage erbB2-overexpressing breast cancer who have completed their primary adjuvant chemotherapy and have no clinical or radiographic evidence of disease (Moy and Goss, 2006). Additionally, in a phase III trial the efficacy and safety of sunitinib (Sutent®), a TKI which inhibits several tyrosin kinase receptors, was reported in patients with gastrointestinal stroma tumor after failure of imatinib, a selective TKI (Demetri et al., 2006).

As promising drug candidates not only for cancer therapy, lipocalins have recently come in the center of attention. Lipocalins represent a family of functional diverse, small proteins comprising 160-180 aa residues and have naturally important biological functions in a variety of organisms (from bacteria to humans) such as storage and transport of vitamins, steroids or metabolic products. Because lipocalins comprise only a single, small polypeptide chain that exhibits a simple set of four hypervariable loops, this protein family provides several benefits for applications in biotechnology and medicine, *e.g* as storage proteins, carrier vehicles for pharmaceutical compounds or as therapeutic drugs (Schlehuber and Skerra, 2005).

In the last few years, lipocalins have been recruited as a scaffold for the design of a new class of engineered binding proteins with antibody-like ligand-binding function termed ”anticalins” (Skerra et al., 2001). Similar to the antibody-antigen-interaction, the mechanism of the anticalin-complex formation with low molecular weight ligands gives way for the generation of novel binding proteins with high affinity and specificity. Anticalins that specifically recognize a tumor surface marker could be useful for drug targeting approaches (Schlehuber and Skerra, 2005).

2. Objective

Human uPAR, which focuses uPA to the tumor cell surface, thereby leading to extracellular matrix degradation and promoting metastasis of tumor cells, represents an attractive target for tumor therapy. Thus, the aim of the present study was to employ a mAb IIIF10-derived genetically engineered scFv to target the uPAR-uPA interaction. For this (i) plasmids should be constructed for the eukaryotic expression of mAb IIIF10-derived single chain antibody (scFv-IIIF10) in a soluble, secreted form or membrane-bound form, (ii) the binding properties of the scFv-IIIF10 should be analyzed *in vitro,* (iii) human ovarian cancer cells (OV-MZ-6#8) should be stably transfected with scFv-IIIF10-encoding expression plasmids and analysed for the effect on primary tumor growth and spread in a *xenograft nude* mouse model in comparison to the vector-transfected control.

3. Materials and Methods

3.1 Materials

3.1.1 Cell lines

The ovarian cancer cell line OV-MZ-6 was established from ascites of a patient with a serous-papillary ovarian carcinoma FIGO IV (Möbus et al., 1992). This cell line was subcloned in the clinical research unit of the ”Frauenklinik der TU München“, characterized and further cultured as OV-MZ-6#8 (Fischer et al., 1998; Lutz et al., 2001).
The lymphoma cell line U937 was established from the pleural effusion of a patient with diffuse lymphoma (ATTC, Rockland, USA).
The chinese hamster ovary cells (CHO-K1) and chinese hamster lung fibroblasts (V79) were purchased from ATTC, Rockland, USA.

3.1.2 *E. coli* bacterial strain

The *E. coli* strain XL1-Blue and K91 (Stratagene, Heidelberg) are facultative anaerob, gram-negative rod shaped bacterial cells which have been used for cloning experiments.

3.1.3 Mammalian expression vector pSecTag2/HygroB

The vector pSecTag2/HygroB (Invitrogen) is a fusion vector encompassing 5749 base pairs **(Figure 6)**. Expression is driven by the strong human Cytomegalovirus (CMV) immediate-early promoter/enhancer, secretion is supported by the murine Ig κ-chain V-J2-C signal peptide (Boshart et al., 1985; Coloma et al., 1992). A polyadenylation signal and transcription termination sequences of the bovine growth hormone stabilize mRNA. The ampicillin resistance gene and hygromycin-B resistance gene ensure selection (Gritz et al., 1983).

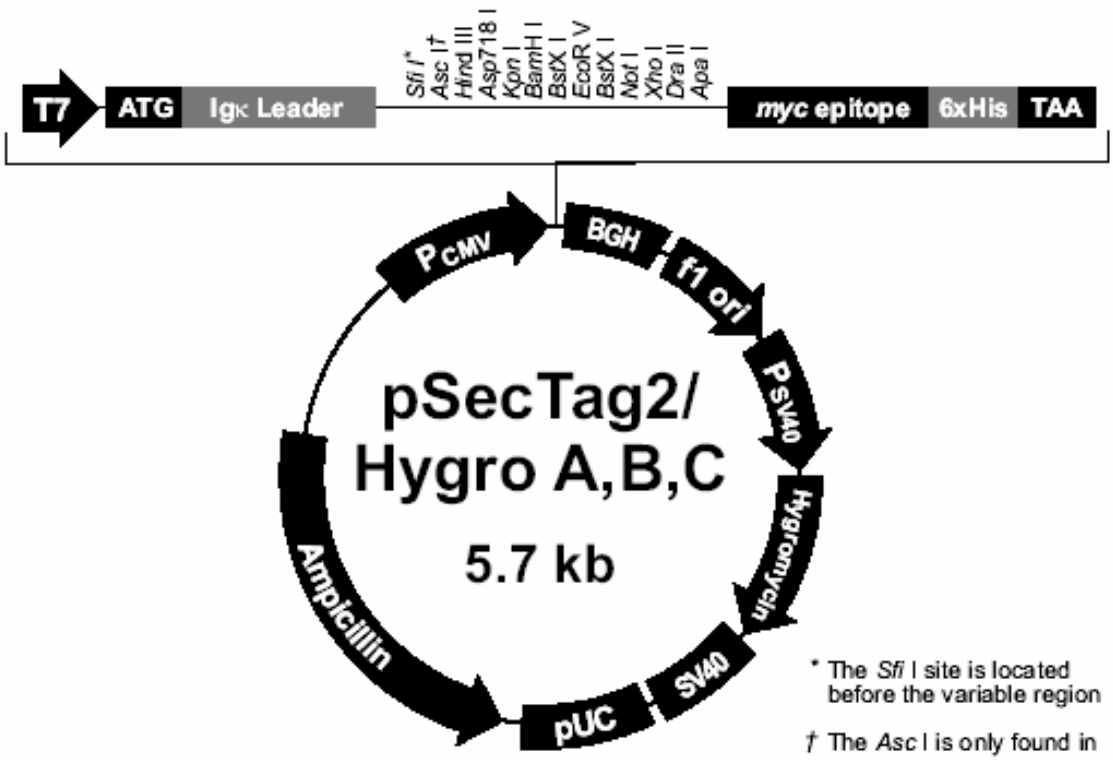

Figure 6: ***Plasmid graphic map of pSecTag2/HygroB***. The vector pSecTag2/HygroB was used as an expression plasmid to express scFv-IIIF10 in different eukaryotic cell lines: Promoter sequence of Cytomegalovirus (CMV), secretion is supported by the murine Ig κ-chain V-J2-C signal peptide, *c-myc* epitope and histidine tag easy protein detection. The ampicillin resistance gene and hygromycin-B resistance gene ensure selection.

3.1.4 Chemicals

The most chemicals used were from Sigma, Munich Germany or Merck, Darmstadt, Germany.

3.1.5 Instruments

autoclave	H+P Labortechnik GmbH, Oberschleißheim
centrifuges	Biofuge Fresco and Varifuge RF, Heraeus Instruments, Osterode; Centrifuge 5402, Eppendorf GmbH, Hamburg
electrophoresis chambers	Biorad, München
ELISA-reader	Titertek Multiscan MCC/340, Labsystems, Finnland
FACScalibur sort cytofluorometer	Becton Dickinson, USA
incubator	RFI-100, Infors HAT Technik, Einsbach
photometer	Ultrospec Plus Spectrophotometer, Pharmacia, Freiburg
pH meter	Knick electronic measuring instruments, Berlin
drying cubicle	WTC, Binder, Tuttlingen
scales	BP 1200, Sartorius, Göttingen Sartorius Basic, Sartorius, Göttingen
semi dry blotting chamber	Fast Blott, Biometra, Göttingen
thermocycler	Perkin-Elmer, Langen
water treatment plant	Purelab Plus UF, USF, Rambach
vortexer	Vortex Genie 2, Bender&Hobein AG, Basel, Switzerland

3.2 Methods

3.2.1 Molecular Biology

3.2.1.1 *E. coli* culture

For generation of eukaryotic expression plasmids *E. coli* bacteria type XL-blue (Stratagene, Heidelberg) were used.

E. coli is a facultative anaerob, gram-negative rod shaped bacterium. It is cultivated in full medium on LB-agar plates or in LB-liquid medium, containing mineral- and ammonium salts, carbohydrates and sugars. *E. coli* XL-blue cells display a generation time of 20 min under optimal conditions and can grow up to $3x10^9$ cells/ml media at a temperature of 37°C.

In most cases, the antibiotic ampicillin is added at a concentration of 100 µg/ml LB-medium for selection of the plasmid. The culture is incubated in sterile polystyrol tubes (Greiner, Frickenhausen) at 37°C over night under 220 rpm rotation.

To isolate bacterial clones transformed with the DNA of interest, cultured bacteria are spread on LB-agar plates containing 100 µg ampicillin/ml medium and incubated over night at 37°C. The next day, single colonies are selected with sterile pipette tips and incubated again in LB medium. For further control of positive clones, the probes are subjected to DNA-preparation and gel electrophoresis.

All culture media, reaction tubes and materials are autoclaved and heat-sensitive substances are sterile filtered.

LB-medium:
10 g/l Trypton, pH 7,0
5 g/l Bacto Yeast Extract
10 g/l NaCl
in 1 l aqua dest.
for agar plates add 1,5% agar

3.2.1.2 Long term storage of *E. coli*

For long term storage, 1.5 ml of a stationary bacterial culture is centrifuged in an Eppendorf tube (13,000 rpm, 30 sec, RT), re-suspended in 15% glycerine and shock frozen in an ethanol bath, then stored at –80°C.

3.2.1.3 Plasmid preparation from *E. coli* (Mini-prep)

For isolation of recombinant plasmid-DNA from *E. coli,* 5 ml of bacterial culture are grown over night (37°C, 220 rpm). The culture is then filled in 1.5 ml Eppendorf tubes and centrifuged at 13,000 rpm for 20 sec. 100 µl Lysis-buffer is added and vortexed for 30 sec at maximum speed, then incubated 10 min at RT. 200 µl of freshly prepared NaOH/SDS solution is added, carefully mixed and incubated at RT for 5 min. The solution turns clear now. 150 µl of cooled KAc-solution is added and incubated on ice for 30 min. The solution precipitates now. After 15 min centrifugation at 4°C 13,000 rpm, the supernatant is collected and 400 µl phenol-chlorophorme is added (P:C:I-extraction), vortexed shortly and centrifuged again at 13,000 rpm at RT. The upper phase is collected and mixed well with 800 µl cooled $EtOH_{abs.}$ (ethyl alcohol precipitation). After incubation at RT exactly for 5 min, the solution is centrifuged at 13,000 rpm at RT for 15 min. The supernatant is discarded and the pellet containing the isolated plasmid DNA is dried in a SpeedVac for 5 min. The pellet is then re-suspended in 90 µl TE and 10 µl RNAse solution (1 mg/ml) and incubated at 37°C for 15 min. 40 µl 4 M LiCl and 260 µl H_2O_{bidest} are added and P:C:I-extraction with 400 µl P:C:I is performed. The upper phase is well mixed with 800 µl $EtOH_{abs}$, incubated on ice for 5 min and centrifuged 15 min at 13,000 rpm at 4°C. The supernatant is discarded and the pellet dried in a SpeedVac for 5 min. For further analysis the pellet is re-suspended in 30 µl $H_2O_{bidest.}$

Lysis buffer:	50 mM Glucose (0.9 g/100 ml) 25 mM Tris-Cl, pH 8.0 10 mM EDTA, pH 8.0
NaOH/SDS-solution:	1% SDS 0.2 N NaOH
KAc-solution:	3 M potassium acetate, pH 4.8
RNAse-solution:	1 mg/ml in 50% glycerine 1:10 diluted in TE buffer (TE: 10 mM Tris-Cl, pH 8.0 and 1 mM EDTA, pH 8.0)
P:C:I	phenol:chlorophorm:isomylalcohol, 25:25:1

3.2.1.4 Plasmid preparation from *E. coli* for DNA-sequencing

For sequencing, DNA was purified with the High Pure Plasmid Isolation Kit (Quiagen, Hilden) according to the manufacturer's manual. All sequencing was performed by Toplab in Martinsried (Munich, Germany).

3.2.1.5 Restriction analysis of DNA-fragments

Restriction analysis is a central method in cloning experiments to produce specific DNA-fragments of interest depending on the endonuclease being used. Restriction endonucleases can hydrolyse DNA specifically under optimal buffer conditions, which are given by commercial companies.
A restriction analysis is typically performed in a sterile Eppendorf tube with a reaction volume between 10 µl and 100 µl. 1/10 Vol. 10x reaction buffer and DNA are added and filled up to the end-volume with H_2O_{bidest}. 2 to 54 units of endonuclease per µg of DNA are used. The added solution should not exceed 10% of the end volume, as the glycerine of the storing buffer can disturb the reaction. Then the reaction is performed within a minimum of 1 h at 37°C.

3.2.1.6 Ligation of DNA fragments with T4-ligase

For ligation vector DNA and the DNA fragment, treated with restriction endonucleases described above, are mixed in a 1:5 - 1:10 ratio in a reaction end volume of 21 µl. 4 µl 5x ligase buffer and 3 µl 10 mM ATP are added. After adding 1 µl T4-DNA-ligase, the solution is incubated at 25°C for 3.5 h. The resulting ligation product is then used for transformation in *E. coli*.

5x ligation buffer	250 mM Tris/HCl, pH 7.6 50 mM $MgCl_2$ 15% polyethylene glykol (8,000 g/mol) 5 mM DTT

3.2.1.7 Transformation of plasmid DNA in *E. coli*

To transport DNA into bacteria, a so-called transformation is performed. Plasmid DNA is brought to the surface of bacteria and transferred into the bacteria *via* heat shock. Competent *E. coli* are slowly defrosted on ice for 20-30 min. 8 µl of ligation solution are mixed with 42 µl TE on ice and 100 µl competent *E. coli* are added and incubated on ice for 25 min, then heat-shocked at 37°C (1 min 45 sec) and incubated on ice again for 3-5 min. 1 ml TY-media is added and mixed gently, then incubated at 220 rpm at 37°C for 1 h and subjected to centrifugation at 5,000 rpm for 1 min at RT. The supernatant is discarded and the pellet re-suspended in 200 µl LB-medium. Cells are then evenly spread on LB-agar plates containing 100 µg/ml ampicillin and incubated at 37°C over night to grow selected clones containing the plasmid of interest.

2x TY-medium: 16 g/l Trypton, pH 7.0
10 g/l yeast extract
5 g/l NaCl

3.2.1.8 Polymerase chain reaction (PCR)

PCR is a method to amplify specific DNA-fragments (templates). There are three different steps in this process: denaturing, annealing and elongation. DNA is denatured at a temperature of 94°C, leading to complete separation of both DNA strands. The added oligonucleotide primers are hybridised to the single strand template-DNA with an annealing temperature of about 55°C, depending on the primer. At a temperature optimum of 72°C, the Taq-polymerase is then working to elongate the primers. This results in a double-strand DNA which is an exact copy of the template. As the Taq-polymerase is working on both separated strands of the template-DNA, the amount of template-DNA is theoretically doubled in one single cycle. The specificity of the DNA-sequence is given by (commercially synthesized) primers, which usually consist of 15-21 bp.
The samples are placed in a thermocycler and go through the following cycle profile, then stored at -20 °C for further analysis:

1x	denaturation template at 94°C for 5 min
10x	denaturation at 94°C for 30 sec
	annealing at ca. 55°C for 30 sec
	elongation at 72°C for ca. 1 min (ca. 1,000 bp per min)
20x	denaturation at 94°C for 30 sec
	annealing at 55°C for 30 sec
	elongation at 72°C for 1 min
1x	prolonged elongation at 72°C for 7 min

To amplify fragments of over 1.5 kb size, *i.e.* "long range PCR", the Expand High Fidelity PCR Kit from Roche was used according to the manufacturer`s manual.

Standardized PCR mix (end volume 50 µl):

10x buffer with $MgCl_2$	4.5	µl
dNTP	5.0	µl
Primer up	5.0	µl
Primer do	5.0	µl
DNA (0.1 µg)	x	µl
Taq-Polymerase (10 U/µl)	0.25	µl
H_20_{bidest}	x	µl

The following primers were used:

TF-HIII	5´-TTG TAT AAG CTT TCA GGC ACT ACA AAT ACT GTG-3´
TF-B	5´-TTG TAT GGA TCC GCT TTC TCC TGG CCC ATA CAC-3´
scFv-HIII	5´-TTG TAT AAG CTT CAG GTG CAA CTG CAG CAG TC-3´
scFv-B	5´-TTG TAT GGA TCC CCG TTT GAT TTC CAG CTT GG-3´
TCD-do	5´-TTA TTG GAT CCA GAG AAA TAT TCT ACA TCA T-3´
TCD-up	5´-TTA TTC TCG AGT TAT GAA ACA TTC AGT GGG G-3´
GPI-do	5´-TTA TTG GAT CCA ACC ACC CAG ACC TGG ATG-3´
GPI-up	5´-TTA TTC TCG AGT TAG GTC CAG AGG AGA GTG-3´
Xho-scFv	5´-TTG TTT CTC GAG CCC GTT TGA TTT CCA GCT-3´

The following primers were used for nested PCR:

2B-DO 5´-TAC TGC TGC TCT GGG TTC CAG-3´

2B-DO2 5´-G TTC CAG GTT CCA CTG GTG AC-3´

2B UP 5´-TCG ACG GCG CTA TTC AGA TCC-3´

2B-UP2 5´-GA TCC TCT TCT GAG ATG AGT T-3´

3.2.1.9 RT-PCR

RT-PCR analysis was used to test for transcription of the expression cassette encoding soluble, secreted scFv-IIIF10 in OV-MZ-6#8 and CHO cells. $6x10^6$ cells were treated with Trizol® reagent (Life Technologies) according to the manufacturer's manual. One µg RNA of each cell line was isolated and reverse transcribed with oligo(dT) as primer using the 1st strand cDNA Synthesis Kit for RT-PCR (AMV, Roche) and amplified by nested PCR by scFv-IIIF10 specific primers. OV-MZ-6#8 cells stably transfected with the empty vector pSecTag2/HygroB, OV-scFv RNA reverse transcribed without adding oligo(dT) and RT-PCR without RNA all served as controls. A control RT-PCR of the house-keeping gene G6PDH (glucose-6-phosphate dehydrogenase gene, h-G6PDH Housekeeping Gene Set, Roche) was additionally performed to demonstrate the integrity of the RNA.

Standardized PCR mix (end volume 25 µl):

Tris-HCl 10 mM, pH 8.3
KCl 50 mM
MgCl 1.5 mM
dNTP 250 µM
Primer up 1 µM
Primer do 1 µM
cDNA (2 µl)
Taq-Polymerase (1.25 U) (Sigma-Aldrich, Inc.)

Each of the samples and controls were amplified as follows:

1st PCR

1. amplification with primers D87 + U648
2. amplification with primers D267 + U590

2nd PCR

1. amplification with primers D267 + U648
2. amplification with primers D333 + U590

The samples were placed in a thermocycler and went through the following cycle profile, then stored at -20 °C for further analysis:

1x	denaturation template at 94°C for 5 min
25x	denaturation at 94°C for 30 sec
	annealing at 50°C for 30 sec
	elongation at 72°C for 30 sec
1x	prolonged elongation at 72°C for 7 min

The following primers were used:

scFv D87 5´-CAC AAG CTA CGA TAT AAA TTG GG-3´

scFv D267 5´-GAA CTC TGC AGT CTA TTT CTG TG-3´

scFv D333 5´-GAC CAC GGT CAC CGT CTC CTC AG-3´

scFv U590 5´-CCT GTG AAG CGA TCA GGG ACT CC-3´

scFv U648 5´-CAG GTC TTC AGA TTG CAC ATT GC-3´

3.2.1.10 Proteinase K digestion

PCR products are digested by the so called proteinase K, to remove the Taq-polymerase still attached to the DNA. After P:C:I-extraction, 10 µl 10x proteinase K-buffer and 2 µl proteinase K (5 mg/ml) are added to 90 µl PCR-product and incubated for 30 min at 37°C. The proteinase K is then deactivated at 65°C for 10 min and incubated on ice for 5 min. In the end, the DNA is subjected to P:C:I extraction and ethyl alcohol precipitation and the product is stored at –20°C until further analysis.

10x proteinase K-buffer	100 mM Tris/HCL, pH 8.0 50 mM EDTA 5% (v/v) SDS

3.2.1.11 DNA gel electrophoresis

DNA gel electrophoresis is a tool to control the purity and size of the DNA-fragment. For a 1% gel, 0.3 g agarose and 30 ml TBE are mixed and heated in the microwave until the agarose is soluble in TBE. Then the solution is cooled down and 1.5 µl ethidium-bromide is added for visual detection. The DNA fragments, loaded with a 6x DNA loading-buffer (2 µl on 10 µl DNA), together with a marker (1 kb or 100 bp according to the fragment's size) will migrate across the gel within an electric field at 80 Volt for 30 min. Large molecules/DNA-fragments will move slower through the gel than smaller fragments and separation of the different fragments takes place according to their size. The DNA is then visible as a band under UV-light (316 nm) and a photo is taken for the archive.

3.2.1.12 Isolation of DNA from agarose-gels ("freeze and squeeze")

For isolation of DNA fragments from agarose-gels, the corresponding band is cut out with a scalpel and treated with the "freeze and squeeze"-method (Tautz 1983). The piece of gel is incubated in 0.3 M NaAc, 0.1 mM EDTA, pH 7.0 for 20 min, then dried carefully with a tissue paper and put in a filter-Eppendorf tube (Costar, Corning Incorp., NY, spin X centrifuge tube filter, pore size 22 nm, cellulose acetat). After three times freezing at –80°C for 15 min and de-freezing at 37°C for 15 min, the piece of gel is centrifuged at 9,000 rpm for 10 min at RT. The filter is discarded, the volume in the tube measured and the same volume of P:C:I added, the tube is then vortexed and centrifuged at maximum speed for 5 min. A new Eppendorf tube is filled with the supernatant and 1/50 volume $MgCl_2$ in 10% acidic acid is added. Thereafter 3x Vol. cooled 100% EtOH is added and incubated at –20°C for 20 min, then centrifuged at maximum speed at 4°C for 10 min. The resulting pellet is washed with 70% EtOH and centrifuged at maximum speed for 5 min (4°C). The supernatant is discarded and the pellet dried. The pellet containing the DNA from the gel can then be diluted in H_2O_{bidest} or TE for further analysis.

TE-buffer	10 mM Tris/HCl, pH 8.0 1 mM EDTA

3.2.2 Protein chemical methods

3.2.2.1 Solid phase binding assay with rec-uPAR$_{1-277}$

96-well immunoassay plates (MaxiSorp™, Nunc, Denmark) are coated over night at 4°C with 100 µl/well of purified recombinant human soluble uPAR (rec-uPAR$_{1-277}$; 0.5 µg/ml, Magdolen et al. 1995) diluted in MOPS buffer. After washing the plates three times with washing buffer, excess protein binding sites are blocked by incubating the plates with blocking solution (200 µl/well) for 1 h at RT. Thereafter, the plates are incubated over night at 4°C with 100 µl/well of either cell culture supernatant as a negative control, purified fractions of the scFv-IIIF10 or TF$_{1-214}$ in serial dilutions. After washing three times with washing buffer and incubating for 1 h with Ni^{2+}-NTA peroxidase reacting with (His)$_6$-tagged proteins, the plates are washed again and peroxidase reaction is initiated by addition of 100 µl/well of chromogenic substrate (TMB; 3,3´,5,5´-tetramethylbenzidine; KPL, Gaithersburg, Maryland, USA). The enzymatic reaction is stopped with 0.5 M H_2S0_4 and the absorbance measured in a microtiter plate reader at 450 nm.

MOPS buffer	MOPS	100 mM
	NaCl	150 mM
	$CaCl_2$-$2H_2O$	5 mM
washing buffer	PBS/0.05% Tween 20	
blocking solution	PBS/2% BSA	

3.2.2.2 SDS polyacrylamide gel electrophoresis (SDS-PAGE)

SDS-PAGE is a tool to resolve proteins individually in an electric field. Using a discontinuous buffer system that incorporates SDS in the buffer, the proteins are denatured by heating in a buffer containing SDS and a thiol reducing agent such as ß-mercaptoethanol. The resulting polypeptides take a negative charge and migrate across the gel to the anode resulting in different single bands according to their size. In the stacking and resolving gel respectively, different buffers and electrode solutions are used. Samples are compressed into a thin starting

band and proteins are finely resolved and separated individually. Using polyacrylamide gels, one can adjust the size of the pores to the size of the analysed protein, depending on the acrylamide concentration and the amount of polymers.

For SDS-PAGE two gels are prepared: a stacking gel (5%) and a resolving gel (12%). First, the resolving gel is filled between two glass plates (separation distance 1.5 mm). The reaction is initiated by addition of TEMED. Then, the stacking gel is added on top and a comb is used to separate the slots for the different probes.

Prior to loading the gel, the probes are mixed 1:2 with SDS reducing sample buffer and heated at 95°C for 3 min. As a standard, the Molecular Weight Standard, Low Range (Bio-RAD, Krefeld, Germany) is used. Electrophoresis is performed in running buffer under the constant voltage of 150 V. After that, the gel is incubated in fixation solution for 30 min shaking, stained with Coomassie Blue G-250 for 1 h and de-stained with 10% acetic acid for 2 h.

SDS-polyacrylamide resolving gel buffer (12%)

acrylamide/Bis 40% (ml)	2.4
1.5 M Tris/HCl, pH 8.8 (ml)	2
10% SDS (µl)	80
H_2O_{bidest} (ml)	3.46
APS 10% (µl) *	50
Temed (µl) *	10

SDS-polyacrylamide stacking gel buffer (5%)

acrylamide/Bis 40% (ml)	3.6
0.5 M Tris/HCl, pH 6.8 (ml)	7.2
10% SDS (µl)	280
H_2O_{bidest} (ml)	17.2
APS 10% (µl) *	50
Temed (µl) *	10

(*) added immediately prior to pouring the gel

running buffer 14.4 g/l glycine
3.0 g/l Tris base, pH 8.3
1.0 g/l SDS

SDS reducing sample buffer	3.55 ml H_2O_{bidest} 1.25 ml 0.5 M Tris-HCl, pH 6.8 2.5 ml glycerol 2.0 ml 10 % SDS 0.5 ml ß-mercaptoethanol
SDS non-reducing sample buffer	SDS reducing sample buffer without ß-mercaptoethanol
Fixation solution	40% EtOH 10% acetic acid
Coomassie staining	0.1% Coomassie Brilliant Blue G-250 10% acetic acid

3.2.2.3 Western blot

Western blotting is used to transfer proteins from a gel onto a blotting-membrane. After immobilizing the proteins on the membrane, they can then be detected using specific antibodies in combination with different detection methods. To detect the presence of the different histidine-tagged variants of scFv-IIIF10 and TF in cell culture supernatant as well as on the cell surface, semi-dry Western blotting technique is used.

The sample is mixed with an equal volume of SDS reducing sample buffer and incubated for 5 min at 95°C, then loaded into the wells of a 12% SDS polyacrylamide gel. As a standard, BenchMark™ Prestained Protein Ladder (Gibco, Karlsruhe, Germany) is used. After electrophoresis the gel is incubated in 5% blotting solution and a "sandwich" consisting of three layers of Whatman filter paper soaked with 20% methanol in 50 mM boric acid pH 9.0, the PVDF membrane, the gel, three layers of Whatman filter paper soaked in blotting solution, is arranged and subjected to blotting (Fast Blott, Biometra) at 50 V, maximum 5 mA/cm^2 for 2 h. Then, the membrane is blocked in PBS/5% skim milk powder (Merck, Darmstadt, Germany) for 1 h at RT to reduce unspecific binding.

Blots are probed with a mAb directed to a $(His)_5$ epitope (Penta-His ab, Qiagen, Hilden, Germany) diluted 1:1,000 in PBS/1% skim milk powder at 4°C over night. After washing for 2x1 min, 1x15 min, 2x5 min with PBS/1% skim milk powder, the membrane is incubated with a peroxidase labeled secondary anti-mouse antibody (Qiagen) diluted 1:5,000 in PBS/1% skim milk powder and washed again. Finally, the antigen-antibody reaction is visualized using the "ECL Western Blotting Detection Reagent" (Amersham Pharmacia, Freiburg, Germany) according to the manufacturer's manual.

Blotting solution	5% methanol 50 mM boric acid, pH 9.0

3.2.2.4 Stripping of Western blot membranes

To subsequently apply different antibodies to Western blot membranes, membranes can be stripped. First the membrane is incubated in 100 ml stripping solution with 830 µl ß-mercaptoethanol at 50°C for 30 min in a shaker, then washed 6x with H_2O_{bidest} and incubated over night at 8°C in net-gelatine. The next day, the membrane can be re-used for applying other antibodies.

Stripping solution	65 mM Tris-HCl pH 6.8	13 ml (0.5 M)
	2% SDS	20 ml (SDS 10%)
	H_2O_{bidest}	ad 100 ml

3.2.2.5 Purification and concentration of scFv-IIIF10 and TF_{1-214}

Purification of $(His)_6$-tagged proteins from cell culture supernatants is performed using Ni^{2+}-NTA affinity chromatography. This method is based on the interaction of $(His)_6$-tagged proteins with the nickel ion of a tetra-dentate chelating adsorbent.
250 ml of cell culture supernatant from OV-MZ-6#8 cells, CHO-cells and V79-hamsterfibroblasts expressing soluble $(His)_6$-tagged scFv-IIIF10 and sTF_{1-214} are collected from cell culture flasks every second day and then subjected to 1 ml Ni^{2+}-NTA columns (Qiagen).
Purification of the recombinant proteins is performed under native conditions. 1 ml columns are loaded with 0.8 ml Ni^{2+}-NTA and equilibrated with 10 ml PBS pH 7.4. The pH of the cell culture supernatant is checked (pH=7.4) before loading the columns. After a washing step with PBS pH 7.4, the $(His)_6$-tagged proteins are eluted with 0.5 ml PBS/Imidazol 200 mM in 1 ml Eppendorf tubes and stored at -20°C for further analysis.

3.2.2.6 FACS analysis

Binding of purified scFv-IIIF10 from eukaryotic cells to human uPAR was tested by flow cytofluorometry. $5x10^6$ human monocytic U937 suspension cells were stimulated with 1 mM

(final concentration) of PMA (phorbol 12-myristate 13-acetate 4-0 methyl ether, Sigma, Taufkirchen, Germany) for 72 h at 37°C, which makes them adherent and leads to a 10-fold over-expression of cell surface-associated human uPAR. After washing with PBS, cells were incubated with 50 mM glycine/100 mM NaCl, pH 3.0, for 1 min at RT to dissociate endogenous receptor-bound uPA. The acidic buffer was neutralized with an equal volume of 500 mM HEPES/100 mM NaOH, pH 7.5. After a washing step with PBS, cells were re-suspended in PBS/0.1% BSA (10^7 cells/ml) for further analysis. To optimize the fluorescent labelling protocol, the amount of secondary antibody necessary was tested in different concentrations. In order to find a concentration of the second antibody resulting in an acceptable background, $2.5x10^5$ monocytic U937 cells were probed with either 800 ng of control anti-*myc* or *β-Gal* antibodies and different concentrations of ALEXA 488 goat-anti mouse (Molecular Probes) as a secondary antibody. U937cells with PBS/BSA 1% without addition of secondary antibody served as a negative control. Adding secondary antibody ALEXA 488 goat-anti-mouse IgG in the range of 1 µg to 2 µg, *i.e.* about two times the concentration of the primary antibody showed a fluorescence intensity with an acceptable background **(Figure 7)**.

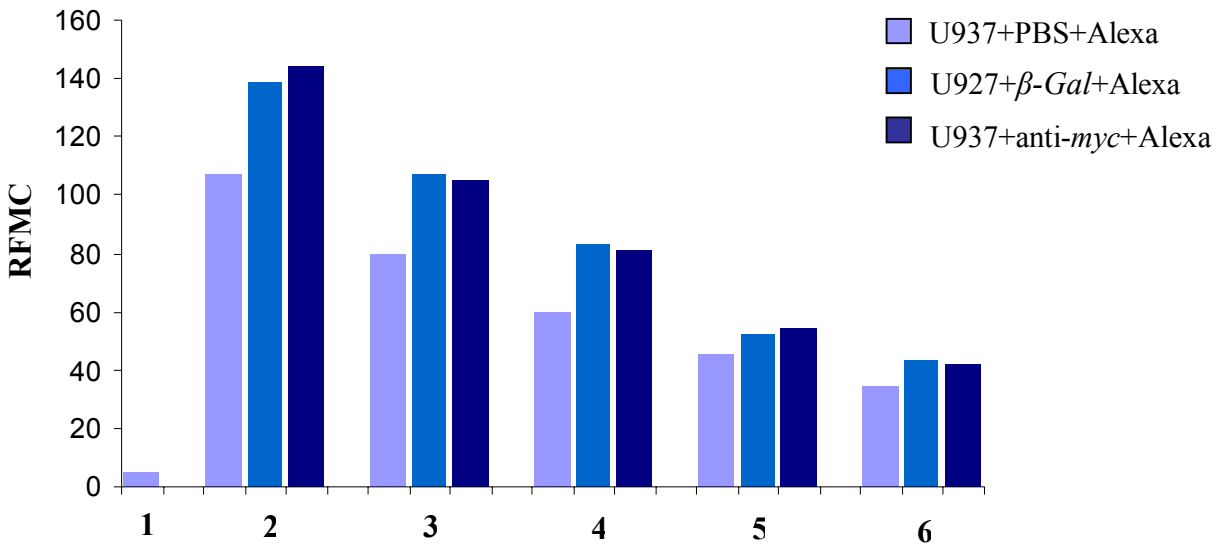

Figure 7: ***Determination of optimal secondary antibody concentration.*** To optimize the fluorescent labelling protocol, $2.5x10^5$ U937 were probed with 800 ng of anti-*myc* and *β-Gal* antibody and different concentrations of ALEXA 488 goat-anti mouse. (1) U937 with PBS/BSA 1% serving as a negative control. (2) 4 µg ALEXA 488. (3) 2 µg ALEXA 488. (4) 1 µg ALEXA 488. (5) 400 ng ALEXA 488, (6) 200 ng ALEXA 488.

Binding of purified scFv-IIIF10 from hamster cells to human uPAR was tested by incubating $2.5x10^5$ U937 cells with eluates of the soluble scFv-IIIF10 and sTF_{1-214} columns for 20 min at RT. Anti-*myc*-antibody (0.8 µg, Invitrogen) directed against the C-terminal *c-myc* epitope of scFv-IIIF10 followed by the fluorescence labeled secondary antibody ALEXA 488 goat-anti-mouse (1.6 µg, Molecular Probes) was added and incubated for another 20 min at RT. Prior to FACS analysis propidium-jodide was added in order to be able to exclude dead cells from analysis. Single cell-associated fluorescence was then quantified by FACS analysis using the FACScalibur cytofluorometer (Becton Dickinson). Autofluorescence of anti-*myc* antibody and Alexa 488 goat-anti-mouse was determined in the absence of the purified protein. sTF_{1-214} eluate was used as a non-binding control protein.

For specificity testing, one sample of scFv-IIIF10 eluate was simultaneously incubated with recombinant human pro-uPA (4 µg) for 30 min. Fluorescence intensities were expressed as relative fluorescence mean channel (RFMC).

3.2.3 Cell biology

3.2.3.1 Cell culture

OV-MZ-6#8 cells are adherent cells and grow as a monolayer attached to the bottom of the culture flask. They are cultured under standard conditions (37°C, 5% CO_2, humid atmosphere) in DMEM (Dublecco´s Modified Eagle Media), containing 10 mM HEPES, 10% fetal calf serum (FCS), penicillin/streptomycin (100 µg/ml, 100 U/ml) (all from Gibco, Karlsruhe, Germany) and 0.27 mM asparagine, 0.55 mM arginine (Sigma, St.Louis, USA). Cells are subcultured 3 times a week. By adding splitting solution EDTA/PBS 1:20 and incubating the adherent cells for 2 min at 37°C, the washed cells detach from the culture flask and are then centrifuged 3 min at 940 rpm, RT. The supernatant is discarded and cells are re-suspended in PBS. According to the amount of cells needed, cells are spread into new culture flasks.

For experiments 70-80% confluent cells between passages 2 to 9 are used. Every second month, cells are tested for mycoplasma contamination using PCR.

U937 cells are monocytic suspension cells cultured under standard conditions in RPMI media containing 10 mM HEPES, 2 mM L-glutamine, 10% FCS and penicillin/streptomycin (100 µg/ml, 100 U/ml). The cells are maintained in culture by transfer of 1 ml cell suspension in 30 ml fresh culture media once a week. For FACS experiments, the cells are stimulated with PMA which make them adherent and lead to a 10 fold over expression of uPAR on the cell surface.

For long term storage, cell pellets of approximately 10^6 cells are re-suspended in 1 ml DMSO/FCS (1:10) in kryo-tubes and shock frozen in an ethanol bath, then stored at –80°C in nitrogen.

3.2.3.2 Stable transfection of V79, CHO and OV-MZ-6#8 cells

For stable transfection of plasmids, SuperFect™ (QIAGEN, Hilden, Germany) was used. Cells were grown in a 6-well plate until they reached 40-60% confluence. 10 µl of SuperFect™ (QIAGEN, Hilden, Germany) and 100 µl of DMEM (without serum and antibiotics) were dissolved.

Two µg DNA of various eukaryotic expression plasmids (pSecTag2/HygroB-scFv-IIIF10, pSecTag2/HygroB-scFv-IIIF10$_{his}$, pSecTag2/HygroB-scFv-IIIF10-GPI, pSecTag2/HygroB-scFvIIIF10-TCD, pSecTag2/HygroB-sTF and empty vector pSecTag2/HygroB) were dissolved each in 100 µl DMEM (without serum and antibiotics), mixed well and incubated for 10 min at RT. DNA- and SuperFect™- solution were mixed together and incubated for 10 min to allow complex formation. Then, 300 µl FCS-free cell culture medium were added to the SuperFect™-DNA mixture and the total volume was transferred immediately to the cells that were previously washed with PBS (Gibco, Karlsruhe, Germany). After 3 h of incubation at 37°C, cells were washed 3 times with PBS and further cultured in 10% FCS DMEM. The day, cells reached 80-90% confluence, the selection of stably transfected cells was started using cell culture medium containing 250 µg/ml hygromycin B (HygroGold, InvivoGen, San Diego, USA). Selected cells were then kept in culture for further investigation.

3.2.3.3 Phage-display

3.2.3.3.1 Phage amplification and purification

Different M13-phages (0108, 0109, 0110, 0114, 0115, 0117 binding to mAb-IIIF10 and an irrelevant non-binding phage as a negative control) were kindly provided by Dr. Volker Böttger, Wilex AG, Munich. For phage amplification, 1 µl of phage suspension was incubated with 200 µl K91 *E. coli* bacteria, grown to late log phase ($OD_{600nm} \approx 1$), for 15 min at 37°C without shaking followed by another 15 min with shaking at 200 rpm. The infected bacteria were then transferred to a 50 ml Falcon tube (polypropylene) with 10 ml 2x TY medium, supplemented with 20 µg/ml tetracycline (Smith et al., 1993) and grown for 24 h at 37°C, gently shaking (200 rpm). The suspension was then centrifuged at 3,400xg and 4°C for 30 min and the supernatant transferred to a new 50 ml Falcon tube. 100 µl were kept for titration. For phage purification/precipitation, 2 ml of PEG/NaCl solution were added to the 10 ml supernatant, mixed by inverting the tube several times and incubated on ice for at least 2 h. The suspension was then centrifuged at 3,400xg and 4°C for 30 min, the supernatant discarded and the phage pellet re-suspended in 1 ml aqua dest. Transferred to a 1.5 ml Eppendorf tube, suspension was spun at 10,000xg and 4°C for 10 min to remove remaining bacteria and cellular debris. The phage supernatant was transferred to a new 1.5 ml tube and 200 µl PEG/NaCl added for a second precipitation, mixed and left on ice for 1 h, then spun at

10,000xg at 4°C for 10 min. The supernatant was poured off, the tube re-spun briefly and the remaining supernatant removed with a pipette. The phage pellet was then re-suspended in 1 ml TBS, filtered through a 0.2 µm syringe filter and stored at 4°C.

PEG/NaCl	100 g polyethylene glycol 8,000 117 g NaCl 475 ml H_2O, then autoclaved

3.2.3.3.2 Phage-titration

To determine the concentration of phage after amplification, phage titration is carried out. It is based on counting bacterial colonies, which had been infected with a dilution series of phage, making them grow on tetracycline selection plates. Therefore, only transforming units, *i.e.* infectious phage particles, are determined.

LB-agar plates were prepared with 20 µg/ml tetracycline and dried with open lid under sterile conditions for several hours. A grid with 1.5x1.5 cm squares (4x4 for a 9 cm petri dish) was drawn on the bottom of each plate. 45 µl TBS were filled into each well of a 96-well microtiterplate and 5 µl of the purified phage added to the first well. Properly mixed by aspirating and dispensing at least ten times, 5 µl were transferred into the next well and continued until 10 serial dilutions had been made. The pipette tip was changed to minimize unwanted carry over of phage. Then 155 µl log phase K91 bacteria were added to each well, mixed carefully with the phage dilution and incubated at 37°C for 30 min. The bacteria in the wells were re-suspended and 10 µl of each dilution spotted onto the prepared agar plate. Waiting until the liquid had completely disappeared the lid was closed and the plate incubated face down over night at 37°C. The colonies at dilutions with well separated clones were counted and the phage concentration of the starting material calculated (**Figure 8**).

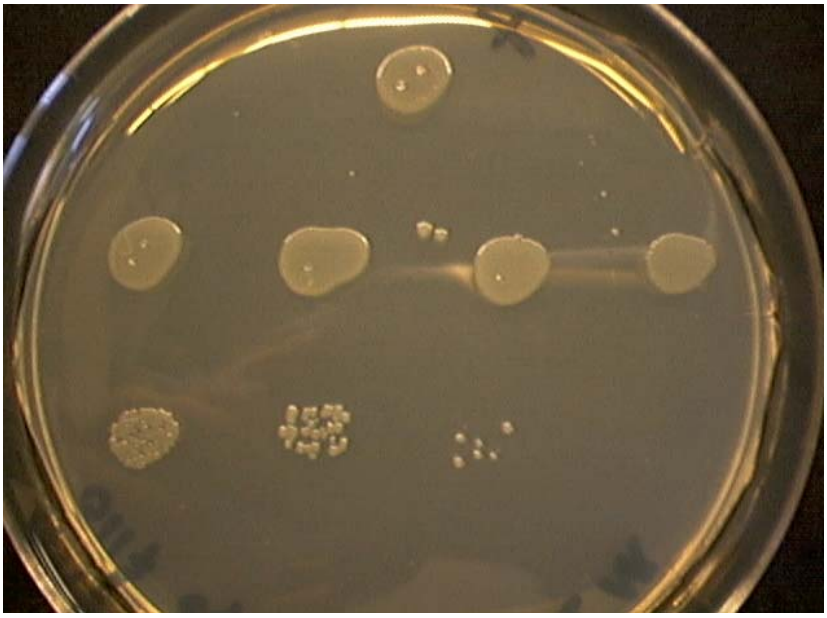

Figure 8: ***Phage titration on agar-plates***. To determine concentration of phages after purification and amplification, phages were titrated and serious dilutions incubated on LB-agar plates with 20 µg/ml tetracycline over night. Then single colonies were counted and phage concentration was calculated.

3.2.3.3.3 Solid phase binding assay phage ELISA

The different purified and amplified phages were then tested in a solid phase binding assay, using mAb-IIIF10 as the solid binding phase, in serial dilutions to verify specificity.

A 96-well microtiter plate was coated with 100 µl mAb-IIIF10 per well (1 µg/nl in PBS, dilution 1:1,000) and incubated over night at 4°C. As a negative control, wells were coated with anti-TF VI C7 (in PBS, 1:500) as a non-binding protein. An irrelevant, non-binding phage served as a second negative control.

The wells were washed with PBS and blocking solution (200 µl PBST-M: PBS, 0.1% Tween 20, 5% milk powder) was added for 30 min to reduce unspecific binding, and washed again. 100 µl phage supernatant diluted in PBST-M (*i.e.* 1:2, 1:20, 1:200) were added and incubated for 2 h at RT, then washed again.

100 µl/well (dilution 1:1,000 in PBST-M) of horseradish peroxidase-labeled anti-M13 monoclonal antibody were added and incubated for 1 h at 37°C. α-M13-HRP is a monoclonal antibody generated from mouse ascites, which is directed against the surface of M13 phages (Amersham Pharmacia Biotech, UK). After washing, phages bound to the mAb-IIIF10 were

visualized by incubating with 100 µl/well of chromogenic substrate (TMB, KPL, Gaithersburg, Maryland, USA). The enzymatic color-reaction was stopped with 1 M H_2S0_4 and absorbance measured in a microtiter plate reader at 450 nm. **Figure 9** below shows the different phage binding to mAb-IIIF10 in comparison to the non-binding control-phage. Phages neither bind to anti-TF VI C7 coated wells nor does the control phage bind to mAb-IIIF10 as a second negative control.

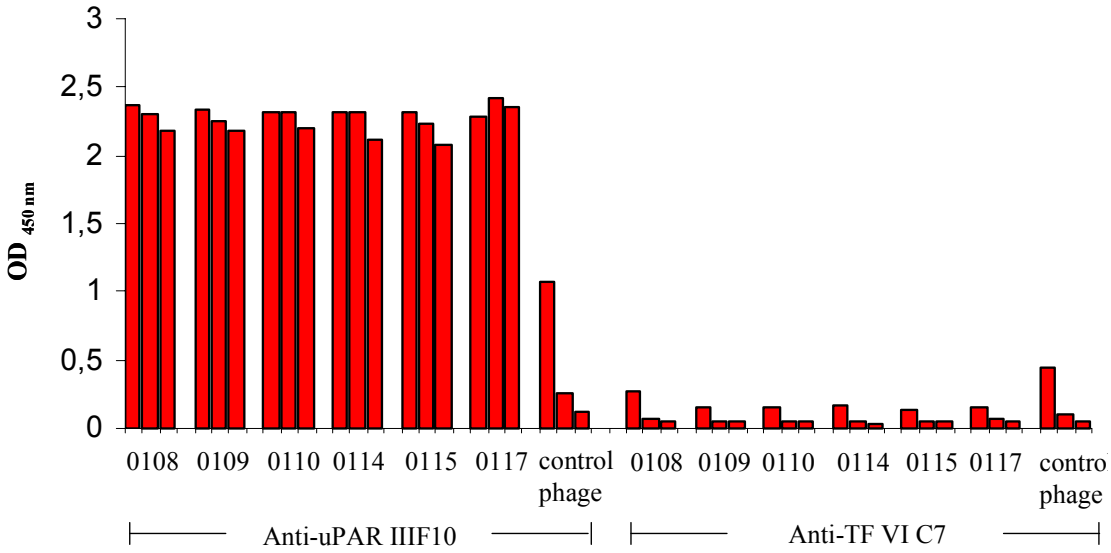

Figure 9: ***Specificity testing of phages in a solid phase binding assay.*** 100 µl phage supernatant in PBST-M in different dilutions (1:2, 1:20, 1:200) were added to a 96-well microtiter plate coated with 100 µl mAb-IIIF10 per well, incubated for 2 h at RT and subjected to horseradish peroxidase-labeled anti-M13 monoclonal antibody. The enzymatic color-reaction was started with chromogenic substrate TMB and absorbance measured in a microtiter plate reader at 450 nm. Phages specifically bind to mAb-IIIF10 coated wells in comparison to the non-binding control phage. Phages did not show significant binding to the mAb TF VI C7 coated wells.

3.2.3.3.4 Phage-binding assay

100,000 cells/well of eukaryotic cells transfected with scFv-IIIF10-GPI or scFv-IIIF10–TCD were seeded onto a 96-well microtiter plate and grown over night in DMEM, 10% FCS at 37°C until about 90-100% confluence. The vector transfected cell line served as a negative control. The next day, phages/DMEM in different dilutions were added to the wells and incubated for 2 h at 37°C. After washing three times with 200 µl DMEM/1% BSA, 100

µl/well (dilution 1:1,000) of the horseradish peroxidase labeled anti-M13 monoclonal antibody was added and incubated for 1 h at 37°C). The wells were then washed two times with 200 µl DMEM/1% BSA and once more with PBS. The adherent cells were visualized by incubating with 100 µl/well of chromogenic substrate TMB. The enzymatic color reaction was stopped with 0.5 M H_2S0_4 and the absorbance measured in a microtiter plate reader at 450 nm.

3.2.3.4 Cell proliferation assay

The proliferation assay was performed to compare the growth rate of vector transfected control cells and cell lines transfected with expression plasmids encoding scFv-IIIF10. 30,000 cells in 1 ml 10% FCS DMEM were seeded in triplicate into the wells of a 24-well plate and incubated for 48 h or 96 h. After incubation cells were washed with PBS, detached from the wells by incubation with 1% (w/v) EDTA/PBS solution and counted in a Neubauer hemocytometer upon Trypan blue exclusion.

3.2.3.5 Cell adhesion assay

3.2.3.5.1 Cell-matrix adhesion assay

The cell-matrix adhesion assay was used to estimate any differences in the adhesive behaviour of the scFv-IIIF10 expressing eukaryotic cell lines to different ECM proteins in comparison to the vector transfected cell line.
Fibronectin (Becton Dickinson, Heidelberg, Germany), vitronectin (Promega) and collagen type IV (Sigma, München, Germany) were diluted in PBS to the final concentration of 10 µg/ml. For coating, 100 µl of the protein solution were added to each well of a 96-well plate in triplicate and incubated over night at 4°C. The next day, wells were washed two times with PBS, blocked with PBS/2% BSA for 3 h at RT and again washed with PBS. Afterwards,
40,000 cells in 100 µl DMEM/0.5%BSA were seeded to each well, the plate was incubated for 2 h at 37°C and washed carefully with PBS to remove non-adherent cells. Adherent cells were then visualized by incubating with substrate solution (50 µl/well + 50 µl/well PBS) for 1 h at 37°C. The resulting color reaction was stopped with the stop solution and the absorbance

measured in a microtiter plate reader at 405 nm. Serial dilutions of cell suspension in a range from 2,500 to 40,000 cells in 50 µl PBS served as a standard.

Substrate solution	15 mM p-nitrophenol-N-acetyl-beta-D-glucosaminide 0.5% Triton X-100 100 mM sodium acetate, pH 5.0
Stop solution	200 mM NaOH 5 mM EDTA

3.2.3.5.2 Cell-cell adhesion assay

The cell-cell adhesion assay was performed to determine the cell-cell interaction of the membrane anchored variants of the scFv-IIIF10 expressed by eukaryotic cells in comparison to the vector transfected control cells. 50,000 cells/100 µl were seeded into each well of a 96-well plate and incubated over night in DMEM. The next day, the adherent cells were washed two times with 100 µl RPMI and the scFv-IIIF10 expressing cells and the control group were incubated with pro-uPA (10 µg/ml RPMI) in quadruplicate for 20 min, then, washed once more. Making cell-cell interaction visible, $3x10^6$ U937 suspension cells were incubated at 37°C over night with a fluorescent lipophilic dye, the carbocyanine DIO 1:100 in RPMI (Molecular Probes, USA). This tracer is weakly fluorescent in water but highly fluorescent and quite photostable, when incorporated into cell membranes. Once applied to cells, the dye diffuses laterally within the plasma membrane, resulting in staining of the entire cell. Transfer of these probes between intact membranes is usually negligible. The next day, 100,000 DIO-labeled U937 per 100 µl RPMI were added to each well and incubated for 3 h at 37°C, washed two times with 100 µl RPMI/well and the extinction was measured in the fluorimeter at 480 nm. Serial dilutions of fluorescence labeled U937 cells in a range from 5,000 to 100,000/well in 100 µl RPMI in triplicate served as a standard. With the standard dilutions and the extinction of the probes, the amount of fluorescence labeled U937, bound to the transfected, adherent eukaryotic cell lines, can be calculated, thereby giving an idea of U937 expressing uPAR on their cell surface and interacting with membrane anchored scFv-IIIF10. Phenol-red-free RPMI medium was used not to interact with the fluorescent dye. The preparations for the experiment were done under reduced exposure to bright light at all times.

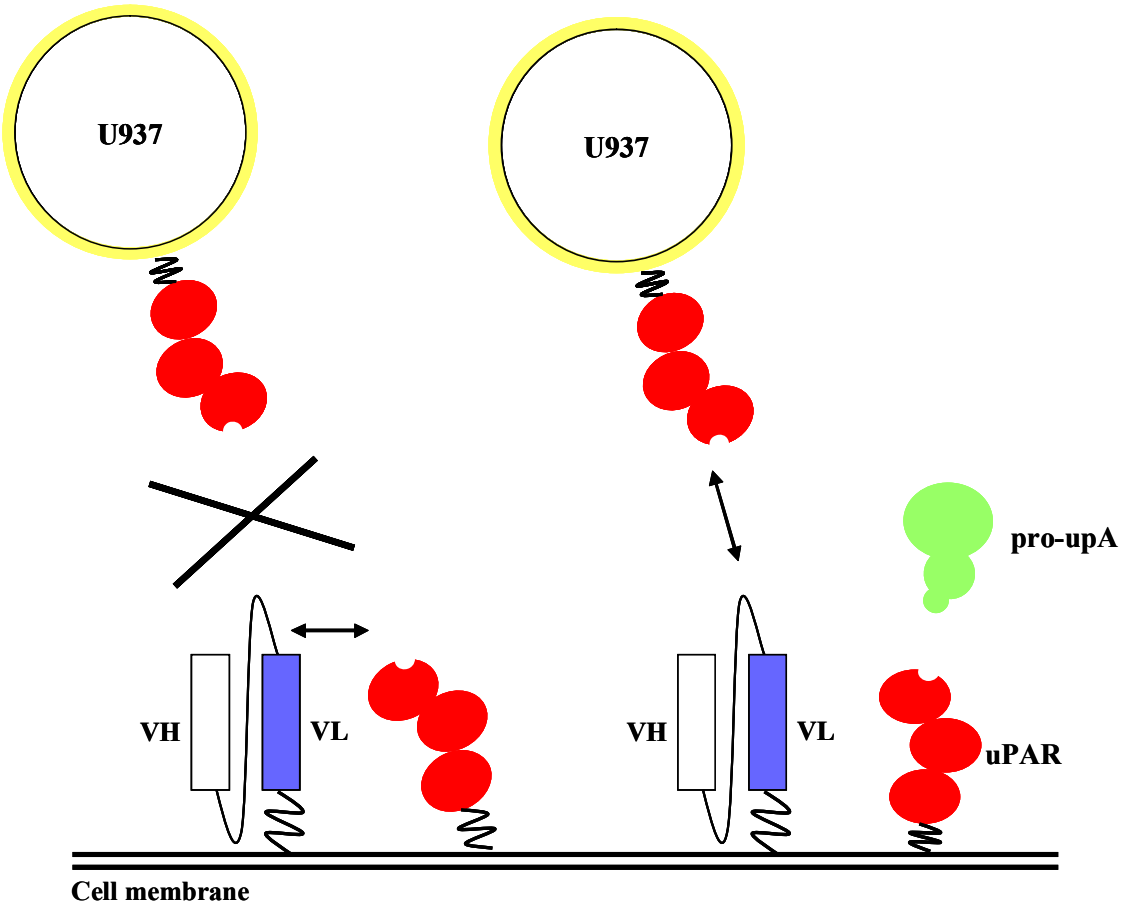

Figure 10: ***Schematic overview of the principle of the cell-cell adhesion assay described above.*** DIO-labeled U937 cells overexpressing uPAR on their cell surface interact with membrane anchored variants of scFv-IIIF10 expressed on the surface of transfected eukaryotic cell lines. At the same time, there might be possible interaction between scFv-IIIF10 and uPAR expressed on the surface of transfected cell lines, thereby inhibiting scFv-IIIF10 and uPAR interaction described before. After pre-incubation with pro-uPA, cell surface associated uPAR/scFv-IIIF10 interaction can be inhibited. scFv-IIIF10 is free for interaction with DIO-labeled U937 cells.

3.2.4 Tumor model

Pathogen-free, female a-thymic (*nu/nu*, CD1) mice (9 weeks old), were purchased from Charles River Laboratories (Sulzfeld, Germany). The animal experiments were performed under semi-sterile conditions in cooperation with Prof. Dr. A. Krüger, Institute for Experimental Oncology, Klinikum rechts der Isar, Munich.

Stably transfected OV-MZ-6#8 cells expressing soluble scFv-IIIF10, transfected with an empty expression plasmid (pRcRSV) and with the trifunctional inhibitor pRcRSV-N-hTimp-1-chCys-uPA$_{19-31}$ (for further details see Krol et al. 2003) were grown until 60-80% confluence. $7x10^6$ cells of each cell line were inoculated into the peritoneal cavity of nude mice. After 56 days, the mice were sacrificed, all intraperitoneal organs including the tumor removed and weighed. These data were taken further as total situs weight. All visible tumor mass was then removed and subsequently weighed. To estimate the differences between individual mice, the ratio of tumor mass to total situs weight was calculated. Tumor of three mice from each group were frozen in liquid nitrogen for further detection of soluble scFv-IIIF10. Blood and ascites were collected, centrifuged at 2,000 xg for 30 min at 4°C and stored at –20°C for further detection.

3.2.5 Statistical analysis

Significant differences in tumour weight over total situs weight between the groups were investigated using a Man-Whitney Rank Sum Test according to the distribution of the data. A level of $p<0.05$ was considered statistically significant.

4. Results

4.1 Mammalian expression plasmids encoding scFv-IIIF10

Previously, the sequence encoding scFv-IIIF10 was isolated from the mRNA of mAb IIIF10-producing hybridoma cells. For this, the fragments encoding the variable regions of heavy (VH) and light (VL) chain were amplified by RT-PCR using gene-specific primers with added restriction sites. VH- and VL-gene segments were then connected *via* a glycine- and serine-rich, flexible linker and expressed as a single-chain antibody (scFv) in *E. coli* (Kirschenhofer et al., 2003).

Using the phagemid vector encoding scFv-IIIF10 as template, an eukaryotic expression plasmid based on the vector pSecTag2/HygroB was generated, encoding scFv-IIIF10 as a secreted, soluble form with a C-terminal *c-myc* epitope as well as a $(His)_6$-tag. These two tags allow for detection and/or purification of the recombinant protein. Expression is driven by the strong viral CMV promoter, secretion is supported by the murine Ig κ-chain V-J2-C signal peptide. In addition, two membrane-anchored variants were designed to display scFv-IIIF10 on the surface of mammalian cells: (i) One fusion harbors the C-terminal sequence of uPAR (aa 294-335 with the Met of the pre-protein being pos. 1). This sequence contains the signals for the attachment of a glycan lipid anchor to a newly formed C-terminus at Gly305 (corresponds to Gly283 of mature uPAR) which results in the cell surface linkage of the recombinant protein *via* a glycosylphosphatidylinositol (GPI) anchor (Sevlever et al., 2000). ii) The other variant harbors the transmembrane and the short cytoplasmic domain (TCD) of tissue factor ($TF_{250-295}$ with the Met of the pre-protein being pos. 1), the cellular receptor for the blood coagulation factor VII. A schematic presentation of the three different scFv-IIIF10-encoded fusion proteins is given in **Figure 11A**, the complete amino acid sequence of the fusion protein encoding the soluble form of scFv-IIIF10 is depicted in **Figure 11B**. In a similar manner, we also generated a pSecTag2/HygroB-based expression vector encoding the extracellular domain of mature tissue factor TF_{1-214} (Magdolen et al., 1998), which served as a control protein for monitoring expression in eukaryotic cells. A schematic overview of the plasmid-constructions is shown in **Figure 12 and 13.**

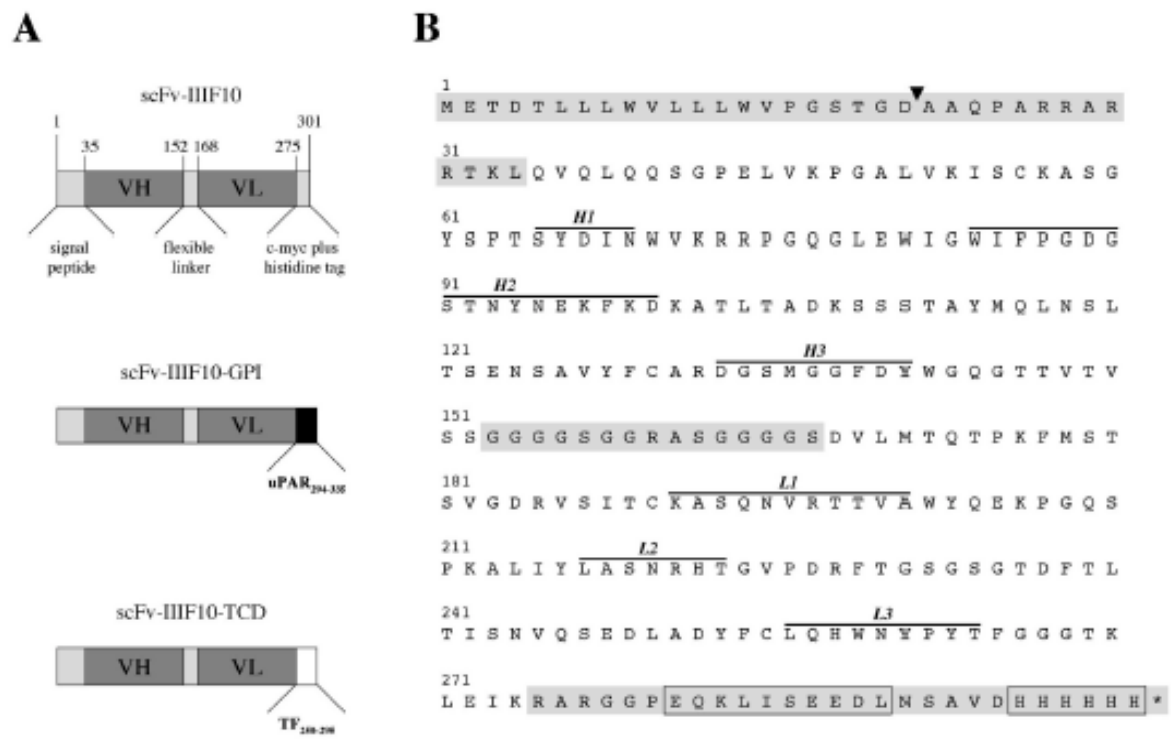

Figure 11: ***Mammalian expression plasmids encoding scFv-IIIF10.***
(A) ScFv-IIIF10 DNA was amplified by PCR using gene-specific primers with added restriction sites and inserted into the expression vector pSecTag2/HygroB (Invitrogen). Three different vectors were generated which encode: i) a soluble, secreted form of scFv-IIIF10 harboring a C-terminally located *c-myc* epitope *plus* a $(His)_6$ tag; ii) scFv-IIIF10 with the C-terminal part of the unprocessed uPAR (encoding $uPAR_{294-335}$ of pre-uPAR) for display of scFv-IIIF10 on the cell surface in a glycan lipid-anchored form; iii) scFv-IIIF10 with the C-terminal part of the unprocessed tissue factor (TF) (encoding $TF_{250-295}$ of pre-TF) for insertion of scFv-IIIF10 into the cell surface via a transmembrane domain.
(B) Complete amino acid sequence of the secreted, soluble form of scFv-IIIF10. N-terminal and C-terminal extensions (encoding the murine Ig κ-chain V-J2-C signal peptide and the *c-myc* epitope *plus* $(His)_6$ tag, respectively) as well as the flexible linker region separating the VH- and VL-chains are indicated by a grey background. The cleavage site of the signal sequence is indicated by an arrowhead, the *c-myc* epitope and the $(His)_6$ tag are boxed. Hypervariable regions within VH and VL (CDRs H1-H3 and L1-L3, respectively) are overlined.

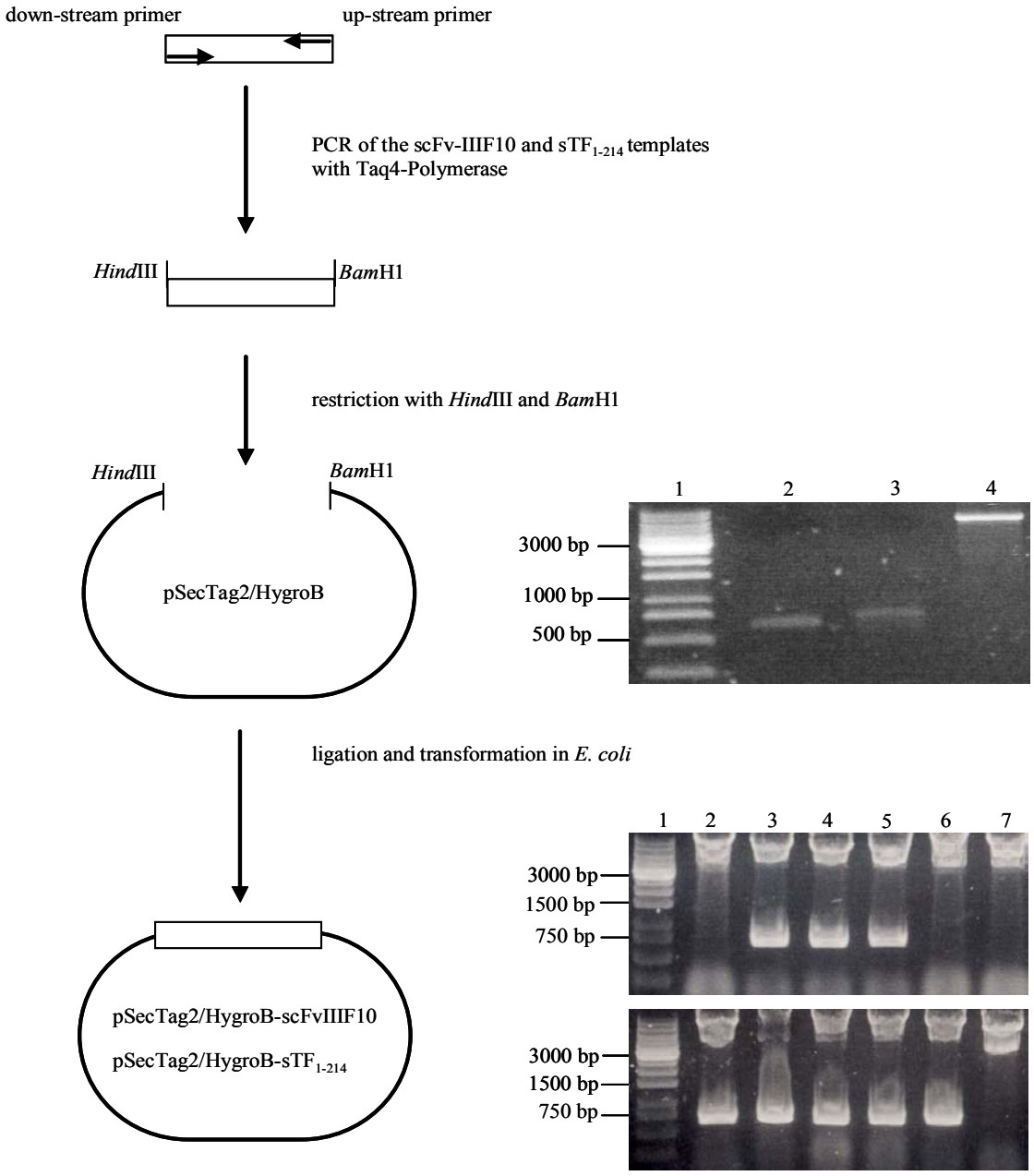

Figure 12. ***Construction of the expression plasmids pSecTag2/HygroB encoding soluble scFv-IIIF10 and soluble TF$_{1-214}$.*** The vector pSecTag2/HygroB (Invitrogen) was subjected to the restriction endonucleases *Hind*III and *Bam*H1 resulting in a cloning site to insert directionally the sequences of the soluble secreted form of scFv-IIIF10 and TF$_{1-214}$. PCR of the templates was performed with the primers scFv-HIII/scFv-B and TFIII/TF-B and PCR-products were subjected to restriction analysis with the endonucleases *Hind*III and *Bam*HI and isolated from the agarose gel *via* "freeze and squeeze" method. The corresponding gel is depicted above: lane 1, 1kb ladder, lane 2, TF (650 bp); lane 3, soluble scFv (735 bp); lane 4, pSecTag2/HygroB.
Fragments were then ligated into the vector pSecTag2/HygroB and transformed into *E. coli*. DNA-preparation from *E. coli* and restriction analysis with *Hind*III and *Bam*HI shows positive clones on the agarose gel. Verified clones were sent for DNA sequencing. Upper panel: lane 1, 1kb ladder; lane 2, negative clone; lane 3 to 5 positive clones for soluble scFv-IIIF10 (735 bp); lane 6 and 7, negative clones. Lower panel: lane 1, 1 kb ladder; lane 2 to 6, positive clones for soluble TF$_{1-214}$ (650 bp); lane 7, negative clone.

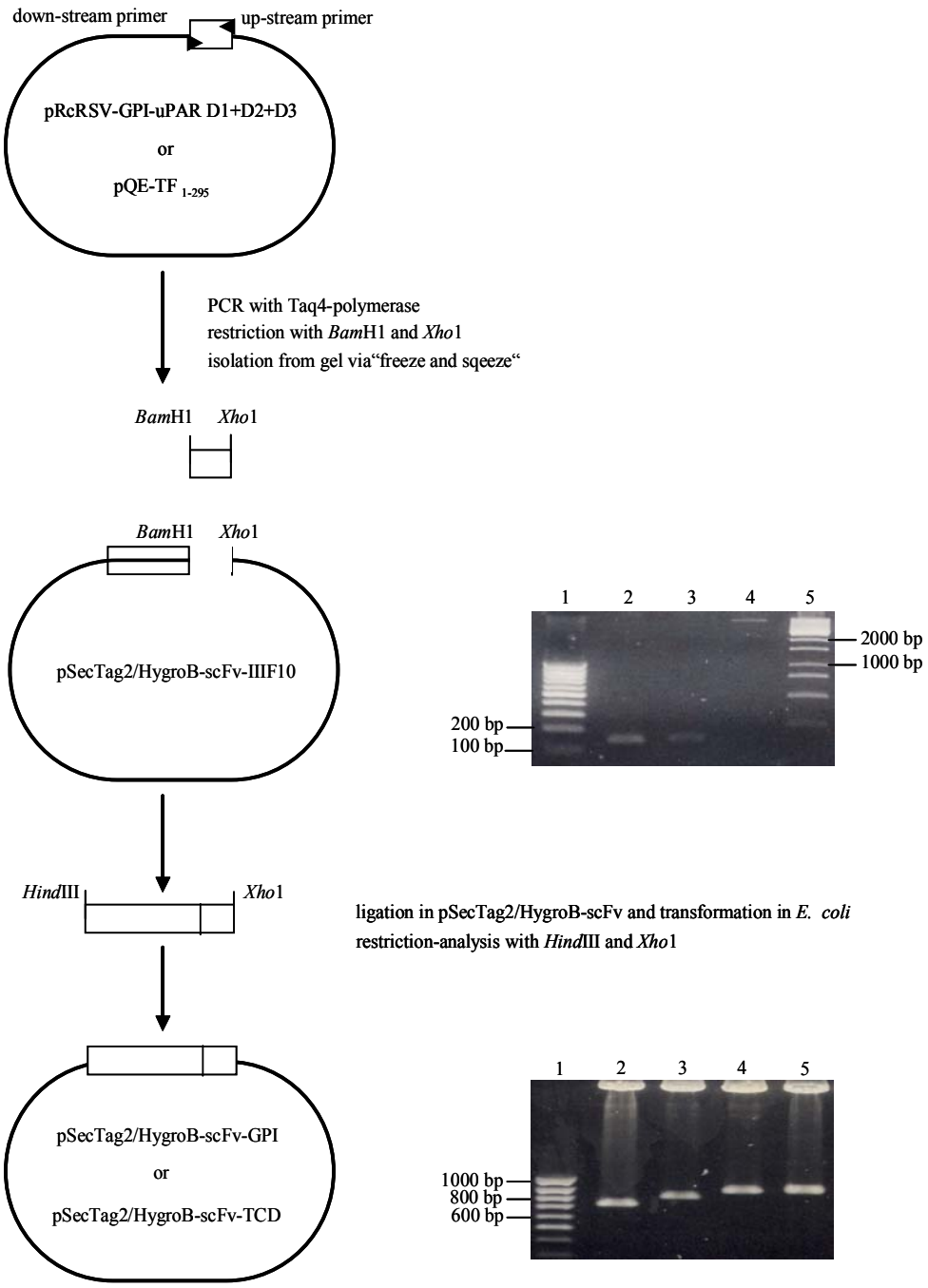

Figure 13: ***Construction of the expression plasmids pSecTag2/HygroB-scFv-IIIF10-TCD and pSecTag2/HygroB-scFv-IIIF10-GPI.*** PCR was performed from pRcRSV-GPI-uPAR D1+D2+D3 encoding the C-terminal part of the unprocessed uPAR for display of scFv-IIIF10 on the cell surface in a glycan lipid-anchored form and from pQE-TF_{1-295} encoding the C-terminal part of the unprocessed tissue factor (TF) for insertion of scFv-IIIF10 into the cell surface *via* a transmembrane domain. Used primers: TCD-do/up and GPI-do/up. PCR-products were subjected to restriction analysis with the endonucleases *Bam*HI and *Xho*1 and isolated from the agarose gel *via* "freeze and squeeze" method. The corresponding gel after gel-isolation is depicted above: lane 1, 100 bp ladder; lane 2, scFv-GPI (141 bp); lane 3, scFv-TCD (153 bp); lane 4, pSecTag2/HygroB-scFv-IIIF10; lane 5, 1kb ladder. Isolated DNA-fragments were then ligated into pSecTag2/HygroB-scFv-IIIF10 and transformed in *E. coli*. Lane 1, 100 bp ladder; lane 2, TF (703 bp); lane 3, scFv (expected size: 788 bp); lane 4, scFv-GPI (876 bp); lane 5; scFv-TCD (888 bp).

4.2 Generation of stable transfectants in eukaryotic cells

Plasmids encoding either of the three variants of scFv-IIIF10, soluble TF_{1-214} and the empty vector pSecTag2/HygroB, respectively were transfected into Chinese hamster ovary cells (CHO), hamster fibroblasts (V79) and the human ovarian cancer cell line OV-MZ-6#8. In addition, OV-MZ-6#8 cells were available, which had been previously transfected with a pRcRSV-derived expression plasmid encoding a trifunctional inhibitor directed against different tumor-associated proteolytic systems and the vector only. These cells were later used in *in vivo* experiments as controls to analyze the effects of scFv-IIIF10 expression on tumor growth and spread (see below). The characterization of the pRcRSV-derived cell lines has been described in detail elsewhere (Krol et al., 2003 a, b). The trifunctional recombinant inhibitor, N-hTIMP-1-chCys-uPA_{19-31} is composed of the N-terminal domain of the human matrix-metalloproteinase inhibitor TIMP-1 and a chicken cystatin variant harboring the uPAR binding site of uPA, chCys-uPA_{19-31}, which in addition to its inhibitory activity towards cysteine proteases interferes with uPA/uPAR-interaction (Muehlenweg et al., 2000).
Subsequently to selection of hygromycin-resistent cells, integration of the pSecTag2/HygroB-derived plasmids into genomic DNA was proven by PCR (**Figure 14A**). For this, genomic DNA was prepared from the various transfectants and used as template for a nested PCR with specific oligodeoxynucleotide primers directed to the DNA encoding the murine signal sequence and the *c-myc* epitope of pSecTag2/HygroB, respectively. The amplification product of the integrated vector corresponded to the expected fragment of 166 bp (not shown), the PCR products of the other stably transfected cell lines varied between 798 bp and 971 bp, depending on the DNA inserted (**Figure 14A**). In order to prove not only integration of the pSecTag2/HygroB-derived plasmids into genomic DNA but also transcription under the control of the strong viral CMV promoter, total RNA was isolated from the transfected cell lines, reverse transcribed and amplified with gene specific oligodeoxynucleotides. **Figure 14B** depicts the results of such a RT-PCR analysis for detection of mRNA encoding the soluble, secreted scFv-IIIF10 in CHO and OV-MZ-6#8 cells. In both cell lines a specific product was amplified, which lacks in the vector-control as expected.

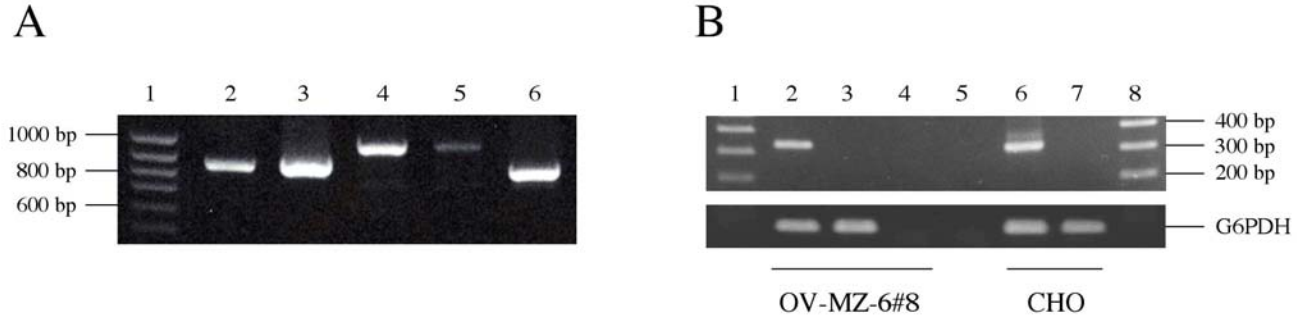

Figure 14: ***Analysis of stably transfected cell lines by PCR.*** Two µg of purified DNA of either expression plasmid were transfected with the SuperFect™ Transfection Reagent into three different mammalian cell lines: CHO, V79 and OV-MZ-6#8.
(A) PCR analysis to test for integration of the expression plasmids into genomic DNA of OV-MZ-6#8 cells. Genomic DNA was isolated from $2x10^6$ cells of the various transfected cell lines and used as template for a nested PCR with pSecTag2/HygroB-specific primers. Lane 1, 100 bp ladder; lane 2, amplification product from OV-scFv (expected size: 877 bp); lane 3, plasmid pSecTag2/HygroB-scFv-IIIF10 as positive control (877 bp); lane 4, OV-scFv-GPI (959 bp); lane 5, OV-scFv-TCD (971 bp); lane 6, OV-sTF (798 bp).
(B) RT-PCR analysis to test for transcription of the expression cassette encoding soluble, secreted scFv-IIIF10 in OV-MZ-6#8 and CHO cells. $6x10^6$ cells were treated with Trizol reagent (Life Technologies) according to the manufacturers manual and total RNA was isolated, reverse transcribed into first/strand cDNA with random and oligo (dT) primers and amplified by scFv-IIIF10 specific primers (expected fragment: 323 bp, upper panel). Lanes 1 and 8, 100 bp ladder; lane 2, OV-scFv; lane 3, OV-MZ-6#8 cells stably transfected with the empty vector pSecTag2/HygroB; lane 4, OV-scFv RNA reverse transcribed w/o oligo(dT) (= control); lane 5, RT-PCR w/o RNA (= control); lane 6, CHO-scFv; lane 7, CHO- pSecTag2/HygroB. The lower panel shows the control RT-PCR of the house-keeping gene G6PDH to demonstrate the integrity of the RNA.

4.3 Purification and characterization of soluble scFv-IIIF10 and soluble TF_{1-214} from eukaryotic cell culture supernatants

Since both, the secreted form of scFv-IIIF10 as well as sTF_{1-214} contain a C-terminal $(His)_6$ tag, these proteins were initially purified from culture supernatants of the transfected eukaryotic cell lines *via* Ni^{2+}-NTA-agarose affinity chromotagraphy under native conditions. Expression and purification of sTF was followed by applying a TF ELISA (Albrecht et al. 1992). The cells produced about 20 ng/ml (CHO cells) to 55 ng/ml sTF per 10^6 cells after 48 h of cultivation. The recovery rates of sTF amounted to 65 to 90% after purification. It has previously been demonstrated that sTF_{1-214} expressed in *E. coli* displays functional activity (Magdolen et al., 1998; Randolf et al., 1998; Albrecht et al., 2002). As tested by a soluble TF

coagulation assay (Magdolen et al., 1998), recombinant human sTF_{1-214} from hamster cells displays a procoagulatory activity as well (data not shown).

Both purified scFv-IIIF10 and sTF were tested by Western blot analysis applying a mAb directed to a $(His)_5$ epitope **(Figure 15A)**. Specific signals were obtained corresponding to proteins of about 30 kDa, which is in line with the deduced molecular weight of scFv-IIIF10 (= 30.4 kDa) and sTF_{1-214} (= 30.3 kDa). In contrast to the stably transfected hamster cell lines, we were not able to purify soluble scFv-IIIF10 from the culture supernatants of OV-MZ-6#8 cells transfected with pSecTag2/HygroB-scFv-IIIF10, even though expression has been proven on the level of transcription. Furthermore, the qualitative analysis suggests that expression is in a similar range as compared to that in CHO cells **(Figure 14B)**. It is tempting to speculate that the produced soluble scFv-IIIF10 binds immediately to human uPAR presented on the (human) OV-MZ-6#8 cells, whereas in the case of the hamster CHO or V79 cells such a cellular binding site is not present and, thus, the recombinant protein accumulates in the cell culture supernatant.

Binding of purified scFv-IIIF10 from hamster cells to uPAR was tested by flow cytofluorometry. Again, scFv-IIIF10 distinctly recognizes native human uPAR, presented on the surface of PMA-stimulated U937 cells **(Figure 15B)**. Simultaneous incubation of scFv-IIIF10 and recombinant human pro-uPA prevents binding of scFv-IIIF10 to the cell surface. Pro-uPA binds to uPAR with a K_D of about 1 nM and, thus, strongly competes with scFv-IIIF10 for interaction with cell surface-associated uPAR. Purified sTF (also containing the *c-myc* epitope used for detection in FACS analysis) does not bind to U937 cells.

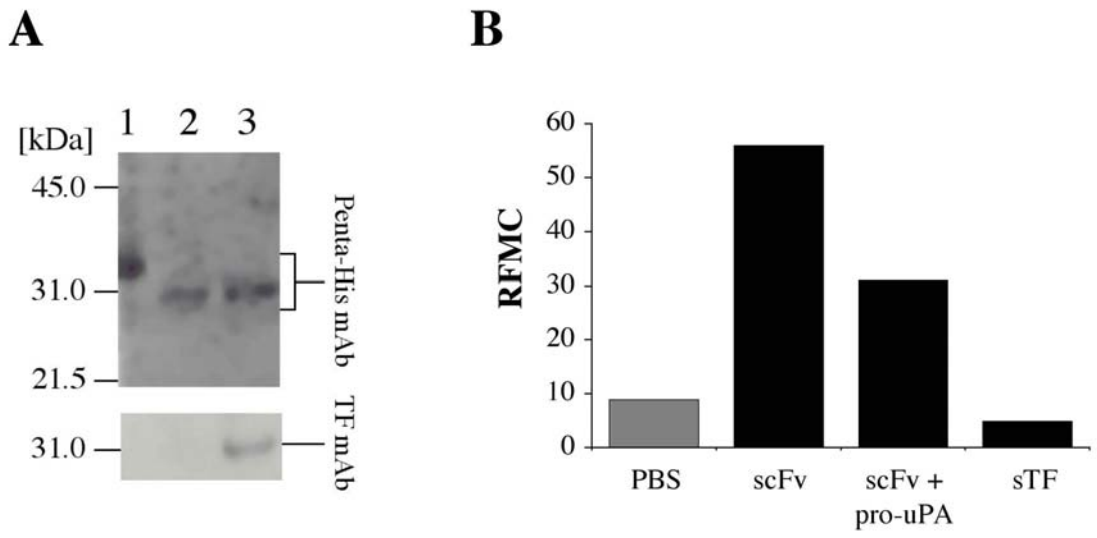

Figure 15: ***Characterization of purified recombinant soluble scFv-IIIF10 and sTF$_{1-214}$ from culture supernatants of hamster cells.*** (His)$_6$-tagged scFv-IIIF10 and sTF$_{1-214}$ were purified from culture supernatants of stably transfected cell lines harboring pSecTag2/HygroB-derived expression cassettes by Ni^{2+}-NTA-agarose affinity chromotagraphy.
(A) Western blot analysis. Eluates from the affinity column were separated by SDS-PAGE and then transferred to PVDF membranes by semi-dry blotting. Subsequently, the blots were probed with a mAb directed to a (His)$_5$ epitope (Penta-His-ab, Qiagen) (upper panel). Lane 1, recombinant (His)$_6$-tagged uPAR from *E. coli* (deduced molecular weight: 33.4 kDa; = control); lane 2, eluate from scFv-IIIF10 column (deduced molecular weight of scFv-IIIF10: 30.4 kDa); lane 3, eluate from sTF$_{1-214}$ column (deduced molecular weight of sTF: 30.3 kDa). As an additional control (lower panel), the Western blot was stripped and re-probed with mAb VIC7 directed to TF (Magdolen et al. 1998). Immuno-reactivity is only observed in lane 3 corresponding to the eluate from the sTF$_{1-214}$ column.
(B) FACS analysis. 2.5x10^5 PMA-stimulated human monocytic acid-treated U937 cells, overexpressing cell surface associated uPAR, were incubated with eluates of the scFv-IIIF10 or sTF$_{1-214}$ columns. Anti-*myc*-antibody directed against a C-terminal *c-myc* epitope of the scFv-IIIF10 followed by the flourescence labeled secondary antibody ALEXA 488 rabbit-anti-mouse were added and single cell associated flourescence quantified by FACS analysis. sTF$_{1-214}$ eluate was used as a non binding protein for negative control. For specificity testing, one sample of scFv-IIIF10 eluate was simultaneously incubated with recombinant human pro-uPA. Recombinant human pro-uPA prevents binding of scFv-IIIF10 to the cell surface.

Additionally, a solid phase binding assay was performed to test interaction of the purified scFv-IIIF10 with uPAR. As can be seen from **Figure 16**, especially fraction I of the scFv-IIIF10 eluate from the Ni^{2+}-NTA-agarose affinity chromotagraphy column contained significant amounts of scFv-IIIF10. Together with the results obtained by FACS analysis, it can therefore be concluded that scFv-IIIF10 is produced and secreted by the eukaryotic cell lines CHO and V79 hamsterfibroblasts in an active form.

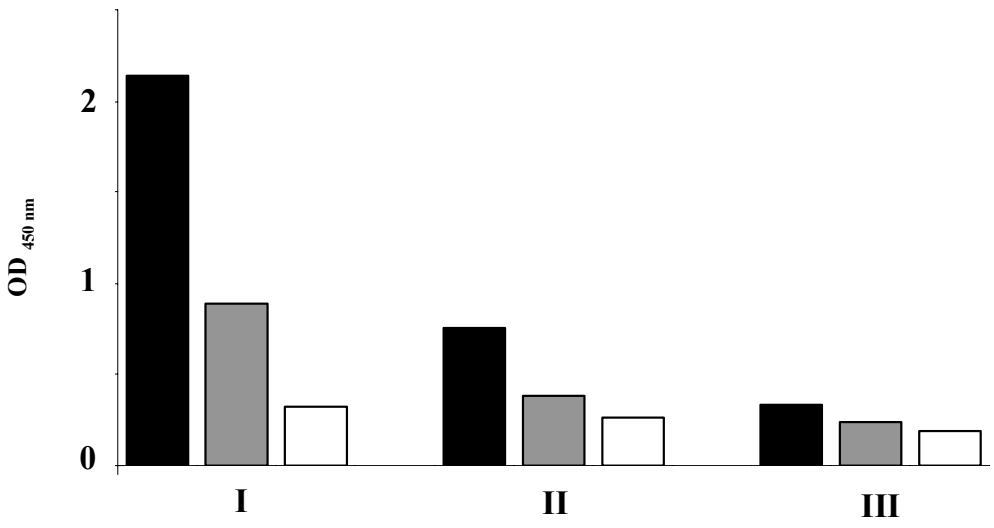

Figure 16: ***Purified recombinant soluble scFv-IIIF10 binding to immobilized uPAR***. 100 µl/well of fraction I, II and III, respectively, of the scFv-IIIF10 eluate were added in serial dilutions to a 96-well immunoassay plate pre-coated with purified recombinant human soluble uPAR (rec-$uPAR_{1-277}$, 0.5 µg/ml): black bar, undiluted; grey bar, diluted 1:3; open bar, diluted 1:10 in PBS. Transfected CHO as well as V79 cell lines produced and secreted detectable amounts of the respective scFv into the cell culture medium, whereas the vector transfected cells did not show any reaction (not shown here).

4.4 Detection of membrane anchored variants of scFv-IIIF10 via M-13 phages

Based on a phage-based random peptide library (Smith and Scott, 1993), different phages selectively binding to the epitope of scFv-IIIF10 were used to characterize stably transfected eukaryotic cell lines expressing recombinant membrane anchored scFv-IIIF10-GPI and scFv-IIIF10-TCD on their cell surface (see **Figure 9**).

M13 Phages were amplified by incubating with *E. coli* bacteria and growing in selection medium with 20 µg/ml tetracycline. After purification and titration, phages were applied to the wells containing adherent, stably transfected eukaryotic cell lines expressing membrane

anchored variants of scFv-IIIF10 (scFv-IIIF10-GPI, scFv-IIIF10-TCD). A peroxidase-labeled monoclonal antibody which is directed against the surface of M13 phages lead to an enzyme-linked color reaction and showed phages bound to the membrane anchored variants of scFv-IIIF10 on the transfected cell lines. **Figure 17** shows scFv-IIIF10-GPI as a functionally present protein on the surface of the transfected CHO cells, whereas scFv-IIIF10-TCD could not be recognized by the phages. This might be due to a reduced expression rate or impaired functionality of the protein either on its way to the cell surface or by possible interference with its transmembrane anchor. Similar results were obtained with V79 hamsterfibroblasts and OV-MZ-6#8 (data not shown).

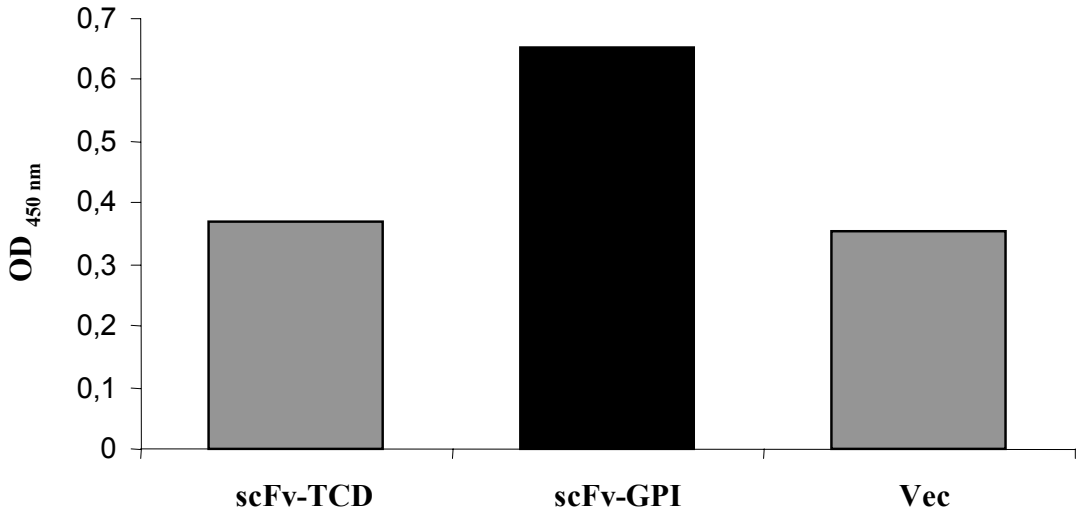

Figure 17: ***Phage-binding assay detecting membrane anchored variants of scFv-IIIF10.***
100,000 cells/well of CHO cells stably transfected with scFv-IIIF10-GPI, scFv-IIIF10–TCD or the vector only, were seeded onto 96-well microtiter plates in quadruplicate and grown until about 90-100% confluence. M13-phages (phage 0110, titer $4x10^{11}$) were added and incubated for 2 h at 37°C. A horseraddish peroxidase labeled anti-M13 monoclonal antibody (dilution 1:1,000) was added and adherent cells expressing scFv-IIIF10 on their surface visualized by enzymatic color reaction with TMB. The vector transfected cell line served as a negative control.

4.5 Interaction of membrane bound scFv-IIIF10 with human uPAR

To test the interaction of the scFv-IIIF10 expressed on the cell surface of eukaryotic cell lines with uPAR, an adhesion assay was performed. For this, stably transfected eukaryotic cells expressing scFv-IIIF10-GPI, scFv-IIIF10-TCD, sTF and vector transfected control cells were

seeded onto 96-well plates and cultured over night. The next day, fluorescence labeled human U937 overexpressing uPAR were added and incubated. Fluorescence of adherent U937cells was measured in the fluorimeter and number of adherent U937 cells calculated. As the membrane-associated uPAR expressed on the surface of the transfected cells might interact with membrane bound scFv in its neighbourhood, wells were pre-incubated with pro-uPA before adding U937 cells. In comparison to the wells containing the vector only or wells not pre-incubated with pro-uPA, an increased number of fluorescence labeled U937 could be detected **(Figure 18)**. Vector transfected cells and sTF did not show a distinct increase of binding of fluorescently labeled U937 cells. Similar results were obtained with V79 hamsterfibroblasts and OV-MZ-6#8 (data not shown).

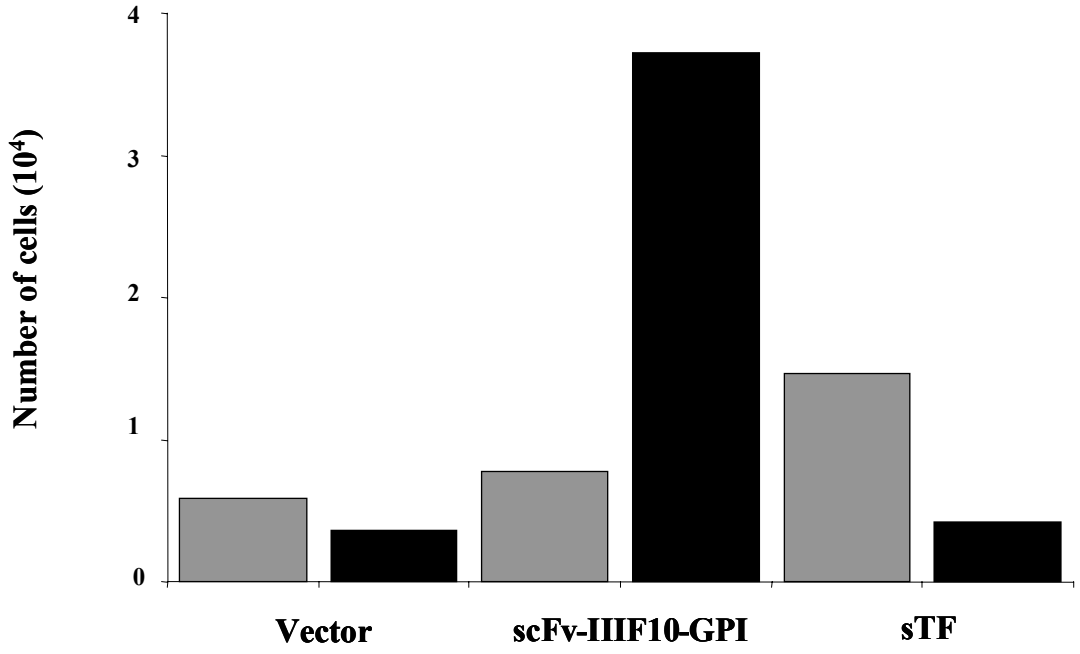

Figure 18: ***Determination of cell-cell interaction of membrane bound scFv-IIIF10-variants.***
To determine the interaction of transfected CHO cells expressing membrane bound scFv-IIIF10 with uPAR expressed on the surface of U937 cells, an adhesion assay was performed. 50,000 cells were seeded into each well of a 96-well plate and incubated over night. 100,000 DIO-labeled U937 were added to the wells and incubated. Extinction was measured in the fluorimeter at 480 nm. scFv-IIIF10-GPI expressing cells pre-incubated with pro-uPA (black bar) interact with an increased number of fluorescently labeled U937 compared to not pre-incubated cells and vector only (grey bar).

4.6 Characterization of proliferation of OV-MZ-6#8 cells transfected with soluble scFv-IIIF10

The proliferative behavior of the stably transfected cells was examined in *in vitro* proliferation assays under normal culturing conditions. Cells were subcultured in 24-well plates with serum containing medium for 48 h and 96 h, then counted using a Neubauer hemocytometer. As shown in **Figure 19A**, proliferation rates of transfected OV-MZ-6#8 cell lines expressing scFv-IIIF10 were comparable to the rates obtained with the vector control cell line OV-pRcRSV.

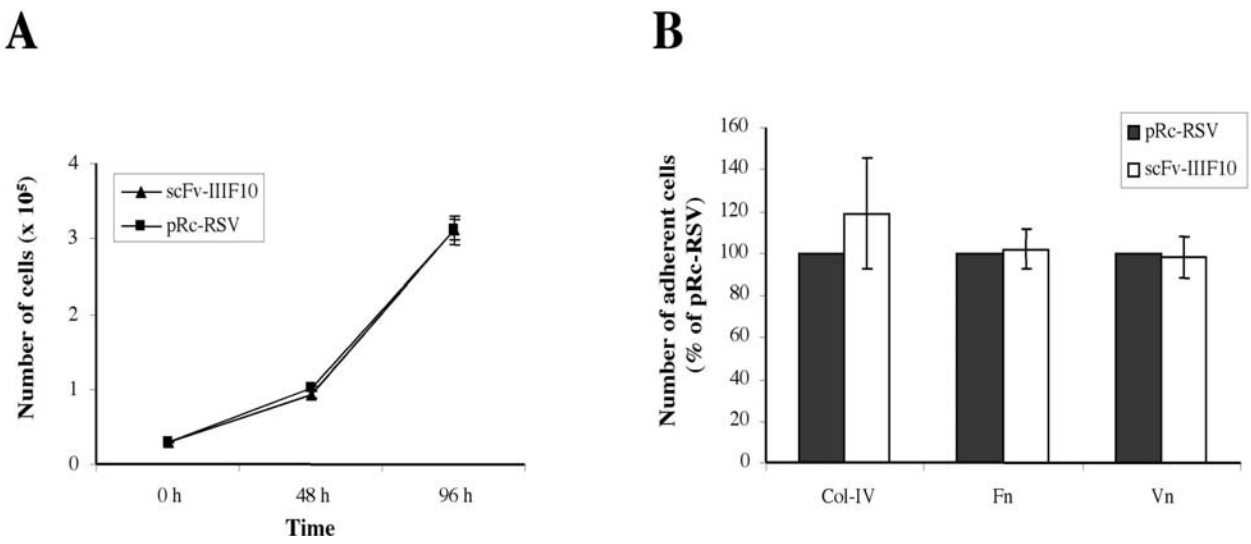

Figure 19: ***Characterization of OV-MZ-6#8 derived cells expressing single chain antibody directed against uPAR.***
(A) Proliferation of OV-MZ-6#8 derived cells, expressing single chain antibody directed against uPAR (OV-scFv-IIIF10), or transfected with vector pRc-RSV only. 30,000 cells in 1 ml DMEM, 10% (v/v) FCS were seeded into wells of a 24-well plate. After 48 and 96 h of incubation, cells were counted in a Neubauer hemocytometer in the presence of Trypan blue. Expression of single chain antibody scFv-IIIF10 had no influence on cell proliferation compared to OV-MZ-6#8 cells stably transfected with vector only. Three independent experiments were performed in triplicate. Mean values ± SD are indicated.
(B) Adhesion of OV-MZ-6#8 derived cells expressing scFv-IIIF10 (OV-scFv-IIIF10) or transfected with vector only to different extracellular matrix (ECM) proteins. 30,000 cells were seeded into wells of a 96-well plate precoated with collagen type IV (Col-IV), fibronectin (Fn) or vitronectin (Vn). Two hours later non-adherent cells were washed out with PBS and remaining cells were indirectly quantified *via* a hexoaminidase substrate solution. The resulting color reaction was measured on a microtest plate reader at a wave length of 405 nm. Values are given as adhesion in % setting adhesion of OV-pRcRSV at 100%. Expression of scFv-IIIF10 had no influence on cell adhesion to all tested ECM proteins compared to OV-pRc-RSV, Mean values ± SD of four independent experiments performed in duplicate are indicated.

4.7 Determination of the adhesive capacities of transfected OV-MZ-6#8 cells to different ECM-Proteins

In oder to examine the effect of transfection on the adhesive behavior of the transfected cell lines, OV-MZ-6#8 cells transfected with scFv-IIIF10 and with empty vector were seeded on a microtiter plate precoated with components of the extracellular matrix (ECM) such as fibronectin, vitronectin and collagen type IV. Adherent cells were then detected using hexoaminidase-substrate. For OV-scFv-IIIF10 binding to collagen IV, a slightly enhanced binding was observed compared to the binding to vitronectin and fibronectin and the vector-transfected control cells (**Figure 19B**).

4.8 Effects of scFv-IIIF10 secretion on *in vivo* tumor growth of human ovarian cancer cells

We were interested to analyze whether scFv-IIIF10 expression in human OV-MZ-6#8 cells affects primary tumor growth and spread in a *xenograft* nude mouse model and decided to compare three cell lines OV-scFv-IIIF10, OV-pRcRSV (= vector control), and OV-N-hTIMP-1-chCys-uPA$_{19-31}$ expressing a multifunctional inhibitor directed to three different tumor-associated proteolytic systems (see above; Krol et al., 2003a,b) in this model.
For this, we inoculated 7x10^6 OV-scFv-IIIF10 cells into the peritoneum of nude mice, while control mice received the same number of OV-MZ-6#8 cells transfected with an empty expression plasmid (pRcRSV) or with pRcRSV-N-hTIMP-1-chCys-uPA$_{19-31}$ (Krol et al., 2003a,b). After 56 days, the tumor mass within the peritoneal cavity, appearing as focal tumors located below the liver and in the mesenterium, as well as tumor cell layers or colonies along the diaphragm and the inner abdominal wall (*peritoneum parietalis*), was compared between the three groups. Expression of scFv-IIIF10 led to the formation of a smaller intraperitoneal tumor mass (13% reduction) as compared to the control, however, not statistically significant (**Figure 20**). In contrast, significant reduction of tumor mass was observed in mice inoculated with the cell line expressing the trifunctional inhibitor N-hTIMP-1-chCys-uPA$_{19-31}$ (71% reduction) as compared to the tumor mass generated by OV-pRcRSV cells (**Figure 20**; see also Krol et al., 2003b).

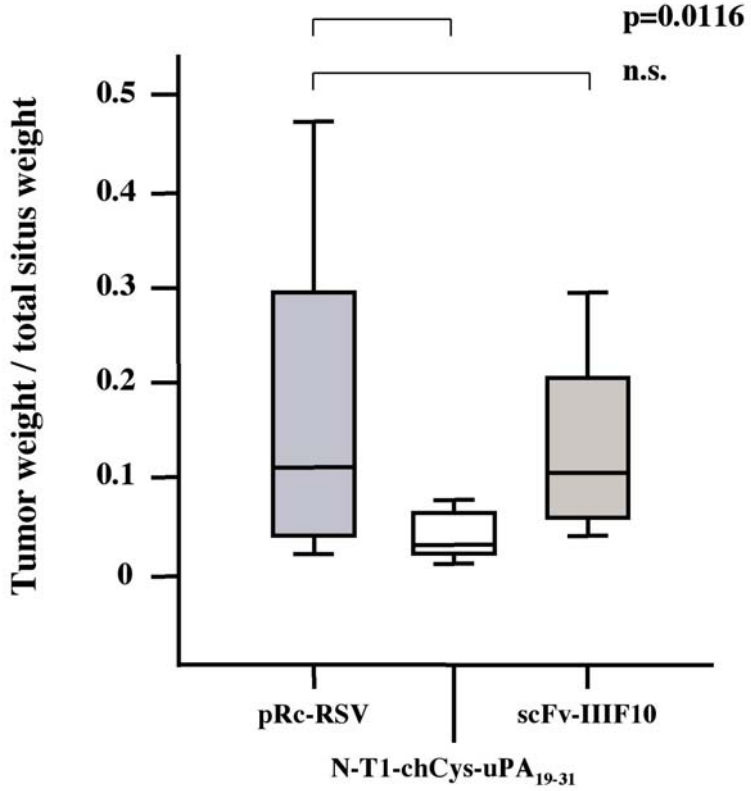

Figure 20: ***In vivo tumor growth of human ovarian cancer cells synthesizing scFv-IIIF10.***
$7x10^6$ OV-scFv-IIIF10, OV-pRcRSV, and OV-N-hTIMP-1-chCys-uPA_{19-31} cells (Krol et al., 2003b) were inoculated into the peritoneal cavity of pathogen-free, female athymic (nu/nu, CD41) mice, 9 weeks old (Charles River, Sulzfeld, Germany). After 56 days, the mice were sacrificed and the relative tumor mass within the total situs determined. To achieve this, all intraperitoneal organs, including the tumor, were removed and weighed. Then, all visible tumor mass was removed and weighed and the data expressed as the ratio of tumor weight over weight of total situs. The OV-derived cell line expressing scFv-IIIF10 (OV-scFv-IIIF10 n=10, median tumor proportion (m.t.p.)= 0.1056) was compared to the control cell line (OV-pRcRSV n=13, m.t.p.=0.1217), stably transfected with the expression plasmid only, and to an OV-derived cell line secreting the trifunctional inhibitor N-hTIMP-1-chCys-uPA_{19-31} (OV-N-hTIMP-1-chCys-uPA_{19-31} n=9, m.t.p.=0.0347), as positive control. The box plot marks the 25th and 75th percentile, the vertical bars above and below indicate the 10th and the 90th percentile, respectively. The median value is indicated by a bold bar. n.s., not significant. Statistical differences in tumor weight over total situs weight between the groups were calculated using Mann–Whitney Rank Sum Test. Values of $p<0.05$ were considered statistically significant.

5. Discussion

5.1 scFv-IIIF10 as a therapeutic molecule

The uPA/uPAR-system is an attractive target for tumor therapy to affect tumor invasion and metastasis (Sperl et al., 2001; Reuning et al., 2003). In the present study, we have selected mAb-IIIF10 directed to the uPA-binding site of uPAR to develop a single-chain antibody, scFv-IIIF10, as a potentially interesting therapeutic molecule. Pro- and eukaryotic expression plasmids were generated expressing scFv-IIIF10 either in a soluble form or attached to the cell membrane *via* a GPI or a transmembrane anchor. The binding properties of the different scFv-IIIF10 variants were analyzed *in vitro*. The soluble form of scFv-IIIF10 was initially purified from cell culture supernatants of the transfected eukaryotic cell lines *via* Ni^{2+}-NTA-agarose affinity chromatography under native conditions. The purified protein was then subjected to different proteinchemical and cell biological methods, demonstrating that soluble scFv-IIIF10 is expressed as a functional protein binding to human uPAR. In cell-cell-adhesion assays it was shown, that membrane anchored, GPI-linked scFv-IIIF10 (scFv-IIIF10-GPI) expressed on the surface of eukaryotic cell lines is recognized by M13 phages selectively binding to the epitope of scFv-IIIF10, whereas the transmembrane form scFv-IIIF10-TCD could not be recognized by the phages. DNA-sequencing analysis confirmed the corresponding DNA sequence encoding pSecTag2/HygroB-scFv-IIIF10-GPI and –TCD. Additionally, integration of both membrane anchored variants (pSecTag2/HygroB-scFv-IIIF10-GPI and –TCD) into genomic DNA was demonstrated by nested PCR (**Figure 12A**). However, a reduced expression rate or failures on the level of intracellular processing and trafficking to the cell surface could be a possible explanation for the M13 phages not being able to recognize the transmembrane-anchored variant of scFv-IIIF10. Furthermore, an impaired functionality of the protein may also be due to a possible interference with its transmembrane anchor.

Subsequently, the effects of scFv-IIIF10 synthesis by ovarian cancer cells on tumor growth and spread were studied in an OV-MZ-6#8 *xenograft* mouse model. In previous studies, a significant anti-tumorigenic effect was achieved in this animal model by blocking uPA/uPAR interaction with synthetic uPA-derived cyclic peptides (Sato et al., 2002) or soluble uPAR (Lutz et al., 2001) as a scavenger for uPA. This illustrates the important role of the uPA/uPAR-system protease system in this tumor model. However, secretion of the single-

chain antibody (scFv-IIIF10) directed against the uPAR did not result in a significant reduction of relative tumor mass. It is possible, that the rather low secretion level of scFv-IIIF10 by the transfected cells does not result in effective and sustained levels of scFv-IIIF10 *in situ* to compete for uPA-binding to all uPAR molecules on the cell surface. Even though DNA-transcription of soluble scFv-IIIF10 could be demonstrated in OV-MZ-6#8 and CHO cells, scFv-IIIF10 was secreted in distinct amounts only from CHO cells and V79 hamster fibroblasts.

Thus, more efficient methods to achieve effective scFv-IIIF10 concentrations *in vivo*, *e.g. via* viral vector-mediated expression of the secretory scFv (Arafat et al., 2002; Solly et al., 2005), may be necessary to demonstrate applicability of scFv-IIIF10 in tumor therapy. As high concentrations of scFvs are needed to achieve therapeutic effects, more research should be done on the possible application of scFv-IIIF10 as a tumor targeting vehicle, as for example described in Menotti et al. (2006). This study demonstrated in a proof of principle experiment that a herpes simplex virus recombinant carrying the insertion of a scFv to HER2/*neu* is able to selectively infect HER/2*neu*-positive cells only. Specific targeting of viruses to tumor cell surface molecules can be used for both oncolytic activity and visualization of tumor cells. This is a new possibility of directing tumor cells more specifically and effectively. Occurring side effects when applying viral vectors might even be reduced.

5.2 Limitations in the design and application of single chain fragments

There are several problems to overcome when using genetically engineered scFvs for clinical application: affinity, specificity, instability, molecular size, biodistribution, immunogenity and high costs in most cases. An immunoreagent like scFv has to meet several criteria for a potential anticancer compound. First of all, selective binding and good affinity is essential for a therapeutic effect. In general, a decrease in binding affinity of the scFvs as compared with intact antibodies is noticed. Some antigen-antibody interaction involves both antigen-binding sites of an intact antibody. Thus, a monovalent scFv has a lower avidity than the divalent IgG. To increase the molecular weight and the functional affinity of an antibody to an antigen, multimerization is an effective method. Several strategies are being used to produce multivalent scFvs for example the addition of a flexible hinge region or a peptide linker. The simplest approach is based on spontaneous formation of non-covalent dimers such as diabodies or trimers (Batra et al., 2002; Hudson et al., 1999).

Min Fang et al. (2004) described the generation and characterization of a bispecific scFv BHL-1 that binds specifically and with good affinity to human CD3 expressed on T-cells and a tumor-associated antigen of human ovarian carcinoma (OC183B2). It was shown that this bispecific scFv could bridge SCOV3 tumor cells and human T-cells and mediates tumor cell lysis *in vitro* and *in vivo*. Biodstribution has shown that scFv BHL-1 could target the tumor *in vivo* with a terminal half life time of 7.7 h. It is particularly important in terms of side effects of application, that there is no reaction in normal human tissue, which has to be determined by immunhistochemistry. Pavoni et al. (2006) developed a human scFv against the carcinoembryonic antigen (CEA) and demonstrated, that this scFv binds selectively and with good affinity to the CEA epitope expressed by metastatic melanoma, colon and lung carcinomas, but poorly or not to normal human tissue.

As the affinity for a tumor-related antigen rises, its penetration is progressively impeded, but specific targeting improves. Adams et al. (2001) demonstrated in a study using a series of antibody mutants of a scFv, that high affinity limits the tumor-localization and intra-tumoral diffusion of small antibody-based molecules. mAbs with very high affinity for tumor antigens stably bind to the first encountered tumor antigen. This could lead to the so called “binding site barrier effect”, *i.e.* patchy and incomplete tumor penetration and could be associated with suboptimal therapeutic effects when therapeutic efficacy is dependent upon uniform delivery to tumor cells (Fujimori et al., 1990; Juweid et al., 1992). Recently, it has been observed that quantitative tumor retention did not significantly increase with enhancements in affinity beyond 10^{-9} M and resulted in lower tumor:blood ratios (Adams et al., 2001).

When applying scFvs, immunogenity can lead to severe side effects such as anaphylactic reactions. Most of the mAbs are murine in nature and systemic administration can lead to the development of a human anti-mouse immunoglobulin antibody response (HAMA). This risk can be reduced, when therapeutic antibodies are humanized, *e.g.* chimeric antibodies as they become less immunogenic (Smith et al., 2004).

Due to their small size, scFvs have the advantage of good tumor penetration compared with whole antibodies, but they are cleared from the blood by the kidneys more rapidly. In several anti-cancer studies it was shown, that scFvs derived from monoclonal antibodies could indeed be targeted to tumors, even improve the penetrating ability for the tumor compared with whole IgG antibodies. However, due to their short serum half-life the retention within the tumor and absolute uptake quantity by the tumor is low in most cases (Colcher et al., 1998).

One way to alter the pharmacology of scFv is to modify its net charge. Charge-modified scFvs with desired isoelectric points have been prepared by inserting negatively charged amino acids on the template of the variable region genes. This can help to overcome undesirable elevations of renal uptake seen with most antibody fragments (Pavlinkova et al., 1999).

5.3 Currently applied therapeutic antibodies in clinical trials

Antibody-based therapeutics have emerged as important components of therapies for an increasing number of human malignancies and are providing an insight into the biology of several malignancies. Some tumor antigens, so-called tumor markers, identified by mAbs, are being used as reliable markers of disease activity in malignancies (CEA, AFP, CA 125, Ca 19-9 etc.). CEA, *e.g.*, is a well characterized tumor-associated glycoprotein that is expressed on endodermally derived gastrointestinal-tract neoplasms and other adenocarcinomas. It is present on the surface of tumor cells and also shed at high levels into the circulation. In a study with a radio-labeled anti-CEA-scFv injected intravenously before surgery, radioimmune-guided surgery was performed to locate tumor tissue in the operative field. 82% true-positive rates of tumor detection were found when examining the excised tissues (Mayer et al., 2000).

Recently, more and more clinical trials are ongoing, applying therapeutic mAbs or scFvs against tumor-associated antigens. They are used as immunologic mediators of cytotoxicity, by blocking receptors or conjugated to a drug, toxin or radionuclide. For example, rituximab is one of the first mAb approved by the FDA (Food and Drug Administration; USA) for therapeutic use in human malignancy. The chimeric anti-CD20 antibody also known as Rituxan® demonstrated in *in vitro* studies that it leads to cell death by multiple mechanisms. Phase II studies demonstrated the efficacy and safety of an antibody therapy with rituximab in patients with previously treated low-grade B-cell lymphoma. There were response rates of 46% to 48% with an acceptable safety profile (McLaughlin et al., 1998).

A commonly used antibody for targeting solid tumors is directed against HER-2/*neu* (c-erbB-2). This is a cell-surface protein from the EGFR (epidermal growth factor receptor) family overexpressed on ca. 25% of primary breast cancer as well as on other carcinomas of the ovary, prostate, lung and gastrointestinal tract. A humanized mAb (trastuzumab) derived from the murine mAb 4D5 was developed recognizing an epitope on the extracellular domain of

HER-2/*neu.* Approximately 15% of women who were previously treated for metastatic breast cancer and were overexpressing HER-2/*neu* respond to trastuzumab (Herceptin®) therapy. A large randomized phase III trial comparing cytotoxic chemotherapy alone or with trastuzumab, showed substantial better efficacy and a 25% increase in survival at 29 months with combination therapy. On the basis of these results trastuzumab was approved by the FDA in 1998 and is now used as a standard therapy either alone or in combination with chemotherapy in the treatment of women with metastatic breast cancer and HER-2/*neu* overexpression, since the beginning of 2006 also in the adjuvant setting (Cobleigh et al., 1999; Slamon et al., 2001; Baselga et al., 2001; Adams et al., 2005; Romond et al., 2005).

One of the receptor blocking mAbs is cetuximab (Erbitux®), a murine-human chimeric anti-EGFR-antibody blocking ligand-receptor interactions, which is used alone or in combination with chemotherapy in patients overexpressing EGFR suffering from colorectal, lung or head and neck cancers (Saltz et al., 2004).

An alternative to targeting a cell-surface receptor expressed on cancer cells is to target the ligand that initiates signalling events through the receptor. An antibody that works with this mechanism is bevazicumab (Avastin®). This is a murine-human chimeric mAb, that blocks binding of VEGF or VEGF-A to their receptors on the vascular endothelium. VEGF is produced by many cancers to stimulate angiogenesis. Bevacizumab is used alone as anti-angiogenic therapy or in combination with chemotherapy in the treatment of metastatic colorectal and lung cancer patients. In a recent phase II trial bevazicumab showed potential benefit in combination with fluorouracil and leucovorin in patients with first-line colorectal cancer (Willett et al., 2004). In a large randomized phase III clinical trial of standard chemotherapy with or without bevazicumab, anti-vascular effects of this antibody-therapy were confirmed (Kabbinavar et al., 2005).

Alemtuzumab (MabCampath®), a humanized anti-CD 52 mAb that efficiently mediates complement fixation, is working as an immue modulator and has been approved for use in chemotherapy-refractory chronic-lymphotic leukaemia. A phase II multicenter study of previous treated patients with low-grade non-Hodgkin lymphoma has reported a response rate of 20%. Alemtuzumab is also being used to deplete T-cells from allogenic transplant grafts in patients with other hematologic malignancies (Lundin et al., 1998, 2002; Ravandi et al., 2006).

5.4 Future prospects of antibody-therapy

In the recent years, antibody therapy has become more and more important, either utilized to eliminate a critical cell-surface antigen or target payloads (*e.g.* radioisotopes, drugs or toxins) to directly kill tumor cells by modulating immune response or to activate prodrugs. The combination with chemotherapy shows applied scFvs or mAbs to raise to even higher efficacy. Bauer et al. (2005) evaluated the effect of anti-uPAR monoclonal antibodies with and without gemcitabine on primary tumor growth, retroperitoneal invasion and hepatic metastasis *in vivo*. Human pancreatic carcinoma cells were injected into the pancreatic tail of nude mice. It was demonstrated that mice systemically treated with a combination of gemcitabine and anti-uPAR mAb led to about 92% tumor reduction compared to the control or either agent alone. In addition, treatment with anti-uPAR mAb or the combination of gemcitabine and anti-uPAR mAb led to complete inhibition of retroperitoneal tumor invasion the tumor capsule remaining intact **(Figure 21)**.

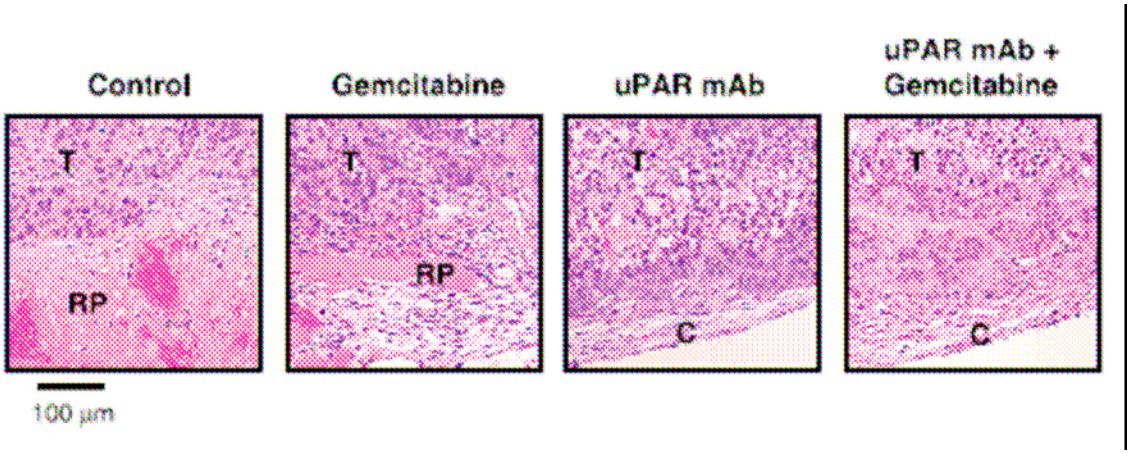

Figure 21: ***Effect of anti-uPAR antibody and gemcitabine on retroperitoneal tumor invasion.*** Photographs demonstrating retroperitoneal invasion by pancreatic tumors treated with nonspecific IgG plus saline (control), gemcitabine, anti-uPAR mAb or anti-uPAR mAb plus gemcitabine. Pancreatic tumor cells invaded the retroperitoneum in the control and gemcitabine-alone group, whereas there was no retroperitoneal invasion and tumor capsules remained intact in the groups treated with anti-uPAR mAb and anti-uPAR mAb plus gemcitabine. T, tumor; RP, retroperitoneum; C, tumor capsule. (Figure 4 from Bauer et al. 2005, p. 7780)

The ability to produce efficient and effective scFvs and mAbs holds great promise. The development of ideal vector systems is paramount and would allow the continued refinement and utilization of antibody-therapy in clinical trials. In summary, by utilizing the extensive

knowledge gained in scFv pre-clinical studies, the combination of improved vectors both in terms of targeting and oncolysis (Solly et al., 2005; Menotti et al., 2006), and an improved ability to modulate the immune system for anti-tumoral effects, holds great promise and provides a strategy for successful gene therapy (Leath et al., 2004).

Considering Herceptin® as a standard therapy for Her2/*neu*-overexpressing cancer patients, the combination of antibody-therapy and chemotherapy shows already great success. In the future, more targeted therapeutics have to be explored for an even more patient specific cancer treatment. In a phase I study phage-display libraries and scFv libraries were used in cancer patients to identify more customized tumor-targeting ligands (Krag et al., 2006). More research has to be done in this field to explore tumor specific as well as patient specific cancer therapies, giving hope for more possibilities in diagnostic and therapy of malignancies in the future.

6. Summary

The cellular receptor (uPAR, CD87) for the serine protease urokinase-type plasminogen activator (uPA) focuses uPA to the tumor cell surface, which results in extracellular matrix degradation and modulation of migration, adhesion and proliferation of tumor cells. Thus, uPAR represents an attractive target for tumor therapy.

In the present study, we have generated expression plasmids encoding a single chain fragment (scFv-IIIF10) of the monoclonal antibody mAb IIIF10, which is directed to uPAR and blocks uPA/uPAR-interaction, either as a soluble form or attached to the cell membrane *via* a GPI anchor or a transmembrane domain. Plasmids encoding either of the three variants of scFv-IIIF10, soluble TF_{1-214} (used as control protein), and the empty vector pSecTag2/HygroB, respectively, were transfected into Chinese hamster ovary cells (CHO), hamster fibroblasts (V79) and the human ovarian cancer cell line OV-MZ 6#8. scFv-IIIF10 was initially purified from cell culture supernatants of the transfected eukaryotic cell lines *via* Ni^{2+}-NTA-agarose affinity chromatography under native conditions and analysed by Western blot. Binding of purified scFv-IIIF10 from hamster cells to uPAR, presented on the surface of PMA-stimulated U937 cells, was tested by flow cytofluorometry. In contrast to hamster cells, we were not able to purify soluble scFv-IIIF10 from the culture supernatants of OV-MZ-6#8 cells transfected with pSecTag2/HygroB-scFv-IIIF10, even though expression has been proven on the level of transcription. In cell-cell-adhesion assays it was shown *via* phage display technology, that membrane-anchored scFv-IIIF10-GPI is expressed on the surface of eukaryotic cell lines.

Furthermore, the effects of scFv-IIIF10 synthesis by ovarian cancer cells on tumor growth and spread were studied in an OV-MZ-6#8 *xenograft* mouse model. However, secretion of the single-chain antibody (scFv-IIIF10) directed against the uPAR did not result in a significant reduction of relative tumor mass. It is possible, that the rather low secretion level of scFv-IIIF10 by the transfected cells does not result in effective and sustained levels of scFv-IIIF10 *in situ* to compete for uPA-binding to all uPAR molecules on the cell surface.

6. Zusammenfassung

Der Rezeptor (uPAR, CD87) für die Serinprotease Urokinase-Typ Plasminogen Aktivator (uPA) fokussiert uPA an der Zelloberfläche und führt somit zum Abbau der extrazellulären Matrix und moduliert Migration, Adhäsion und Proliferation von Tumorzellen. Auf Grund dieser Eigenschaften ist der uPA-Rezeptor in den Mittelpunkt des Interesses für die Entwicklung von Tumortherapeutika gerückt.

In der vorliegenden Arbeit wurden Expressionsplasmide konstruiert, die ein single chain Fragment (scFv-IIIF10) des monoklonalen Antikörpers mAb IIIF10, der gegen uPAR gerichtet ist und die uPA/uPAR-Interaktion blockiert, entweder als lösliche Form oder zellgebunden (mittels eines GPI-Ankers bzw. einer Transmembrandomäne) kodieren. Zusätzlich wurde ein Plasmid für die Expression einer löslichen Form von Tissue Factor (TF_{1-214}) als Kontrollprotein konstruiert. Die verschiedenen Expressionsplasmide (und auch die Vektorkontrolle pSecTag2/HygroB) wurden in *Chinese Hamster Ovary* Zellen (CHO), Hamsterfibroblasten (V79) und in die humane Ovarialtumor-Zellinie OV-MZ 6#8 transfiziert. Um die Bindungseigenschaften der verschiedenen Transfektanten *in vitro* zu analysieren, wurde anfangs löslicher scFv-IIIF10 aus dem Zellkulturüberstand transfizierter Zellen *via* Ni^{2+}-NTA-Agarose-Affinitäts-Chromatographie unter nativen Bedingungen aufgereinigt, mittels Western Blot-Analysen nachgewiesen und die Bindungsfähigkeit von scFv-IIIF10 an uPAR, der auf der Zelloberfläche von PMA-stimulierten monozytären U937 Zellen präsent ist, mittels Durchfluss-Zytofluorometrie verifiziert. Obwohl die mRNA von scFv-IIIF10 auch in OV-MZ-6#8 Zellen gezeigt werden konnte, konnte scFv-IIIF10 auf Proteinebene nur in CHO Zellen und V79 Hamsterfibroblasten nachgewiesen werden. Die scFv-IIIF10-GPI-Variante wurde an der Zelloberfläche von eukaryotischen Zelllinien in Zell-Zell-Adhäsionsassays durch Phage Display Technik nachgewiesen.

Abschließend wurde in einem Tierversuch mit athymischen Nacktmäusen der Effekt von löslichem scFv-IIIF10, exprimiert von OV-MZ-6#8 Zellen, auf Tumorwachstum und Metastasierung untersucht. Die relative Tumormasse wurde durch scFv-IIIF10 nicht signifikant reduziert. Durch die vermutlich eher geringe Expressionsrate scFv-IIIF10 exprimierender Ovarialtumor Zellen konnten keine ausreichenden Konzentrationen *in situ* erreicht werden, um mit uPA an allen uPAR-Molekülen an der Zelloberfläche zu konkurrieren.

7. References

Adams GP. Improving the tumor specificity and retention of antibody-based molecules. *In vivo* 12 (1998) 11-21

Adams GP, Schier R, McCall AM, Simmons H, Horak EM, Alpaugh RK, Marks JD, Weiner LM. High affinity restricts the localization and tumor penetration of single-chain Fv antibody molecules. *Cancer Res* 61 (2001) 4750-4755

Adams GP, Weiner LM. Monoclonal antibody therapy of cancer. *Nat Biotechnol* 23 (2005) 1147-1157

Andreasen PA, Egelund R, Petersen HH. The plasminogen activation system in tumor growth, invasion and metastasis. *Cell Moll Life Sci* 57 (2000) 25-40

Aguirre Ghiso JA, Kovalski K, Ossowski L. Tumor dormancy induced by downregulation of urokinase receptor in human carcinoma involves integrin and MAPK signaling. *J Cell Biol* 147 (1999) 89-103

Albrecht S, Luther T, Grossmann H, Flössel C, Kotzsch M, Müller M. An ELISA for tissue factor using monoclonal antibodies. *Blood Coagul Fibrinolysis* 3 (1992) 263-270

Albrecht S, Magdolen V, Herzog U, Miles L, Kirschenhofer A, Baretton G, Luther T. Soluble tissue factor interferes with angiostatin-mediated inhibition of endothelial cell proliferation by lysine-specific interaction with plasminogen kringle domains. *Thromb Haemost* 88 (2002) 1054-1059

Allgayer H. Molecular regulation of an invasion-related molecule-options for tumor staging and clinical strategies. *Eur J Cancer* 42 (2006) 811-819

Altieri DC, Edgington TS. Sequential receptor cascade for coagulation proteins on monocytes. *J Biol Chem* 264 (1989) 2969-2972

Alvarez RD, Barnes MN, Gomez-Navarro J, Wang M, Arafat W, Strong TV. A cancer gene therapeutic approach utilizing an anti-erbB-2 single chain antibody-encoding adenovirus (AD21): a phase I trial. *Clin Cancer Res* 6 (2000) 3081-3087

Andolfo A, English WR, Resnati M, Murphy G, Blasi F, Sidenius N. Metalloproteases cleave the urokinase-type plasminogen activator receptor in the D1-D2 linker region and expose epitopes not present in the intact soluble receptor. *Thromb Haemost* 88 (2002) 298-306

Andreasen P, Kjoller L, Christensen L, Duffy MJ. The urokinase plasminogen activator system in cancer metastasis: a review. *Int J Cancer* 72 (1997) 1-22

Andreasen P, Sottrup-Jensen L, Kjoller L, Nykjaer A, Moestrup S, Petersen C. Receptor-mediated endocytosis of plasminogen activators and activator/inhibitor complexes. *FEBS Lett* 338 (1994) 239-245

Appella E, Robinson EA, Ullrich SJ, Stoppelli MP, Corti A, Cassani G, Blasi F. The receptor binding sequence of urokinase. A biological function for the growth factor module for proteases. *J Biol Chem* 262 (1987) 4437-4440

Arafat WO, Gomez-Navarro J, Buchsbaum DJ, Xiang J, Wang M, Casado E, Barker SD, Mahasreshti PJ, Haisma HJ, Barnes MN, Siegal GP, Alvarez RD, Hemminki A, Nettelbeck DM, Curiel DT. Effective single chain antibody (scFv) concentrations *in vivo* via adenoviral vector mediated expression of secretory scFv. *Gene Ther* 9 (2002) 256-62

Barinka C, Parry G, Callahan J, Shaw D, Kuo A, Bdeir Khalil, Cines Douglas, Mazar A and Lubkowski J. Structural basis of interaction between urokinase type plasminogen activator and its receptor. *J Mol Biol* 363 (2006) 482-295

Batra SK, Jain M, Wittel UA, Chauhan SC and Colcher D. Pharmacokinetics and biodistribution of genetically engineered antibodies. *Curr Opin Biotechnol* 13 (2002) 603-608

Bauer TW, Liu W, Fan F, Camp E, Yang A, Somicio R, Bucana C, Callahan J, Parry G, Evans D, Boyd D, Mazar A, and Ellis L. Targeting of urokinase plasminogen activator receptor in human pancreatic carcinoma cells inhibits c-Met-and insulin-like growth factoe-I receptor mediated migration and invasion and orthotopic tumor growth in mice. *Cancer Res* 65 (2005) 7775-7781

Bazan JF. Structural design and molecular evolution of a cytokine receptor superfamily. *Proc Natl Acad Sci USA* 87 (1990) 6934-6938

Behrendt N, Ploug M, Patthy L, Houen G, Blasi F, Dano K. The ligand–binding domain of the cell surface receptor for urokinase-type plasminogen activator. *J Biol Chem* 266 (1991) 7842-7847

Blasi F. uPA, uPAR, PAI-1: key intersection of proteolytic, adhesive and chemotactic highways? *Immunol Today* 18 (1997) 415-417

Blasi F. Proteolysis, cell adhesion, chemotaxis, and invasiveness are regulated by the u-PA-u-PAR-PAI-1 system. *Thromb Haemost* 82 (1999) 298-304

Blasi F, Carmeliet P. uPAR: a versatile signalling orchestrator. *Nat Rev Mol Cell Biol* 3 (2002) 932-43

Boshart M, Weber F, Jahn G, Dorsch-Häsler K, Fleckenstein B, Schaffner W. A very strong enhancer is located upstream of an immediate early gene of human cytomegalovirus. *Cell* 41 (1985) 521-530

Böttger V. Epitope-mapping with random peptide libraries. In: *Antibody engineering* (Kontermann R, Dubel S eds), Springer Verlag, Berlin Heidelberg (2001) pp. 460-472

Bromberg M, Bailly M, Königsberg W. Role of protease-activated receptor 1 in tumour metastasis promoted by tissue factor. *Thromb Haemost* 86 (2001) 1210-4

Bromberg M, Konigsberg W, Madison J, Pawashe A. Tissue factor promotes melanoma metastasis by a pathway independent of blood coagulation. *Proc Natl Acad Sci USA* 92 (1995) 8205-8209

Chapman H, Wei Y, Simon DI, Waltz DA. Role of urokinase receptor and caveolin in regulation of integrin signaling. *Thromb Haemost* 82 (1999) 291-297

Chapman H, Wei Y. Protease crosstalk with integrins: the urokinase paradigm. *Thromb Haemost* 86 (2001) 124-129

Chapman H, Vavrin Z, Hibbs J. Macrophage fibrinolytic activity: identification of two pathways of plasmin formation by intact cells and of a plasminogen activator inhibitor. *Cell* 28 (1982) 653-662

Cobleigh MA, Vogel CL, Tripathy D, Robert NJ, Scholl S, Fehrenbacher L, Wolter JM, Paton V, Shak S, Liebermann G, Slamon DJ. Multinational study of the efficacy and safety of humanized anti-HER2 monoclonal antibody in women who have HER-2-overexpressing metastatic breast cancer that has progressed after chemotherapy for metastatic disease. *J Clin Oncol* 17 (1999) 2639-2648

Colcher D, Pavlinkova G, Beresford G, Booth BJ, Choudhury A, Batra SK. Pharmacokinetics and biodistribution of genetically engineered antibodies. *Q J Nucl Med* 42 (1998) 225-41

Coloma MJ, Hastings A, Wims LA, Morrison SL. Novel vectors for the expression of antibody molecules using variable regions generated by polymerase chain reaction. *J Immunol Methods* 152 (1992) 89-104

Cubellis MV, Wun TC, Blasi F. Receptor-mediated internalization and degradation of urokinase is caused by its specific inhibitor PAI-I. *EMBOJ* 9 (1990) 1079-1085

Danø K, Romer J, Nielsen BS, Bjorn S, Pyke C, Rygaard J, Lund LR. Cancer invasion and tissue remodelling-cooperation of protease systems and cell types. *APMIS* 107 (1999) 120-127

Del Rosso M, Fibbi G, Pucci M, D`Alessio S, Del Rosso A, Magnelli L, Chiarugi V. Multiple pathways of cell invasion are regulated by multiple families of serine proteases. *Clin Exp Metstasis* 19 (2002) 193-207

Demetri G, van Oosterom A, Garrett C, Blackstein M, Shah M, Verweij J, McArthur G, Judson I, Heinrich M, Morgan J, Desai J, Fletcher C, Georg S, Bello C, Huang X, Baum C, Casali P. Efficacy and safety of sunitinib in patients with advanced gastrointestinal stromal tumor after failure of imatinib: a randomised controlled trial. *Lancet* 368 (2006) 1329-1338

Deng G, Royle G, Seiffert D, Loskutoff D. The PAI-I/vitronectin interaction: two cats in a bag? *Thromb Haemost* 74 (1995) 66-70

Duffy MJ, O`Grady P, Devaney D, O`Siorian L, Fennelly JJ, Lijnen HJ. Urokinase-plasminogen activator, a marker for aggressive breast carcinoma: preliminary report. *Cancer* 62 (1988) 531-533

Duffy MJ. Urokinase plasminogen activator and its inhibitor, PAI-1, as prognostic markers in breast cancer: from pilot to level 1 evidence studies. *Clin Chem* 48 (2002) 1194-1197

Ehrlich H, Keijer J, Preissner K, Gebbink R, Pannekoek H. Functional interaction of plasminogen activator inhibitor type I (PAI-1) and heparin. *Biochemistry* 30 (1991) 1021-2028

Ellis V, Whawell SA, Werner F, Deadman J. Assembly of urokinase receptor-mediated plasminogen activation complexes involves direct, non-active site interactions between urokinase and plasminogen. *Biochemistry* 38 (1999) 651-659

Fan D, Yano S, Shinohara H, Solorzano C, Van Arsdall M, Bucana CD, Pathak S, Kruzel E, Herbst RS, Onn A, Roach JS, Onda M, Wang QC, Pastan I, Fidler IJ. Targeted therapy against human lung cancer in nude mice by high-affinity recombinant antimesothelin single-chain Fv immunotoxin. *Mol Cancer Ther* 8 (2002) 595-600

Fang M, Zhao R, Yang Z, Zhang Z, Li H, Zhang XT, Lin Q, Huang HL. Characterization of an anti-human ovarian carcinoma x anti-human CD3 bispecific single-chain antibody with an albumin-original interlinker. *Gynecol Oncol* 92 (2004) 135-146

Fazioli F, Resnati M, Sidenius N, Higashimoto Y, Appella E, Blasi F. A urokinase-sensitive region of the human urokinase receptor is responsible for its chemotactic activity. *EMBO J* 16 (1997) 7279-7286

Fischer K, Lutz V, Wilhelm O, Schmitt M, Graeff H, Heiss P, Nishiguchi T, Harbeck N, Kessler H, Luther T, Magdolen V, Reuning U. Urokinase induces proliferation of human ovarian cancer cells: characterization of structural elements required for growth factor function. *FEBS Lett* 438 (1998) 101-105

Fujimori K, Covell DG, Fletcher JE, Weinstein JN. A modelling analysis of monoclonal antibody percolation through tumors: a binding site barrier. *J Nucl Med* 31 (1990) 1191-1198

Gårdsvoll H; Danø K; Ploug M. Mapping part of the functional epitope for ligand binding on the receptor for urokinase-type plasminogen activator by site-directed mutagenesis. *J Biol Chem* 274 (1999) 37995-38003

Gårdsvoll H, Gilquin B, Le Du MH, Ménèz A, Jørgensen TJ, Ploug M. Characterization of the functional epitope on the urokinase receptor. Complete alanine scanning mutagenesis supplemented by chemical crosslinking. *J Biol Chem* 14 (2006) 19260-19272

Gritz L, Davies J. Plasmid encoded Hygromycin B-resistance: the sequence of Hygromycin-B-phophotransferase gene and its expression in *Escherichia coli* and *Saccharomyces cerevisiae*. *Gene* 25 (1983) 179-188

Guillaume-Rousselet N, Jean D, Frade R. Cloning and characterization of anti-cathepsin L single chain variable fragment whose expression inhibits procathepsin L secretion in human melanoma cells. *Biochem J* 367 (2002) 219-227

Harbeck N, Kates RE, Look MP, Meijer-van Gelder ME, Klijn JG, Krüger A, Kiechle M, Jänicke F, Schmitt M, Foekens J. Enhanced benefit from adjuvant chemotherapy in breast cancer patients classified high risk according to urokinase-type plasminogen activator (uPA) and plasminogen activator inhibitor type 1 (*n* = 3424). *Cancer Res* 62 (2002) 4617-4622

Helfrich W, Haisma HJ, Magdolen V, Luther T, Bom VJ, Westra J, van der Hoeven R, Kroesen BJ, Molema G, de Leij L. A rapid and versatile method for harnessing scFv antibody fragments with various biological effector functions. *J Immunol Methods* 237 (2000) 131-145

Herbst RS, Maddox AM, Rothenberg ML. Selective oral epidermal growth factor receptor-tyrosine kinase inhibitor ZD 1839 is generally well-tolerated and has activity in non-small-cell lung cancer and other solid tumors. Results of a phase I trial. *J Clin Oncol* 20 (2002) 3815-3825

Hidalgo M, Siu LL, Neumunaitis J, Rizzo J, Hammond LA, Takimoto C, Eckhardt SG, Tolcher A, Britten CD, Denis L, Ferrante K, Von Hoff DD, Silberman S, Rowinsky EK. Phase I and pharmacologic study of OSI-774, an epidermal growth factor receptor tyrosine kinase inhibitor, in patients with advance solid malignancies. *J Clin Oncol* 19 (2001) 3267-3279

Hooper JD, Clements JA, Quigley JP, Antalis TM. Type II transmembrane serine proteases. Insights into an emerging class of cell surface proteolytic enzymes. *J Biol Chem* 276 (2001) 857-860

Høyer-Hansen G, Ploug M, Behrendt N, Rønne E, Danø K. Cell surface acceleration of urokinase-catalysed receptor cleavage. *Eur J Biochem* 243 (1997) 21-26

Høyer-Hansen G, Rønne E, Søberg H, Behrendt N, Ploug M, Lund LR, Ellis V, Danø K. Urokinase plasminogen activator cleaves its cell surface receptor releasing the ligand binding domain. *J Biol Chem* 267 (1992) 18224-18229

Hudson PJ. Recombinant antibodies: a novel approach to cancer diagnosis and therapy. *Expert Opin Investig Drugs* 9 (2000) 1231-1242

Ichinose A, Fujikawa K, Suyama T. The activation of pro-urokinase by plasma kallikrein and its activation by thrombin. *J Biol Chem* 261 (1986) 3486-3489

Jänicke F, Prechtl A, Thomssen C, Harbeck N, Meisner C, Untch M, Sweep CG, Graeff H, Schmitt M, for the German Chemo N0 Study Group. Randomized adjuvant therapy trial in high-risk lymph node negative breast cancer patients identified by urokinyse-type plasminogen activator and plasminogen activator inhibitor type I. *J Natl Cancer Inst* 93 (2001) 913-920

Jänicke F, Schmitt M, Graeff H. Clinical relevance of the urokinase-typ and tissue-type plasminogen activators and of their type-1 inhibitor in breast cancer. *Semin Thromb Hemost* 17 (1991) 30-12

Juweid M, Neumann R, Paik C, Perez-Bacete MJ, Sato J, van Osdol W, Weinstein JN. Micropharmacology of monoclonal antibodies in solid tumors: direct experimental evidence for binding site barrier. *Cancer Res* 52 (1992) 5144-5153

Kabbinavar FF, Schulz J, McCleod M, Patel T, Hamm JT, Hecht JR, Mass R, Perrou B, Nelson B, Novotny WF. Addition of bevacizumab to bolus fluorouracil and leucovorin in first-line metastatic colorectal cancer: results of a randomized phase II trial. *J Clin Oncol* 23 (2005) 3697-3705

Kay BK, Winter J & McCafferty J. Phage display of peptides and proteins. A laboratory manual. *Academic Press* (1996) London

Kirschenhofer A, Magdolen V, Schmitt M, Albrecht S, Krol J, Farthmann J, Kopitz C, Prezas P, Krüger A, Luther T, Böttger V. Recombinant single chain antibody scFv-IIIF10 directed to human urokinase receptor. *Recent Res Devel Cancer* 5 (2003) 9-25

Koblinski JE, Ahram M, Sloane BF. Unraveling the role of proteases in cancer. *Clin Chim Acta* 291 (2000) 113-135

Krag D, Shukla G, Shen G, Pero S, Ashikaga T, Fuller S, Weaver D, Burdette-Radoux and Thomas C. Selection of tumor-binding ligands in cancer patients with phage display libraries. *Cancer Res* 66 (2006) 7724-7733

Kristensen P, Eriksen J, Blasi F, Dano K. Two alternatively spliced mouse urokinase receptor mRNAs with different histological localization in the gastrointestinal tract. *J Cell Biol* 115 (1991) 1763-1771

Krol J, Sato S, Rettenberger P, Assfalg-Machleidt I, Schmitt M, Magdolen V, Magdolen U. Novel bi- and trifunctional inhibitors of tumor-associated proteolytic systems. *Biol Chem* 384 (2003a) 1085-1096

Krol J, Kopitz C, Kirschenhofer A, Schmitt M, Magdolen U, Krüger A, Magdolen V Inhibition of intraperitoneal tumor growth of human ovarian cancer cells by bi- and trifunctional inhibitors of tumor-associated proteolytic systems. *Biol Chem* 384 (2003b) 1097-1102

Kroon ME, Koolwijk P, van Goor H, Weidle UH, Collen A, van der Pluijm G, van Hinsbergh VW. Role and localization of urokinase receptor in the formation of new microvascular structures in fibrin matrices. *Am J Pathol* 154 (1999) 1731-1742

Kruithof E, Baker M, Bunn C. Biological and clinical aspects of plasminogen activator inhibitor type 2. *Blood* 86 (1995) 4007-4024

Le Y, Murphy P, Wang J. Formyl-peptide receptors revisited. *Trends Immunol* 23 (2002) 541-548

Leath CA, Douglas JT, Curiel DT, Alvarez RD. Single-chain antibodies: A therapeutic modality for cancer gene therapy. *Int J Oncol* 24 (2004) 765-771

Leissner P, Verjat T, Bachelot T, Paye M, Krause A, Puisieux A, Mougin B. Prognostic significance of urokinase plasminogen activator and plasminogen activator inhibitor-1 mRNA expression in lymph node- and hormone receptor positive breast cancer. *BMC Cancer* 6 (2006) 1-9

Llinas P, Le Du MH, Gardsvoll H, Dano K, Ploug M, Gilquin B. Crystal structure of the human urokinase plasminogen activator receptor bound to an antagonist peptide. *EMBO J* 24 (2005) 1655-1663

Look M, van Putten W, Duffy M, Harbeck N, Christensen I, Thomssen C, Kates R, Spyratos F, Fernö M, Eppenberger-Castori S, Sweep F, Ulm K, Peyrat JP Martin P, Magdelenat H, Brünner N, Duggn C, Lisboa B, Bendahl P, Quillien V, Daver A, Ricolleau G, Meijer-van Gelder M, Manders P, Fiets E, Blankensein M, Broet P, Omain S, Daxenbichler G, Windbichler G, Cufer T, Borstnar S, Kueng W, Beex L, Klijn J, O`Higgins N, Eppenberger U, Jänicke F, Schmitt M, Foekens J. Pooled analysis of prognostic impact of urokinase-type plasminogen activator and its inhibitor PAI-1 in 8377 breast cancer patients. *J Nat Cancer Inst* 94 (2002) 116-128

Lundin J, Kimby E, Bjorkholm M, Broliden PA, Celsing F, Hjalmar V, Mollgard L, Rebello P, Hale G, Waldmann H, Mellstedt H, Osterborg A. Phase II trial of subcutaneous anti-CD52 monoclonal antibody alemtuzumab (Campath-1H) as first-line treatment for patients with B-cell chronic lymphatic leukaemia (B-CLL). *Blood* 100 (2002) 768-773

Luther T, Flössel C, Weber F, Haroske G, Kotzsch M, Müller M. Expression von Tissue Factor und Urokinase im Menschlichen Brustkrebs: Beziehungen zu Prognosefaktoren. *Verh Dtsch Path* 78 (1994) 532

Luther T, Magdolen V, Albrecht S, Kasper M, Riemer C, Kessler H, Graeff H, Müller M, Schmitt M. Epitope-mapped monoclonal antibodies as tools for functional and morphological analyses of the human urokinase receptor in tumor tissue. *Am J Pathol* 150 (1997) 1231-1244

Lutz V, Reuning U, Kruger A, Luther T, von Steinburg SP, Graeff H, Schmitt M, Wilhelm OG and Magdolen V. High level synthesis of recombinant soluble urokinase receptor (CD87) by ovarian cancer cells reduces intraperitoneal tumor growth and spread in nude mice. *Biol Chem* 382 (2001) 789-798

Ma Z, Webb DJ, Jo M, Gonias SL. Endogenously produced urokinase-type plasminogen activator is a major determinant of the basal level of activated ERK/MAP kinase and prevents apoptosis in MDA-MB-231 breast cancer cells. *J Cell Sci* 114 (2001) 3387-3396

Magdolen V, Rettenberger P, Lopens A, Oi H, Lottspeich F, Kellermann J, Creutzburg S, Goretzki L, Weidle U, Wilhelm O, Schmitt M, Graeff H. Expression of the human urokinase-type plasminogen activator receptor in E. coli and Chinese hamster ovary cells: Purification of the recombinant proteins and generation of polyclonal antibodies in chicken. *Electrophoresis* 16 (1995) 813-816

Magdolen V, Albrecht S, Kotzsch M, Haller C, Bürgle M, Jacob U, Großer M, Kessler H, Graeff H, Müller M, Schmitt M, Luther T. Immunological and functional analyses of the extracellular domain of human tissue factor. *Biol Chem* 379 (1998) 157-165

Magdolen V, Bürgle M, de Prada NA, Schmiedeberg N, Riemer C, Schroeck F, Kellermann J, Degitz K, Wilhelm OG, Schmitt M, Kessler H. Cyclo^{19,31}[D-Cys19]-uPA$_{19-31}$ is a

potent competitive antagonist of the interaction of urokinase-type plasminogen activator with its receptor (CD87). *Biol Chem* 382 (2001) 1197-1205

Martin P, Kelly C, Carney D. Epidermal growth factor receptor-targeted agents for lung cancer. *Cancer Control* 13 (2006) 129-140

Mayer A, Tsiompanou E, O´Malley D, Boxer GM, Bhatia J, Flynn AA, Chester KA, Davidson BR, Lewis AA, Winslet MC, Dhillon AP, Hilson AJ, Begent RH. Radioimmunoguided surgery in colorectal cancer using a genetically engineered anti-CEA single chain Fv antibody. *Clin Cancer Res* 6 (2000) 1711-1719

McCafferty J, Fitzgerald KJ, Earnshaw J, Chiswell DJ, Link J, Smith R and Kenten J. Selection and rapid purification of murine antibody fragments that bind a transition-state analog by phage display. *Appl Biochem Biotechnol* 47 (1994) 157-171; discussion 171-173

McLaughlin P, Grillo-Lopez AJ, Link BK, Levy R, Czuczman MS, Williams ME, Heyman MR, Bence Bruckler I, White CA, Cabanillas F, Jain V, Ho AD, Lister J, Wey K, Shen D, Dallaire BK. Rituximab chimeric anti-CD20 monoclonal antibody therapy for relapsed indolent lymphoma: half of patients respond to a four dose treatment program. *J Clin Oncol* 16 (1998) 2825-2832

Menotti L, Cerretani A and Campadelli-Fiume G. A Herpes Simplex Virus recombinant that exhibits a single-chain antibody to HER2/neu enters cells through the mammary tumor receptor, independently of the gD receptors. *J Virol* (2006) 5531–5539

Min Fang, Zhao R, Yang Z, Li H, Zhang XT, Ling Q, Huang HL. Characterization of an anti-human ovarian carcinoma x anti-human CD3 bispecific single chain antibody with an albumin-original interlinker. *Gynecol Oncol* 92 (2004) 135-146

Moller LB, Pollänen J, Ronne E, Pedersen N, Blasi, F. N-linked glycosylation of the ligand binding domain of the human urokinase receptor contributes to the affinity for its ligand. *J Biol Chem* 268 (1993) 11152-11159

Möbus V, Gerharz C, Press U, Moll R, Beck T, Mellin W, Pollow K, Knapstein P, Kreienberg R. Morphological, immunohistochemical and biochemical characterization of 6 newly established human ovarian carcinoma cell lines. *Int J Cancer* 52 (1992) 76-84.

Montuori N, Visconte V, Rossi G, Ragno P. Soluble and cleaved forms of the urokinase receptor: degradation products or active molecules? *Thromb Haemost* 93 (2005) 192-198

Montuori N, Carriero MV, Salzano S, Rossi G, Ragno P. The cleavage of the urokinase receptor regulates its multiple functions. *J Biol Chem* 277 (2002) 46932-46939

Moy B and Goss P. Lapatinib: Current status and future directions in breast cancer. *Oncologist* 11 (2006) 1047–1057

Muehlenweg B, Assfalg-Machleidt I, Parrado SG, Bürgle M, Creutzburg S, Schmitt M, Auerswald EA, Machleidt W, Magdolen V. A novel type of bifunctional inhibitor directed against proteolytic activity and receptor/ligand interaction. *J Biol Chem* 275 (2000) 33562-33566

Muehlenweg B, Sperl S, Magdolen V, Schmitt M, Harbeck N. Interference with the urokinase plasminogen activator (uPA) system: A promising therapy concept for solid tumors. *Expert Opin Biol Ther* 1 (2001) 683-691

Myers KA, Ryan MG, Stern PL. Targeting immune effector molecules to human tumor cells through genetic delivery of 5T4-specific scFv fusion proteins. *Cancer Gene Ther* 9 (2002) 884-896

Nykjaer A, Conese M, Christensen EI, Olson D, Cremona O, Gliemann J, Blasi F. Recycling of the urokinase receptor upon internalization of the uPA:serpin complexes. *EMBO J* 16 (1997) 2610-2620

Ny T, Mikus P. Plasminogen activator inhibitor type 2. A spontaneously polymerizing serpin that exists in two topological forms. *Adv Exp Med Biol* 425 (1997) 123-30

Oh P, Li Y, Yu J, Durr E, Krasinska KM, Carver LA, Testa JE, Schnitzer JE. Subtractive proteomic mapping of the endothelial surface in lung and solid tumors for tissue specific therapy. *Nature* 429 (2004) 629-635

Ott I, Fischer EG, Miyagi Y, Mueller BM, Ruf W. A role for tissue factor in cell adhesion and migration mediated by interaction with actin-binding protein 280. *J Cell Biol* 140 (1998) 1241-1253

Pavlinkova G, Beresford G, Booth BJ, Batra SK, Colcher D. Charge-modified single chain antibody constructs of monoclonal antibody CC49: generation, characterization, pharmacokinetics and biodistribution analysis. *Nucl Med Biol* 26 (1999) 27-34

Pavoni E, Flego M, Dupuis ML, Barca S, Petronzelli F, Anastasi AM. D'Alessio V, Pelliccia A, Vaccaro P, Monteriu G, Ascione A, De Santis R, Felici F, Cianfriglia M and Minenkova O. Selection, affinity maturation and characterization of a human scFv antibody against CEA protein. *BMC Cancer* 6 (2006) 41

Pedersen N, Schmitt M, Ronne E, Nicoletti MI, Hoyer-Hansen G, Conese M, Giavazzi R, Dano K, Kuhn W, Jänicke F, et al. A ligand-free, soluble urokinase receptor is present in the ascitic fluid from patients with ovarian cancer. *J Clin Invest* 92 (1993) 2160-2167

Ploug M, Rønne E, Behrendt N, Jensen AL, Blasi F, Danø K. Cellular receptor for urokinase plasminogen activator. Carboxy-terminal processing and membrane anchoring by glycosyl-phosphatidyl-inositol. *J Biol Chem* 266 (1991) 1926-1933

Ploug M, Ellis V, Danø K. Ligand interaction between urokinase-type plasminogen activator and its receptor probed with 8-anilino-1-naphthalenesulfonate. Evidence for a hydrophobic binding site exposed only on the intact receptor. *Biochemistry* 33 (1994) 8991-8997

Ploug M, Rahbek-Nielsen H, Ellis V, Roepstorff P, Danø K: Chemical modification of the urokinase-type plasminogen activator and its receptor using tetranitromethane. Evidence for the involvement of specific tyrosine residues in both molecules during receptor-ligand interaction. *Biochemistry* 34 (1995) 12524-12534

Ploug, M. Identification of specific sites involved in ligand binding by photoaffinity labeling of the receptor for the urokinase-type plasminogen activator. Residues located at equivalent positions in uPAR domains I and III participate in the assembly of a composite ligand binding site. *Biochemistry* 37 (1998) 16494-16505

Ploug M, Rahbek-Nielsen H, Nielsen PF, Roepstorff P, Danø K. Glycosylation profile of a recombinant urokinase-type plasminogen activator receptor expressed in Chinese hamster ovary cells. *J Biol Chem* 273 (1998) 13933-43

Ploug M, Gårdsvoll H, Jorgensen TJ, Lonborg Hansen L, Danø K. Structural analysis of the interaction between urokinase-type plasminogen activator and its receptor: a potential target for anti-invasive cancer therapy. *Biochem Soc Trans* 30 (2002) 177-183

Pollänen JJ. The N-terminal domain of human urokinase receptor contains two distinct regions critical for ligand recognition. *Blood* 82 (1993) 2719-2729

Potempa J, Korzus E, Travis J. The serpin superfamily of proteinase inhibitors: structure, function and regulation. *J Biol Chem* 269 (1994) 15957-15960

Rabbani SA, Gladu J. Urokinase receptor antibody can reduce tumor volume and detect the presence of occult tumor metastases in vivo. *Cancer Res* 62 (2002) 2390-2397

Rabbani SA, Mazar AP. The role of the plasminogen activation system in angiogenesis and metastasis. *Surg Oncol Clin N Am* 10 (2001) 393-415

Ragno P. The urokinase receptor: a ligand or a receptor? Story of a sociable molecule. *Cell Mol Life Sci* 63 (2006) 1028-1037

Randolph G, Luther T, Albrecht S, Magdolen V, Müller W. Role of tissue factor in adhesion of mononuclear phagocytes to and trafficking through endothelium *in vitro*. *Blood* 11 (1998) 4167-4177

Ravandi F and O'brien S. Alemtuzumab in CLL and other lymphoid neoplasms. *Cancer Invest* 24 (2006) 718-725

Reff ME, Heard C. A review of modifications to recombinant antibodies: attempt to increase efficacy in oncology applications. *Crit Rev Oncol Hematol* 40 (2001) 25-35

Rettenberger P, Wilhelm O, Oi H, Weidle UH, Goretzki L, Koppitz M, Lottspeich F, König B, Pessara U, Kramer MD, Schmitt M, Magdolen V. A competitive chromogenic assay to study the functional interaction of urokinase-type plasminogen activator with its receptor. *Biol Chem* Hoppe-Seyler 376 (1995) 587-594

Reuning U, Sperl S, Kopitz C, Kessler H, Krüger A, Schmitt M and Magdolen V. Urokinase-type plasminogen activator (uPA) and its receptor (uPAR): development of antagonists of uPA/uPAR interaction and their effects *in vitro* and *in vivo*. *Curr Pharm Des* 9 (2003) 1529-1543

Reuning U, Magdolen V, Wilhelm O, Fischer K, Lutz V, Graeff H. Multifunctional potential of the plasminogen activation system in tumour invasion and metastasis. *Int J Oncol* 13 (1998) 893-906

Romond E, Perez E, Bryant J, Suman V, Geyer C, Davidson N, Tan-Chiu E, Martino S, Paik S, Kaufman P, Swain S, Pisansky T, Fehrenbacher L, Kutteh L, Vogel V, Visscher D, Yothers G, Jenkins R, Brown A, Dakhil S, Mamounas E, Lingle W, Klein P, Ingle J and Wolmark N. Trastuzumab plus adjuvant chemotherapy for operable HER2-positive breast cancer. *N Engl J Med* 353 (2005) 1673-1684

Sampson MT, Kakkar AK. Coagulation proteases and human cancer. *Biochem Soc Trans* (2002) 201-207

Saltz LB, Meropol NJ, Loehrer PJ, Needle MN, Kopit J, Mayer RJ. Phase II trial of cetuximab in patients with refractory colorectal cancer that express the epidermal growth factor receptor. *J Clin Oncol* 22 (2004) 1201-1208

Sanz L, Kristensen P, Blanco B, Facteau S, Russell SJ, Winter G, Alvarez-Vallina L. Single-chain antibody-based gene therapy: inhibition of tumor growth by in situ production of phage derived human antibody fragments blocking functionally active sites of cell-associated matrices. *Gene Ther* 9 (2002) 1049-1053

Sato S, Kopitz C, Schmalix WA, Muehlenweg B, Kessler H, Schmitt M, Krüger A, Magdolen V. High-affinity urokinase-derived cyclic peptides inhibiting urokinase/urokinase receptor-interaction: effects on tumor growth and spread. *FEBS Lett* 528 (2002) 212-216

Schlehuber S, Skerra A. Lipocalins in drug discovery: from natural ligand-binding proteins to “anticalins”. *Drug Discov Today* 10 (2005) 23-33

Schmitt M, Wilhelm OG, Reuning U, Krüger A, Harbeck N, Lengyel E. The urokinase plasminogen activator system as a novel target for tumour therapy. *Fibrinolysis* 6 (2000) 114-132

Schmitt M, Jänicke F, Graeff H. Tumour-associated proteases. *Fibrinolysis* 6 (1992) 3-26

Schmitt M, Harbeck N, Thomssen C, Wilhelm O, Magdolen V, Reuning U, Ulm K, Höfler H, Jänicke F, Graeff H. Clinical impact of the plasminogen activation system in tumor

invasion and metastasis: prognostic relevance and target for therapy. *Thromb Haemost* 78 (1997) 285-296

Sevlever D, Chen R, Medof ME. Synthesis of the GPI anchor in paroxysmal nocturnal hemoglobinuria and the glycophosphoinositol-linked proteins. *Academic press* (2000) 199-220

Skerra A. "Anticalins": a new class of engineered ligand-binding proteins with antibody-like properties. *J Biotechnol* 74 (2001) 257-275

Smith GP, Scott JK. Library of peptides and proteins displayed on filamentous phage. *Methods Enzymol* 217 (1993) 228-257

Smith KA, Nelson PN, Warren P, Astley SJ, Murray PG, Greenman J. Demystified...recombinant antibodies. *J Clin Pathol* 57 (2004) 912-917

Sperl S, Mueller MM, Wilhelm OG, Schmitt M, Magdolen V, Moroder L. The uPA/uPA-receptor system as a target for tumor therapy. *Drug News Perspect* 14 (2001) 401-411

Solly S, Nguyen T, Weber A and Horellou P. Targeting of c-Met and urokinase expressing human glioma cells lines by retrovirus vector displaying single-chain variable fragment antibody. *Cancer Biol Ther* 4 (2005) 987-992

Sun J, Pons J, Craik CS. Potent and selective inhibition of membrane-type serine protease 1 by human single-chain antibodies. *Biochemistry* 42 (2003) 892-900

Taniguchi T, Kakkar AK, Tuddenham EG, Williamson RC, Lemoine NR. Enhanced expression of urokinase receptor induced through the tissue factor-factor VII_a pathway in human pancreatic cancer. *Cancer Res* 58 (1998) 4461-4467

Tautz D and Renz M. An optimized freeze-squeeze method for the recovery of DNA fragments from agarose gels. *Anal Biochem* 132 (1983) 14-19

Vitaliti A, Wittmer M, Steiner R, Wyder L, Neri D, Klemenz R. Inhibition of tumor angiogenesis by a single-chain antibody directed against vascular endothelial growth factor. *Cancer Res* 60 (2000) 4311-4314

Waltz D, Chapman H. Reversible cellular adhesion to vitronectin linked to urokinase receptor occupancy. *J Biol Chem* 269 (1994) 14746-14750

Wei Y, Lukashev M, Simon D, Bodary S, Rosenberg S, Doyle MV, Chapman HA. Regulation of integrin function by the urokinase receptor. *Science* 273 (1996) 1551-1555

Wilhelm O, Wilhelm S, Escott GM, Lutz V, Magdolen V, Schmitt M, Rifkin D, Wilson E, Graeff H, Brunner G. Cellular glycosylphosphatidyl-specific phospholipase D regulates urokinase receptor shedding and cell surface expression. *J Cell Physiol* 180 (1999) 225-235

Willett CG, Boucher Y, di Tomaso E, Duda DG, Munn LL, Tong RT, Chung DC, Sahani DV, Kalva SP, Kozin SV, Mino M, Cohen KS, Scadden DT, Hartford AC, Fischman AJ, Clark JW, Ryan DP, Zhu AX, Blaszkowsky LS, Chen HX, Shellito PC, Lauwers GY, Jain RK. Direct evidence that VEGF- specific antibody bevazicumab has antivascular effects in human rectal cancer. *Nat Med* 10 (2004) 145-147

8. Curriculum vitae and publications

Curriculum vitae

Personal details

date of birth	19.04.1975
place of birth	Munich
marital status	single

Parents

father:	Dr. med. Otto Kirschenhofer, general practitioner
mother:	Dr. med. Elisabeth Kirschenhofer, general practitioner

Education

1981-1985	Grundschule Riedering, Riedering
1985-1994	Ignaz Günther Gymnasium, Rosenheim
1994	Abitur

Medical education

11/1996-05/2005	study of medicine, Ludwig-Maximilians-Universität, München
09/1998	pre-clinical examination
04/2000	first state examination
08/2002	second state examination
05/2004	third state examination

Internship

01/1999	clinical research at SmithKline Beecham Pharmaceuticals, Munich

02/1999	department of gynaecology and obstetrics, Klinikum Rosenheim
09/1999	department of internal medicine, Hospital General Jose Parres, Cuernavacca, Mexico
05/2000	department of anesthesia and intensive care, Allgemeines Krankenhaus der Stadt Wien, Austria
09/2000	department of neonatology, Mercy Hospital for Women, Melbourne, Australia
02/2001	general medical practice of Dres. E. und O. Kirschenhofer, Riedering

Clinical clerkship

02/2003-05/2003	department of gynaecology and obstetrics, Klinikum der Universität München Großhadern, Prof. Dr. med. H. Hepp
06/2003-07/2003	department of internal medicine, Berner Klinik, Montana, Schweiz, Dr. med. C. Vaney
08/2003-09/2003	department of internal medicine, Nepean Hospital, Sydney University, Australia, Prof. Dr. med. N. Talley
10/2003-01/2004	department of surgery, Chirurgische Klinik Innenstadt, Ludwig-Maximilians-Universität München, Prof. Dr. med. W. Mutschler

Specialization in gynaecology and obstetrics

08/2004-11/2006	intern at the department of gynaecology and obstetrics, Klinikum Rosenheim, Prof. Dr. med. Th. Beck
since 12/2006	intern at the department of gynaecology and obstetrics Universitätsklinikum Großhadern, Ludwig-Maximilians-Universität München, Prof. Dr. med. K. Friese

Publications

Kirschenhofer A, Magdolen V, Schmitt M, Albrecht S, Krol J, Farthmann J, Koptitz C, Prezas P, Krüger A, Luther T, Böttger V. Recombinant single chain antibody scFv-IIIF10 directed to human urokinase receptor. *Recent Res Devel Cancer* 5 (2003) 9-25

Albrecht S, Magdolen V, Herzog U, Miles L, Kirschenhofer A, Baretton G, Luther T. Soluble tissue factor interferes with angiostatin-mediated inhibition of endothelial cell proliferation by lysine-specific interaction with plasminogen kringle domains. *Thromb Haemost* 88 (2002) 1054-1059

Krol J, Kopitz C, Kirschenhofer A, Schmitt M, Magdolen U, Krüger A, Magdolen V Inhibition of intraperitoneal tumor growth of human ovarian cancer cells by bi- and trifunctional inhibitors of tumor-associated proteolytic systems. *Biol Chem* 384 (2003) 1097-1102

Lebenslauf

Persönliche Daten

Geburtsdatum	19.04.1975
Geburtsort	München
Familienstatus	ledig

Eltern

Vater:	Dr. med. Otto Kirschenhofer, Allgemeinarzt
Mutter:	Dr. med. Elisabeth Kirschenhofer, Allgemeinärztin

Schulische Ausbildung

1981-1985	Grundschule, Riedering
1985-1994	Ignaz Günther Gymnasium, Rosenheim
1994	Abitur

Medizinische Ausbildung

11/1996	Beginn des Studiums der Humanmedizin an der Ludwig-Maximilians-Universität, München
09/1998	Physikum
04/2000	Erstes Staatsexamen
08/2002	Zweites Staatsexamen
05/2004	Drittes Staatsexamen

Praktikum/Famulatur

01/1999	Praktikum in der klinischen Forschung bei SmithKline Beecham Pharmaceuticals, München
02/1999	Famulatur im Fach Gynäkologie am Klinikum Rosenheim
09/1999	Famulatur im Fach Innere Medizin am Hospital General Jose Parres, Cuernavacca, Mexico
05/2000	Famulatur im Fach Anästhesie und Intensivmedizin am Allgemeinen Krankenhaus der Stadt Wien, Österreich
09/2000	Famulatur im Fach Neonatologie am Mercy Hospital for Women, Melbourne, Australien

02/2001	Famulatur in der Gemeinschaftspraxis für Allgemeinmedizin und Sportmedizin Drs. E. und O. Kirschenhofer, Riedering

Praktisches Jahr

02/2003-05/2003	Gynäkologie am Klinikum der Universität München Großhadern unter Prof. Dr. med. H. Hepp
06/2003-07/2003	Innere Medizin an der Berner Klinik, Montana, Schweiz unter Dr. med. C. Vaney
08/2003-09/2003	Innere Medizin am Nepean Hospital, Sydney University, Australien unter Prof. Dr. med. N. Talley
10/2003-01/2004	Chirurgie an der Chirurgischen Klinik Innenstadt, Ludwig-Maximilians-Universität München unter Prof. Dr. med. W. Mutschler

Gynäkologische Facharztausbildung

08/2004-11/2006	Assistenzärztin der Gynäkologie und Geburtshilfe, Klinikum Rosenheim unter Prof. Dr. med. Th. Beck
seit 12/2006	Assistenzärztin der Gynäkologie und Geburtshilfe, Universitätsklinikum Großhadern unter Prof. Dr. med. K. Friese

Veröffentlichungen

Albrecht S, Magdolen V, Herzog U, Miles L, Kirschenhofer A, Baretton G, Luther T. Soluble tissue factor interferes with angiostatin-mediated inhibition of endothelial cell proliferation by lysine-specific interaction with plasminogen kringle domains. *Thromb Haemost* 88 (2002) 1054-1059

Kirschenhofer A, Magdolen V, Schmitt M, Albrecht S, Krol J, Farthmann J, Koptitz C, Prezas P, Krüger A, Luther T, Böttger V. Recombinant single chain antibody scFv-IIIF10 directed to human urokinase receptor. *Recent Res Devel Cancer* 5 (2003) 9-25

Krol J, Kopitz C, Kirschenhofer A, Schmitt M, Magdolen U, Krüger A, Magdolen V Inhibition of intraperitoneal tumor growth of human ovarian cancer cells by bi- and trifunctional inhibitors of tumor-associated proteolytic systems. *Biol Chem* 384 (2003) 1097-1102